“FEDERICO II” UNIVERSITY OF NAPLES

Division of Pharmacology, Department of Neuroscience
Reproductive Sciences and Dentistry, School of Medicine

PhD in Neuroscience

XXXIV Cycle

PhD thesis

Study of the remyelinating and neuroprotective potential of novel pharmacological compounds targeting the Na^{+}/Ca^{+2} exchanger NCX3 in oligodendrocytes or the endocannabinoid and melatoninergic systems in brain explants

PhD Coordinator
Prof. Maurizio Taglialatela

Tutor
Prof. Francesca Boscia

Candidate
Dr. Mariarosaria Cammarota

Academic Year 2021/2022

INDEX

Abbreviations

$[Ca^{+2}]_i$	Intracellular calcium concentration
$[Na^{+}]_i$	Intracellular sodium concentration
AA	Arachidonic acid
AANAT	Aryl-alkyl-amine-N-acetyl transferase
AD	Alzheimer's Disease
AEA	Anandamide
AL	Active lesion
APC	Antigen-Presenting Cell
ALS	Amyotrophic Lateral Sclerosis
BED	5-amino-N-butyl-2-(4-ethoxyphenoxy) benzamide hydrochloride
bFGF	Basic fibroblast growth factor
BBB	Blood-Brain-Barrier
BSA	Bovine Serum Albumin
bHLH	Basic Helix–Loop–Helix
BMPs	Bone Morphogenetic Proteins
CaCA	Calcium-Cation-Antiporters
cAMP	cyclic Adenosine Monophosphate
CAMKIIβ	Calcium/Calmodulin-dependent protein kinase IIβ
CA	Chronic Active
CB	Cannabinoid Receptors
c-JNK	c-Jun N-terminal kinase
CNS	Central Nervous System
CC	Corpus Callosum
CIS	Clinically Isolated Syndrome
CNPase	2',3'-Cyclic Nucleotide-3-Phosphodiesterase
DAGL	Diacylglycerol Lipases
DMSO	Dimethyl Sulfoxide solution
DSE	Depolarization-induced suppression excitation
DSI	Depolarization-induced suppression inhibition
EAE	Experimental Autoimmune Encephalomyelitis
EC	Endocannabinoid system
ECs	Endocannabinoids
ERK	Extracellular signal-regulated kinases

FAAH	Fatty acid amide hydrolase
GPR55	G-protein receptor 55
HLA	Human Leukocyte Antigen
HIOMT	Hydroxy-indole-O-methyltransferase
5-HTP	5-hydroxytryptophan
IFN-γ	gamma Interferon
IL	Inactive Lesion
I_{NCX}	NCX currents
LPS	Lipopolysaccharide
MAG	Myelin Associated Glycoprotein
MAPK	Mitogen-activated protein kinases
MAGL	Monoacyl Glycerol Lipase
MBP	Myelin Basic Protein
MEK	Mitogen-activated protein kinase kinases
MOG	Myelin Oligodendrocyte Glycoprotein
MRI	Magnetic Resonance Imaging
MS	Multiple Sclerosis
MT1	Melatonin receptor type 1
MT2	Melatonin receptor type 2
NAWM	Normal-Appearing White Matter
NAPE	N-acylphosphatidyl-ethanolamine
NAPE-PLD	N-acylphosphatidyl-phospholipase D
NAS	N-acetyl-serotonin
NCX	Na^+/Ca^{2+} exchanger
NCX3	Na^+/Ca^{2+} exchanger type 3
NMDA	N-Methyl-D-Aspartate
NO	Nitric oxide
OPCs	Oligodendrocyte precursor cells
OEA	Oleoylethanolamide
PEA	Palmitoylethanolamide
PD	Parkinson's disease
PDGF-AA	Platelet-derived growth factor-AA
PPAR	Peroxisome proliferator-activated receptors

P60	Postnatal day 60
PKA	Protein kinase A
PPMS	Primary Progressive Multiple Sclerosis
PLP	Proteolipid Protein
PNS	Peripheral Nervous System
SPMS	Secondary Progressive Multiple Sclerosis
QR2	Quinone reductase
RRMS	Relapsing-Remitting Multiple Sclerosis
ROS	Reactive oxygen species
RZR/ROR	Nuclear orphan receptors
RyR	Ryanodine Receptor
RL	Remyelinating Lesions
SPMS	Secondary Progressive Multiple Sclerosis
TBI	Traumatic Brain Injury
Wo	Washout
α_2-NKA	sodium/potassium-transporting ATPase subunit alpha-2.

Summary

Neurodegeneration, neuroinflammation, and failure of regenerative processes contribute to the pathogenesis of several neurodegenerative disorders including multiple sclerosis (MS). Indeed**,** MS treatment are primarily immunomodulatory, but no neuroprotective or remyelinating therapies are available to prevent the accumulation of neurological deficit and progression of the disease.

Currently, a significant effort is underway to develop molecules with the potential to halt the neurodegenerative and demyelination processes, modulate the microglia/macrophage response to neuroinflammation and stimulate myelin repair, particularly for the treatment of progressive MS forms, for which current therapies are relatively ineffective.

In the present research project, we investigated the neuroprotective and remyelinating potential of two distinct pharmacological treatments modulating ionic or lipid homeostasis and contributing to distinct signaling pathways important for oligodendrocyte differentiation and neuroprotection.

The Na^+/Ca^{2+} exchanger NCX3 is an important regulator of sodium and calcium homeostasis in oligodendrocyte lineage, and a recent work performed by our research group demonstrated that $[Ca^{2+}]_i$ transients mediated by NCX3 play an important role during oligodendrocyte differentiation and myelin formation. The observation that any change in NCX activity dynamically affect Na^+ and Ca^{2+} fluxes and that Na^+ and Ca^{2+} gradients tightly control the kinetics and directionality of NCX operation indicates that more studies are required to understand the pharmacological effects of selective NCX3 blockers in oligodendroglia and neuronal cells under demyelinating conditions. These studies are fundamental to develop and identify novel neurorepair strategies targeting NCX exchangers.

In the first part of the thesis, we investigated, by means of biochemical, morphological and functional analyses, the pharmacological effects of the NCX3 inhibitor, the 5–amino-N-butyl-2–(4–ethoxyphenoxy)-benzamide hydrochloride (BED), on NCXs expression and activity, as well as intracellular $[Na^+]_i$ and $[Ca^{2+}]_i$ levels, during treatment and following drug washout both in human MO3.13 oligodendrocytes and rat primary oligodendrocyte precursor cells (OPCs). BED exposure antagonized NCX activity, induced OPCs proliferation and $[Na^+]_i$ accumulation. By contrast, 2 days of BED washout after 4 days of treatment significantly upregulated low molecular weight NCX3 proteins, reversed NCX activity, and increased intracellular $[Ca^{2+}]_i$. This BED-free effect was accompanied by an upregulation of NCX3

expression in oligodendrocyte processes and accelerated expression of myelin markers in rat primary oligodendrocytes.

Collectively, these findings show that the pharmacological inhibition of the NCX3 exchanger with BED blocker maybe followed by a rebound increase in NCX3 expression and reversal activity that accelerate myelin sheet formation in oligodendrocytes. In addition, they indicate that a particular attention should be paid to the use of NCX inhibitors for possible rebound effects and suggest that further studies will be necessary to investigate whether selective pharmacological modulation of NCX3 exchanger may be exploited to benefit demyelination and remyelination in demyelinating diseases.

Another interesting attractive target for MS treatment is the endocannabinoid system (EC) which consists to a complex network of endocannabinoid ligands, cannabinoid receptors and enzymes responsible for synthesizing and degrading endocannabinoids (ECs). Enhancing endogenously-released cannabinoid ligands through the inhibition of the degrading fatty acid amide hydrolase (FAAH) enzyme in the brain may provide therapeutic effects more safely and effectively than administering drugs directly acting at the cannabinoid receptors. FAAH inhibition prevents the breakdown of anandamide (AEA), oleoylethanolamide (OEA) and palmitoylethanolamide (PEA), producing potentially therapeutic effects, some through cannabinoid receptors and some through peroxisome proliferator-activated receptors (PPAR). Currently, FAAH inhibitors are under clinical investigation for the treatment of Tourette Syndrome (NCT02134080), and chronic pain. Furthermore, a large number of studies highlight the beneficial role of melatonin in neuroinflammatory disorders. Melatonin, a neurohormone produced by the pineal gland, regulates the sleep wake-cycle and exerts potent antioxidant, anti-inflammatory, immunomodulatory, and neuroprotective effects. In experimental models of MS, melatonin prevented demyelination, axonal injury and stimulated OPCs differentiation and remyelination. It is currently used as dietary supplement for the short-term treatment of insomnia but its use has also been proposed as add-on therapy in several neuroinflammatory conditions.

In the second part of the thesis, we investigated the neuroprotective effects of a novel pharmacological compound, UCM-1341, a bivalent ligand with FAAH inhibitory activity and melatonin receptors agonism. To this aim, we set up models of excitoxic and neuroinflammatory damage in rat hippocampal explant cultures to study the time – and dose-dependent effects of compounds on cell death. Our expression studies showed that FAAH protein levels early increased in CA1 hippocampal neurons and astrocytes after the

neuroinflammatory insult. At later time points, the increased FAAH immunosignal persisted in astrocytes, but not in neurons, and emerged in microglia, particularly in that one surrounding damaged cells. By using an antibody recognizing melatonin receptors we found that MT1 levels persistently increased after the insult while MT2 proteins decreased after a transient upregulation.

Our neuroprotection studies showed that while the damage occurring in the CA1 and the less vulnerable CA3 region in slices exposed to NMDA concentrations was not greatly affected by UCM-1341, the bivalent ligand exerted a marked dose-dependent neuroprotection against LPS+IFN-γ-induced neuroinflammatory damage and attenuated axonal demyelination. More interestingly, we showed that cotreatment of slices with the reference compounds melatonin or URB-597 exerted a greater neuroprotection against LPS+IFN-γ exposure, if compared to single compounds applications. This effect was comparable to that observed with UCM-1341, thus indicating that the reference compounds exerted a synergistic neuroprotective actions against LPS+IFN-γ-induced inflammatory damage. Finally, by performing biochemical and quantitative colocalization analyses we showed that UCM-1341 had also protective effects on astrocyte and microglia cells and polarized microglia/macrophages to a foamy phenotype expressing the anti-inflammatory M2 marker CD206.

Collectively, our findings demonstrated that the combined modulation of EC and melatoninergic signaling exerted potent neuroprotective effects against the neuroinflammatory damage in hippocampal explant cultures. The modulation effects of UCM-1341 on microglia activities might contribute to the synergistic beneficial effects against the inflammatory injury. Nevertheless, further studies will be required to understand whether enhancing the EC and melatoninergic tone with UCM-1341 may represent a novel neuroprotective strategy to treat neuroinflammatory conditions.

I. INTRODUCTION

1. Multiple sclerosis

Originally described as "La Sclérose en Plaques" by Charcot in 1868, multiple sclerosis (MS) is one of the most common demyelinating disorder characterized by chronic inflammation, oligodendroglia and axonal degeneration in the white and grey matter of the brain and spinal cord (Charcot et al, 1868). MS is the primary cause of non-traumatic neurologic disability in young adults between age of 20 to 40 (Compston and Coles, 2008). Although the cause of MS pathogenesis remains unclear, a complex interaction between genetic and environmental factors lead to an immune response against self myelin antigens, causing local inflammation that results in demyelination, gliosis, and axonal degeneration. The area of myelin loss, called "plaques" or "lesions", is visible with magnetic resonance imaging (MRI) (Lucchinetti et al, 2000) and can differ among patients at different disease stages.

Myelin sheath allows electrical impulses to transmit quickly and efficiently along the nerve cells. If myelin is damaged, these impulses slow down, causing demyelinated areas. Nevertheless, when the axons are not irreversible damaged, demyelination may be followed by a spontaneous regenerative process, called *remyelination*, in which new myelin is restored to the axons and a proper axonal conduction and trophic support is re-established. (Franklin et al, 2008). This myelin repair process contributes to clinical recovery after a relapse in relapsing-remitting RRMS (Patrikios et al, 2006). As the disease progresses, the remyelination capacity of OPCs diminishes and chronically demyelinated axons became more vulnerable to degeneration. Neurodegeneration and failure of remyelination characterize the progressive MS forms, and contribute to the accumulation of neurological disability without clinical recovery (Correale et al, 2019). MS therapies are primarily immunomodulatory, and no neuroprotective or remyelinating MS treatments are yet available.

1.1 Epidemiology

The number of people with MS increased from 2.3 million in 2013 to 2.8 million in 2020. This highlights the many barriers and inequalities that people with MS face in accessing diagnosis, treatment and care (Atlas of MS, 2013). MS can develop at any time in life; the onset of the disease is typically observed in individuals aged from 20 to 40 years and widespread also amongst children. It is more prevalent in women than men, probably as consequence of the effects of the genetic and environmental exposures, gonadal hormones, and lifestyle (Greer et al, 2011). The prevalence and incidence of MS increases at higher

latitudes mainly in North Americans and Caucasians of Northern European ancestry. Thus, MS is more common in areas farthest from the equator but this is not a general rule since the prevalence may differ significantly among ethnic groups previously migrated and living in the same geographic area regardless of distance from the equator (Atlas of MS, 2013). MS is not classified as a hereditary disease; indeed, it is not genetically transmitted. Epidemiological studies have shown that members of the same family have an approximately 3-5% risk of developing the disease. The first identified mutations that impact MS susceptibility were specific human leukocyte antigen (HLA) variants within the major histocompatibility complex (MHC) gene complex, outlining the important role of the immune system for MS development. However, like other autoimmune diseases, MS is a complex genetic disorder following a polygenic etiology and a multitude of MS-associated genes outside the MHC locus were identified during large genome-wide association studies (Gourraud, et al 2012)

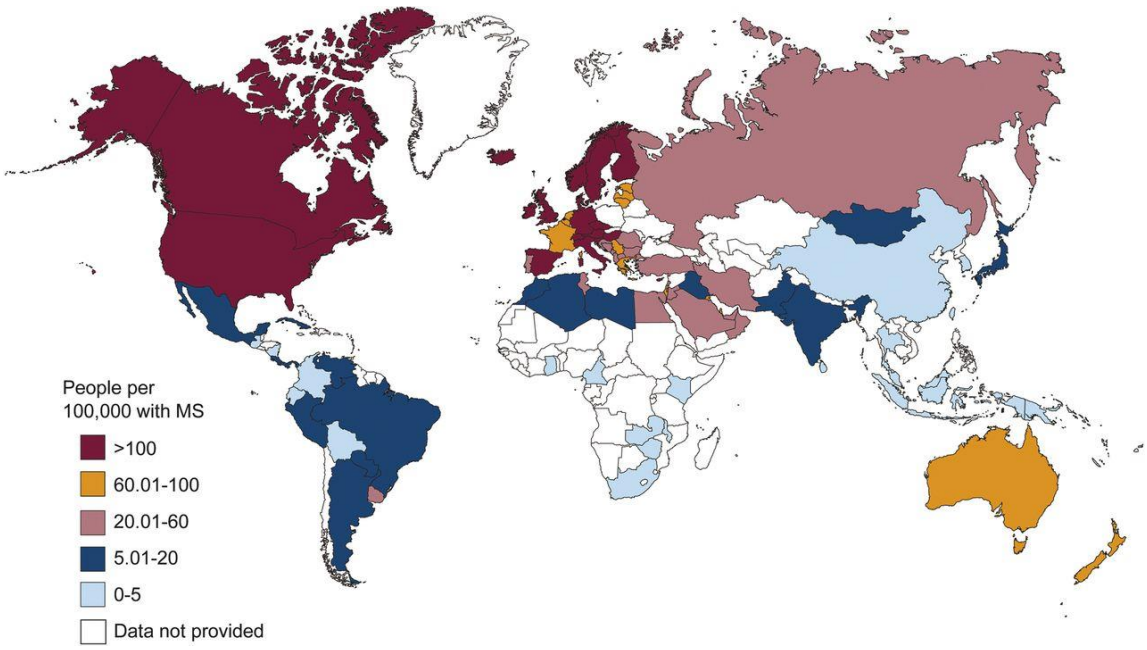

Figure 1. Prevalence of MS estimated in the world from *Atlas of MS, 2013*.

1.2 Etiology

Studies support the opinion that MS is caused by early exposure to some environmental trigger in genetically susceptible individuals (Compston and Coles, 2008). Epstein-Barr virus (EBV) infection, smoking, and low vitamin D levels are the environmental factors that have shown the strongest and most consistent association with the disease development. Low vitamin D levels are also associated with higher disease activity. Other risk factors include obesity and high salt intake. The role of EBV in the pathogenesis and MS progression has been related to the promotion of both autoimmune B- and T-cell responses, and epigenetic changes. The free radicals in the cigarette can also play a role in the pathogenesis and development of the disease by affecting the DNA and the neuronal structure. These findings suggest a complex relationship between environmental and genetic factors in determining who develops MS.

1.3 Pathological mechanisms

Several pathological mechanisms have been proposed over time. Blood–brain barrier (BBB) dysfunction during MS can lead to ion dysregulation, altered signalling homeostasis, as well as entry of immune cells and molecules into the CNS. The first pathogenic event of MS is the inflammatory response that start with the break of the immunological tolerance in the peripheral blood, and the increase of autoreactive lymphocytes that, after crossing the BBB recognizes and attacks self-components of myelin. T cells, B cells and antigen-presenting cells (APCs), including macrophages, infiltrate the CNS, and mediate a cascade of events such as the release of cytokines, chemokines, and antibodies against myelin antigens, thus amplifying the inflammatory response leading to tissue damage. Lymphocytes expressing molecules on their surface such as the integrin α4 β1 (VLA-4), binds the VCAM-1 present on the brain vascular endothelium and cross the BBB. Inside the brain, T cells, macrophages and resident microglia operate in synergy to release pro-inflammatory cytokines, such as interleukin-23 (IL-23), IFN-γ and tumour-necrosis factor-α (TNF–α). In parallel, B cells (plasma cells) produce myelin specific antibodies, which interact with the terminal complex in the complement cascade to produce membrane-attack complexes that further damage oligodendroglial cells leading to myelin sheath injury and, consequently, to neuronal and axonal degeneration (Goverman et al, 2011)

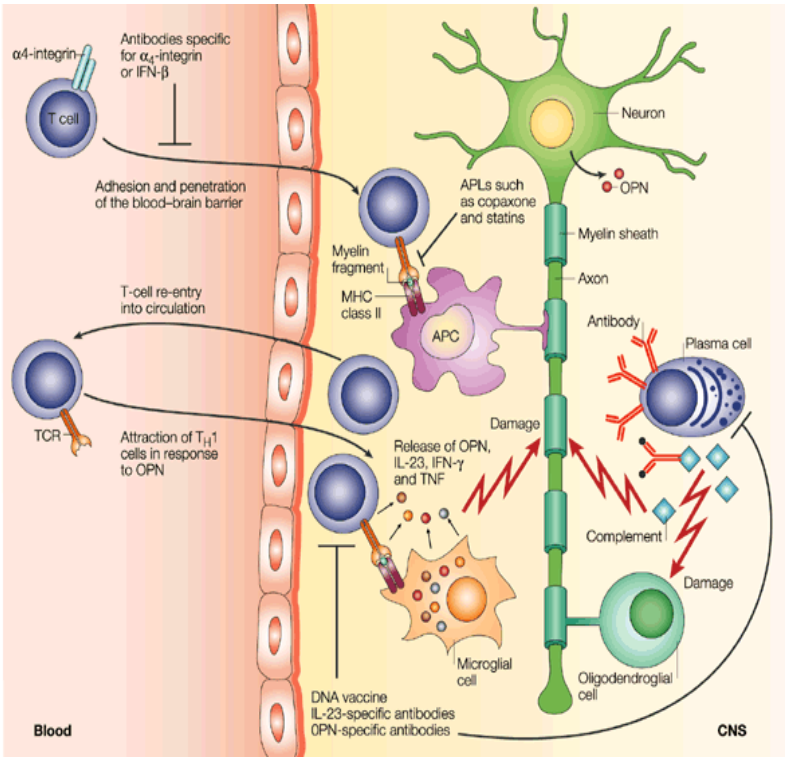

Figure 2. The auto-immune mediated pathophysiological mechanism in MS. T cells, B cells and antigen-presenting cells (APCs), including macrophages, enter the CNS and attacks oligodendrocytes, the myelin forming cells from Steinman and Zamvil, 2003, *Nature reviews immunology*.

1.4 MS hallmarks

The main pathological hallmark of MS is the formation of lesions or plaques visible with MRI. These lesions are not restricted to the white matter, but are also abundant in the grey matter of the cortex, the deep brain stem nuclei and the spinal cord (Lassman et al, 2001). Plaques are the result of a complex myelin damage characterized by demyelination, inflammation, axonal damage, oligodendrocyte loss and astrogliosis. Remyelinated shadow plaques may be also observed, but when axons are severely injured, remyelination fails (Compston and Coles, 2008).

Demyelination is the pathological process in which myelin sheaths are lost from around axons. The acute loss of a myelin internode is associated with conduction block, and chronically, can be compensated by Na^+ channels redistribution along the denuded axolemma, allowing the non saltatory conduction along the demyelinated segments. **Inflammation** is the mechanism by which immune and CNS-resident cells secrete a range of inflammatory mediators that lead to neuronal demyelination and, eventually, damage.

Astrogliosis is characterized by proliferative astrocytes in the focal area of damage, accompanied by an increased synthesis of GFAP protein.When the axons are still active, myelin damage can be restored by a remyelination processes activated by oligodendrocyte precursors (Kornek et al, 1999). During MS relapses, myelin is restored. After continuous event of relapses, ongoing inflammation contribute to the propagation of the **axonal injury**, as occur in primary-progressive (PPMS) or secondary-progressive MS (SPMS) patients.

1.5 Heterogeneity of lesions

MS lesions are classified as active, chronic active, inactive lesions and remyelinating, according to the presence/absence and distribution of macrophages/microglia (inflammatory activity) and the presence/absence of ongoing demyelination (demyelinating activity). Lesions are usually placed in the periventricular area, cerebellum and brain stem, but also in cervical and/or thoracic spinal cord (Trapp et al, 1998; Lassman et al, 1998; Lucchinetti et al, 2000; Bo et al, 2003; Kuhlmann et al, 2017).

Active lesions. They are the initial phenotype of MS lesions, in general found in relapsing-remitting patients or at early disease stages, but also detected in MS patients with SPMS. They are hypercellular and characterized by myelin loss and a dense infiltration of monocytes/macrophages or microglia with a foamy morphology. T cells are localized both perivascularly and diffusely throughout the lesion area, but lower in number if compared to microglia/macrophages. Astrogliosis with increased GFAP expression is a hallmark of the active lesion. Active lesions can be further separated into lesions with ongoing myelin destruction (demyelinating lesions) and lesions in which the destruction of myelin has ceased, but macrophages are still present (post-demyelinating lesions). This distinction is based on the presence or absence of myelin degradation products within the cytoplasm of macrophages/microglia.

Mixed active/inactive lesions or chronic active lesions. They are demyelinated and characterized by a hypocellular lesion core and a rim of activated microglia/macrophages at the lesion border. The center of these lesions is almost completely depleted of macrophages/microglia. Interestingly, only in these lesions are found hypertrophied astrocytes, while moderate T-cell infiltrates are present perivascularly or distributed diffusely throughout the lesion center (Frischer et al, 2015).

Inactive lesions. They are sharply demarcated, hypocellular, and almost completely depleted of mature oligodendrocytes. Only few T cells are present within the lesion and the density of

microglia is strongly reduced, if compared to the normal appearing white matter (NAWM) (Hametner et al, 2013). In these lesions it is evident the axonal swelling and damage. The lesion border is devoid of macrophage/microglia but astrocytes form a gliotic scar. Typically, these lesions are observed in patients with disease more than 15 years and/or secondary progressive MS without attacks.

Remyelinating lesions. MS lesions can be either partly or completely remyelinated but not exclusively located at the lesion border, and remyelinated axons can be identified by MBP staining of thinner myelin sheaths and by pale staining intensity of Luxol fast blue staining. Approximately 20% of the lesions display extensive remyelination and are so-called shadow plaques (Patrikios et al, 2006; Goldschmidt et al, 2009). Remyelination may occurs also in active and demyelinating lesions and may differ among lesions.

Outside the focal MS lesions diffuse white matter changes and microglia activation have been observed in the NAWM at some distance from a lesion or within the periplaque white matter (PPWM) directly adjacent to the lesion.

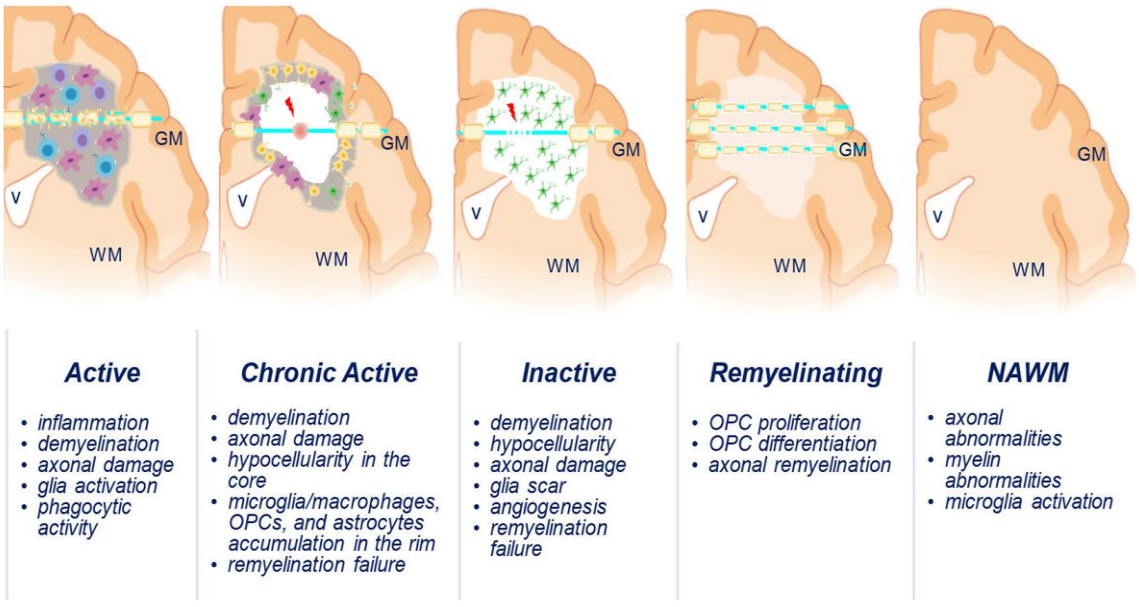

Figure 3. Schematic representation of active (AL), chronic active (CA), inactive (IL), and remyelinating (RL) lesions, and normal-appearing white matter (NAWM) and corresponding lesions features. Boscia et al, 2021, *Frontiers in Cellular Neuroscience*

1.6 Clinical course and main symptoms

The first attack of the disease is named clinically isolated syndrome (CIS), but according to the MS diagnostic criteria, the diagnosis of MS can be done when CIS is accompanied by MRI findings (old lesions or scars) that confirm that an earlier episode of damage occurred in a different location in the CNS. In 2017, the International Panel on Diagnosis of Multiple Sclerosis revised the McDonald 2010 criteria for the diagnosis of MS. Importantly, the 2017 revisions have elevated the role of CSF-specific oligoclonal band (OCB) and enhanced the value of imaging findings by including cortical lesions and symptomatica lesions and more specific MRI lesion criteria (Thompson et al, 2018).

MS phenotypes can be categorized as relapsing-remitting (RR-MS), primary progressive (PPMS) and secondary progressive (SPMS). Evidence of disease activity and clinical progression, which reflects an ongoing inflammatory or neurodegenerative processes, may impact prognosis, therapeutic decisions, and outcomes.

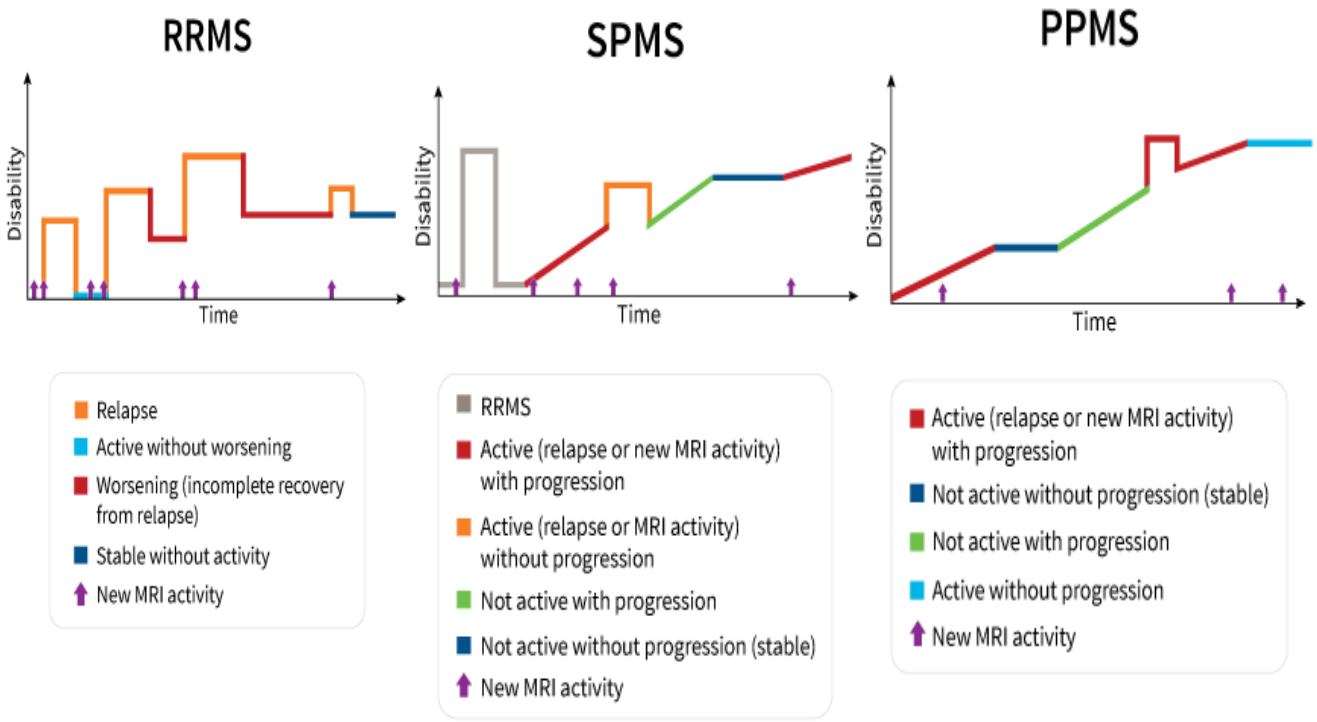

Figure 4. Clinical course of multiple sclerosis according to Lublin et al, 2014, *Neurology*

RRMS forms can be further classified as active (with relapse or evidence of new MRI activity over a specified period of time) or not active, as well as worsening (with a confirmed increase in disability following a relapse) or not worsening. The accumulation of neurological signs and symptoms may evolve years later into SPMS, distinguished into two new groups according to the presence or not of signs of disability progression (Lublin et al, 2014). Up to 15% of MS patients develop directly PPMS disease after the clinical onset. PPMS forms are characterized by a gradual worsening of disability from the onset of symptoms, without early relapses or remissions, although patients may experience occasional plateaus in the disease course. PPMS can be further characterized as either active or not active, as well as with progression or without progression. (Thompson et al, 2017). The most frequent symptoms are fatigue and difficulty of walking. Damaged nerve communication can lead to weakness, tremor, and spasticity (involuntary tightness). Some patients present vision problems (i.e. diplopia) related to unclear vision and pain on ocular movement. Patients also experience neurological disorders such as speech disorders, dizziness, tremor, cognitive deficits leading to memory and in problem- solving skills impairment, lost in attention and altered perception of environment, acute or chronic pain. The most common MS-associated CNS conditions include pain in the lower extremities, paroxysmal pain, which is divided into Lhermitte's phenomenon and trigeminal neuralgia, as well as thermal and mechanical sensory abnormalities (Kanchandani et al, 1982)

1.7 Diagnosis

The diagnosis of MS is based on a combination of clinical findings, neuroimaging, and laboratory data, that show the dissemination in space and time, referred to the presence of lesions in different CNS anatomical locations such as infratentorial, juxtacortical, cortical, periventricular, and spinal cord. The physicians use some criteria to diagnose MS (Figure 5):

1) the finding of at least two separated damaged areas in the CNS, including brain, spinal cord and optic nerve;

2) the evidence that the damage occurred during the course of time;

3) the exclusion of other neurological diseases causing similar neurological symptoms. The *MRI* is the most sensitive diagnostic test for MS. Lesions, depicted as "patchy" or multifocal areas in the white matter, can be efficiently observed by using T2-weighted MRI images. According to the 2010 McDonald criteria, the disease dissemination in time (DTI) can be evaluated by the presence of at least one new T2-weighted or gadolinium enhancing lesion on the next follow-up MRI or the simultaneous presence of asymptomatic gadolinium-enhanced

and non-enhanced lesions at any time (Filippi et al, 2016). The chemical compound gadolinium, also known as "contrast", is injected in patients to evaluate the presence of active lesions. In fact, gadolinium normally does not pass through the BBB but, in some pathologies, such as MS, in which the BBB is disrupted, the gadolinium enters in the brain and spinal cord, allowing the visualization of MS lesions lighting them up on MRI scans as brighter spots. MRI is commonly considered an easy and not invasive exam to acclaim the appearance and evolution of plaques, although in some patients is required more in depth analysis of the clinical picture obtained by analysis of cerebrospinal fluid (CSF) and neurophysiological tests. The *lumbar puncture*, also known as spinal tap, is an invasive test used to evaluate the content of cells and molecules in the CSF used to exclude other diseases in the differential diagnosis of MS. Most patients affected by MS present abnormal results in this test (Stangel et al, 2013). In the CSF of MS patients are commonly found elevated levels of IgG antibodies, as well as specific proteins called oligoclonal bands, and sometimes certain products of the breakdown of myelin (McDonald et al, 2001, Link et al, 2006). The presence of all these markers suggest an abnormal response mediated by immune system against self-component of the myelin.

The *evoked potential (EP)* test can reveal damaged areas in the brain, spinal cord and in the optic nerve that other tests, i.e. the neurological test, may not detect. The EP test measures the electrical activity of the brain in response to the stimulation of specific sensory nerve pathways. Specific types of sensory input are sounds, light or sensations. The decrease in electrical fiber conduction relies to the demyelinating event in course. Since the diagnosis of MS requires evidence of demyelination in two distinct areas of the CNS, EP test could be useful to recognize a second demyelinating event that remains undiagnosed with other tests.

	Number of Lesions With Objective Clinical Evidence	Additional Data Needed for a Diagnosis of MS
≥ 2 clinical attacks	≥ 2	None (but MRI recommended)
≥ 2 clinical attacks	1 (as well as clear-cut historical evidence of a previous attack involving a lesion in a distinct anatomical location†)	None (but MRI recommended)
≥ 2 clinical attacks	1	Dissemination in space demonstrated by an additional clinical attack implicating a different CNS site or by MRI
1 clinical attack	≥ 2	Dissemination in time demonstrated by an additional clinical attack or by MRI OR demonstration of CSF-specific oligoclonal bands
1 clinical attack	1	Dissemination in space demonstrated by an additional clinical attack implicating a different CNS site or by MRI AND Dissemination in time demonstrated by an additional clinical attack or by MRI OR demonstration of CSF-specific oligoclonal bands

Figure 5. Criteria for Diagnosis of Multiple Sclerosis. Thompon et al, 2018, *The Lancet*

2. The myelin-forming cells: oligodendrocytes

The main target of the aberrant autoimmune attacks in MS are the oligodendrocytes. The term *oligodendroglia* was introduced by Rio Hortega to describe those non-neuronal cells that show few processes also known with the term "neuroglia" or "glia" (Rio Hortega DP Histogenesis). Glial cells are found in the CNS and PNS, are smaller than neurons but are greater in number and are not provided with axons and dendrites. He distinguished macroglial cells astrocytes, oligodendrocytes and ependymal cells to "microglia", which are the immune sentinels in the brain, capable of orchestrating a potent inflammatory response. Early research viewed glial cells as the "glue" which support nervous system functions. In more recent years, the presence of numerous receptors and neurotransmitters in glia suggested a complex glial-neuronal network, providing not only functional support, but also having a role during development or recovery from neural injury and during modulation of synaptic action and propagation of nerve signals.

Oligodendrocytes (from G*reek:* cells with few branches) described by Virchow in the 19th century are the myelinating cells of the CNS, generated from oligodendrocyte progenitor cells (OPCs). The latter are progenitors for myelinating oligodendrocytes expressing the proteoglycan neuron-glial antigen 2 (NG2), providing a source of new oligodendrocyte, protoplasmic astrocytes, and neurons (Annunziato et al, 2013; Boscia et al, 2016). OPCs generate new oligodendrocytes migrating into developing white matter from their germinal zones, and, thanks to the high migratory capacity, they can populate the brain and spinal cord generating mature oligodendrocytes (OLs) myelinating the entire CNS during the postnatal period. A small percentage (5-9%) of OPCs generated during development and distributed in all brain regions are maintained in a slowly proliferating 'quiescent' stage up to adulthood (Dawson et al, 2003). These adult OPCs are capable of self-renewal, differentiation, and remyelination after CNS injury (Fernandez-Castaneda et al, 2016). Oligodendrocytes and axons have a reciprocal signaling relationship in which oligodendrocytes receive cues from axons that direct their myelination and oligodendrocytes subsequently shape axonal structure and conduction, partly controlled by neurotransmitters (Karadottir el al, 2007). OPCs are proliferative, but extrinsic factors, as neuronal activity may control and promote oligodendrocyte development (Barres et al, 1999; Bergles et al, 2015). They also display a homeostatic role in buffering extracellular potassium during neuronal activity (Menichella et al, 2006) and release neuroptrophins, such as glial- and brain-derived neurotrophic factors (GDNF and BDNF) which supports the axonal functionality and outgrowth, and preserve

neuronal circuitries (Du and Dreyfus, 2002; Wilkins et al, 2003). Oligodendrocyte diversity is well appreciated by the specific expression patterns of antigenic markers. Recently, a single-cell RNA sequencing study analyzed the transcriptome of oligodendrocyte isolated from 10 different regions of the antero-posterior and dorsal-ventral axis in the CNS of young and adult mice. These experiments led to the identification of 12 different subpopulations, distributed at different stages of maturation from OPCs to myelinating oligodendrocytes (Marques et al, 2016). The different oligodendrocyte populations may have distinct functions within the brain (Foerster et al, 2019). Further studies identified two functionally distinct populations of OPCs in the zebrafish spinal cord. One subset, retained near neuronal somas and dendrites, elaborate process networks and to exhibit remarkably high calcium activity, being apparently involved in the modulation of neuronal transmission. These cells rarely differentiate into mature oligodendrocyte but retain the capacity to divide in an activity- and calcium-dependent manner, producing a second OPCs subpopulation characterized by higher motility, capable of migrating toward axon-rich regions and differentiate into myelinating oligodendrocytes (Marisca et al, 2020).

Myelinating oligodendrocytes may contact up to 40 segments in the CNS (Peters et al, 1991), and the number of processes that form myelin sheaths from a single oligodendrocyte varies according to the CNS region and, possibly, the species. Myelinating oligodendrocytes communicate lifelong with axons, and are required for the long-term integrity and survival of axons. *Satellite oligodendrocytes* are ubiquitously found throughout the cortex and hippocampus in rodents and humans; its mainly role is the regulation ionic homeostasis and the microenvironment around neurons (Baumann et al, 2001).

2.1 Oligodendrocyte differentiation stages

The maturation of OPCs requires a series of intermediate stages as proliferation, migration, differentiation, and myelination that lead mature myelinating oligodendrocytes to finally generate the insulating sheath. (Emery et al, 2010; Barateiro et al, 2014; Elbaz et al, 2019).

Oligodendrocyte precursor cells (OPCs), are proliferative cells characterized by a great migratory capacity. At this stage OPCs express the platelet-derived growth factor receptor α (PDGF-Rα), the ganglioside A2B5, and the proteoglycan NG2 (Pringle et al, 1992; Nishiyama et al, 1996). OPCs cells have a bipolar or stellate morphology, with only few processes that are short in length and emanate from the opposing poles of the cell body. After this step of differentiation OPCs give rise to ***preoligodendrocytes*** *(or late OPC),* that extend multipolar

short processes and express markers such as the sulfatide O4 (Sommer et al, 1981) and the GPR17 protein (Boda et al, 2011) which persist until the immature oligodendrocytes stage.

The immature or pre-myelinating oligodendrocytes continue to express the O4 and begin to express the galactocerebroside C (Yu et al, 1994). They become post-mitotic cells with long ramified branches and are committed to the oligodendroglial lineage (Armstrong et al, 1992; Gard et al, 1989).

In the final stage, ***the mature myelinating oligodendrocytes (OLG)*** extend membranes that form compact enwrapping sheaths around the axons and express, in an orderly manner, myelin proteins e.g. myelin basic protein (MBP), proteolipid protein (PLP), myelin associated glycoprotein (MAG), and finally myelin oligodendrocyte glycoprotein (MOG) (Reynolds et al, 1988; Scolding et al, 1989; Zhang, 2001).

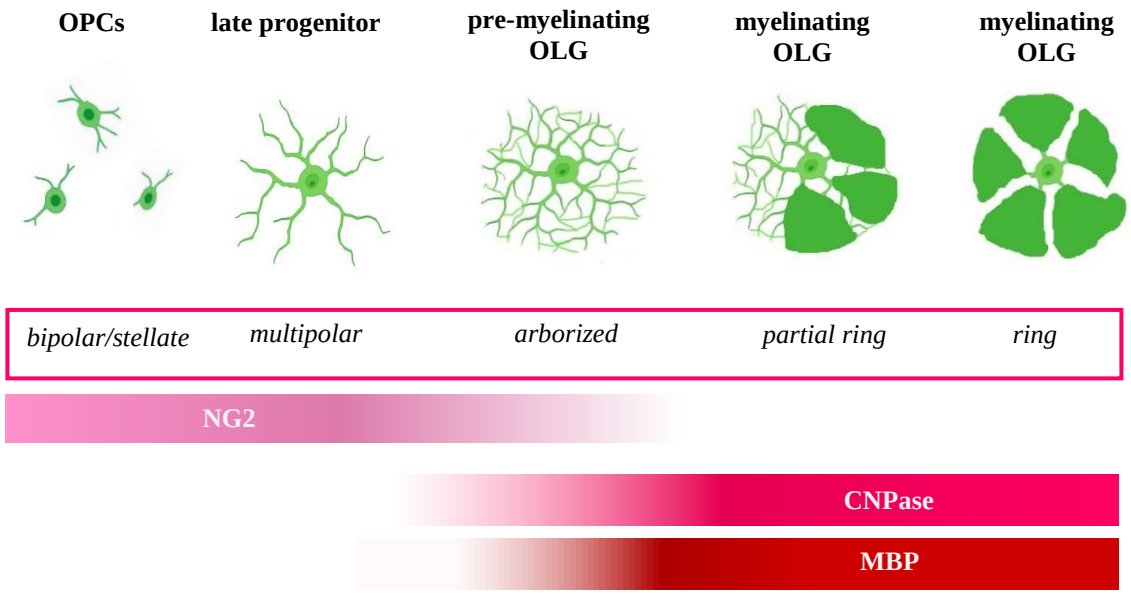

Figure 6. Schematic drawing of the oligodendrocyte lineage cells. Adapted from Cammarota et al, 2021, *Biomedicine and Pharmacotherapy.*

2.2. Myelin composition

The term *myelin* was coined by the german pathologist Rudolf Ludwig Virchow in (1821–1902). Myelin is critical for the function of the nervous system and represents one of the most complex cell–cell interactions of the body. Myelin is a specialized multilamellar membrane, characterized by a high proportion of lipids and low protein, tightly wrapped around nerve fibers produced by oligodendrocyte and Schwann cells, respectively in the CNS and PNS. Normal conduction of nerve impulses depends on the insulating properties of the myelin sheath surrounding the axon. Not all axons are covered with myelin, indeed, they can be either myelinated or unmyelinated and it is myelin's chemical composition of mainly lipids that gives the white matter its characteristic color. Nevertheless, myelinated axons are also present in the grey matter, where large fraction of myelin enwraps the axons of parvalbumin-positive fast-spiking interneurons (Benamer et al, 2020). When myelin sheath wraps the nerve fibers, accelerates the propagation of electrical impulses along axons. During saltatory conduction, action potentials jump across internodes, specialized gaps in the myelin sheath called node of *Ranvier*, where the axon is uncovered and sodium channels are clustered (Baumann et al, 2001; Jessen et al, 2004; Freeman et al, 2016; Cohen et al, 2020). The speed of impulse conduction, is determined by the high specificity of myelin that cause a decrease in capacitance accompanied with increase in electrical resistance across the axolemma. Myelin permits rapid and efficient signal transmission for long distances, and increases the nervous system's information processing capacity. *Myelination* or *myelinogenesis* develops postanatally. It begins after birth, reaching a pick at P20 and being almost concluded at P60 (Baumann et al, 2001; Vincze et al, 2008) while in humans, the myelinating process begins early in the 3rd trimester proceeding after birth through the early adult life. The threshold for axon diameter myelination ranges is from 0.2 μm in CNS to 1 μm in the PNS (Waxman et al, 1972; Voyvodic et al, 1989). Formation of myelin is a complex process, which requires energy to synthetize all lipids membrane and other proteins components by oligodendrocytes. Incorrectly formed myelin can result in severe disturbances of motor and sensory functions.

Myelin is a poorly hydrated structure containing 40% water, 70-85% of lipids and 15-30% of proteins. This lipid-to-protein ratio is very peculiar to the myelin membrane. The *cholesterol* is a critical lipid component for myelin membrane growth (Saher et al, 2005) and synthesis. The *galactolipids*, mostly represented by galactosylceramides (GalC) and its sulfated derivative sulfatide, represent 20% of lipid dry weight. Galactosylceramides contribute to myelin formation and stability, though they are not essential for myelin synthesis. Myelin also

contains minor galactolipids (3% of total galactose) such as fatty esters of cerebroside, acylgalactosylceramides, and galactosyldiglycerides and phospholipids, such as *phosphatidylcholines.*

Proteins and glycoproteins constitute 30% of the total protein and about 10% of the dry weight of myelin.

The *proteolipid proteins (PLP)* is a hydrophobic protein that accounts for about 50% of the protein content of adult CNS myelin. It is a structural component of myelin, providing stability and maintaining the compact lamellar structure. In humans, point mutations in PLP are the cause of Pelizaeus–Merzbacher disease (PMD), a neurologic disorder of myelin metabolism (Osorio et al, 2018)

The myelin basic protein (MBP) is the second most abundant protein of myelin, which has been referred to as the "executive molecule of myelin" (Boggs, 2006), being essential for oligodendrocyte homeostasis and myelin formation. Mbp mRNA is transported from the nucleus to the plasma membrane and is translated locally at the axon–glial contact site. MBP acts as a linker and scaffolding protein (Eylar et al, 1971), and post-translational modifications of MBP, including acetylation, phosphorylation, and methylation play an important role for compaction of myelin membranes. The lack of functional MBP in the Shiverer (*shi*) mice results in a severe hypomyelinated CNS phenotype demonstrating its importance for myelin synthesis (Readhead et al, 1990). In addition to structural tasks, MBP has the ability to bind signaling molecules such as Fyn kinase which is important for morphological differentiation and myelination, and MBP binding to the plasma membrane modulates voltage-operated Ca^{2+} channels, thereby affecting Ca^{2+} responses in the cell (Smith et al, 2011).

The enzyme *2',3'-cyclic nucleotide 3'-phosphodiesterase or CNPase* is the third most abundant myelin protein, representing 4% of CNS myelin proteins. CNPase is encoded by a single gene that consists of four exons and two promoters, giving rise to two RNA transcripts, one of which will generate two isoforms of CNPase of 46 kDa, and 48 kDa. CNPase is able to catalyzes the hydrolysis of 2',3'-cyclic nucleotides to produce 2'-nucleotides in vitro, but the physiologically substrate in vivo is still unclear. It is considered a marker for myelin-forming cells, because is the earliest myelination-specific protein expressed by oligodendrocytes and is expressed in both myelinating and nonmyelinating oligodendrocytes and schwann cells. CNPase is both membrane bound and linked to microtubules, but it has also been observed associated with mitochondria. The role of this enzyme is not yet clear, although over

expression mutations suggest that CNPase plays a role in myelin compaction (Sprinkle et al, 1989; Cammarota et al, 2021)

Myelin-associated glycoprotein (MAG) represents 1% of the total protein found in CNS myelin and the 0.1% in the PNS. MAG plays an important role in the axon-myelin interactions by functioning as recognition molecule (Pfeiffer et al, 1993) helping oligodendrocyte to recognize myelinated from unmyelinated axons (Li et al, 1994; Montag et al, 1994). MAG knockout mice display a normal myelination process, while exhibiting subtle periaxonal structural abnormalities and develops a dying-back oligodendropathy which affects both myelin and axons (Lassmann et al, 1997; Siegel et al, 1999)

Myelin Oligodendrocyte Glycoprotein (MOG) was later identified as a minor glycoprotein specific for CNS myelin. MOG protein is mostly located on the outermost lamellae of compact myelin sheaths in the CNS. It is a surface marker of oligodendrocyte maturation and unique CNS component able to induce an antibody-mediated response and a T-cell mediated immune reaction in the animal model for MS, the experimental autoimmune encephalomyelitis (EAE) (Linington et al, 1988).

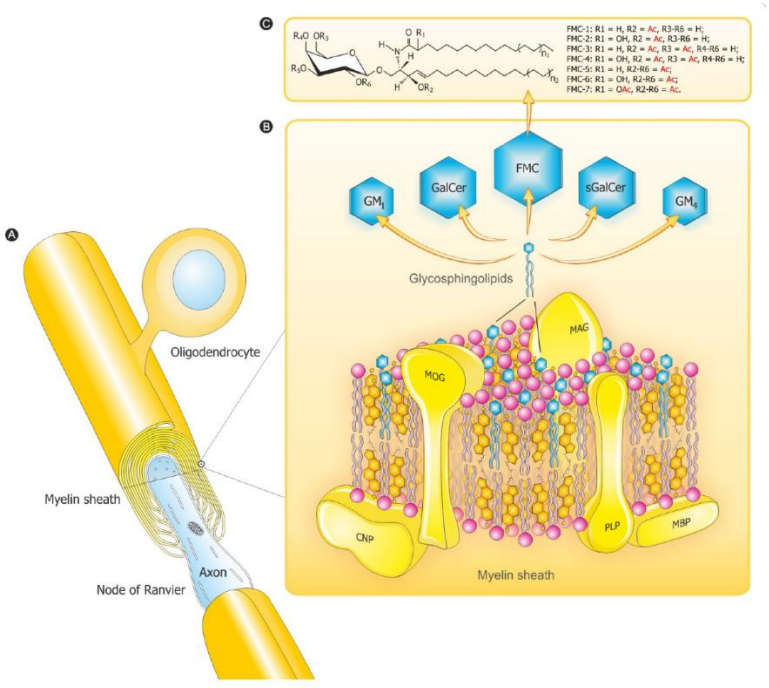

Figure 7. Structural features of CNS myelin. (A) Architecture; (B) 3D-molecular composition and conformation-based assembly and (C) sphingosine 3-*O*-acetylated galactosylceramide series from Podbielska et al, 2013, *Brain Sciences.*

3. Myelination and remyelination

The wrapping of myelin around axons requires specific lipid-protein interactions that lead to the formation of the dense and intraperiodic lines of myelin. The myelination process is a multistep process including: *migration of OPC and proliferation*; *adhesion of OPC to the axon; wrapping around the axon*; *compaction.* First *OPC migrates* adjacent to the axons to myelinate, while maintaining mitotic divisions. Next, the expression of immature oligodendrocyte markers and adhesion proteins such as integrins and laminins mediate the *adhesion of OPCs* to the axon. Oligodendrocytes start to form the myelin sheath by spiral *wrapping*, that finally undergo to *compaction* phase (Baumann et al, 2001). Myelination is a unique cellular process that induces oligodendrocytes to changes their morphology by promoting a reorganization of the actin cytoskeleton (Novak et al, 2011), and also have a dramatic impact on the structure and physiology of the axon (Snaidero et al, 2014). The variation in myelin thickness or internodal length influences the timing of conduction velocity in neurons, and two structural myelin parameters define the rate of axonal transduction: a) the *g-ratio*, corresponding to the diameter of the myelin sheath compared to the wrapped axon, and b) the *internode segments* corresponding the length and spacing of adjacent myelin sheath segments (Wu et al, 2012a).

The ratio of the inner axonal diameter to the total outer diameter (g-ratio) is used as a structural index of optimal axonal myelination (Das et al, 2011). Based on the speed of fiber conduction, the optimal g-ratio value for CNS is approximately 0.77, while in the PNS is approximately 0.6 (Chomiak et al, 2009)

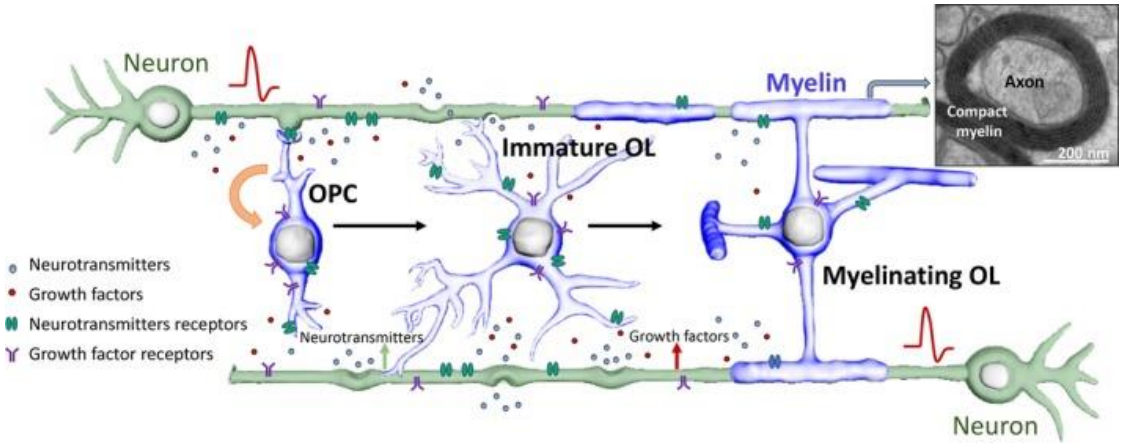

Figure 8. Schematic showing oligodendroglial lineage development and de novo myelination. During development subventriculat cells in the CNS (brain and spinal cord) give rise to committed oligodendrocyte precursor cells (OPCs), which can proliferate and or then terminally differentiate into post-mitotic immature oligodendrocytes (OL). In response to the appropriate extracellular cues, these immature OL can further mature and become myelinating oligodendrocytes, ensheathing receptive axons and forming compact myelin. Action potential firing by active neurons results in the release of neurotransmitters (such as glutamate, GABA, ATP or acetylcholine) and or growth factors (such as platelet-derived growth factor, brain-derived neurotrophic factor or neuregulin) via synaptic and non-synaptic mechanisms, and exert multifaceted influence upon both oligodendroglial lineage development and axonal ensheathment. This process is regulated not only at the level of oligodendroglial proliferation and differentiation but also at the level of individual axons. Faria et al, 2018, *Journal of Neurochemistry*

3.1 Innate and adaptive myelination

CNS myelination has an intrinsic and adaptive phase. The intrinsic myelination phase occurs around birth and in early childhood, it is an innate program of myelin development that proceeds independent of nervous system activity. Adaptive myelination occurs according to the need of a neuronal network, it is modified by experience and lead to an inter-individual variability in myelination throughout the brain regions. While an innate program of oligodendrocyte differentiation occurs in isolated culture settings, physiologic oligodendrocyte lineage dynamics and myelination are subject to extrinsic regulation. Recent studies demonstrated that neuron and glia communication is likely to be important to shape myelination according to the need of the neuron and its network. Ca^{2+} elevation appears to be a common response to glutamate receptor agonists in OPCs and oligodendrocytes. Indeed, glutamate is released from myelinated axons after action potentials by a rise in Ca^{2+} levels mediated by GluN2D and GluN3A-containing NMDA receptors (Burzomato et al, 2010; Micu et al, 2016). OPCs are able to respond to neuronal activity (Sontheimer et al, 1989; Barres et al, 1990; Wyllie et al, 1991; Borges et al, 1994; Holzwarth et al, 1994; Patneau et al, 1994; Ber-ger, 1995, Liu et al, 1995). Also the AMPA receptors have been proposed to play an important role in oligodendrocyte development. Recently, AMPA receptor has been detected at synapse connecting OPCs to neuronal axons of both white (Kukley et al, 2007; Ziskin et al, 2007) and grey matter (Bergles et al, 2000). Unmyelinated axons extent glutamatergic synapses to near OPCs which activate in return through binding on their AMPA/kainate (KA) receptors. As major effect, the OPCs stop to proliferate and initiate the maturation program towards the mature myelinating oligodendrocytes which extent their processes to wrap the axon and enrolling it with the concentric myelin sheaths (Kukley et al, 2007, Ziskin et al, 2007). The number of AMPA receptors at synapses is reduced when OPCs differentiate into

mature oligodendrocytes (De Biase et al, 2010; Kukley et al, 2010). In mature myelinating oligodendrocytes the expression of AMPA receptors is lower and mainly confined at the soma (Salter et al, 2005; Káradóttir et al, 2007). There is evidence that the initial induction of myelin synthesis may be regulated and driven within OPC processes by vesicular glutamate release (Wake et al, 2011). It is now clear that the neuronal function drive proliferation of OPC, oligodendrogenesis and myelination of axons.

3.2 Demyelination and remyelination

Remyelination is a spontaneous process in which myelin sheaths reinvest demyelinated axons, restoring saltatory conduction and resolving functional deficits after a demyelinating insult (Smith et al, 1979; Jeffery et al, 1999; Liebetanz et al, 2006). The remyelination process is sustained by a population of adult CNS stem/precursor cells, referred to as adult OPCs. In the brain, adult OPCs constitutes 3% of total cells in the gray matter and 9% in white matter (Nishiyama et al, 2001). After the insurgence of demyelinating injury, local OPCs rapidly pass by a "quiescent" to a regenerative phenotype. The rapid OPCs proliferative response has been observed in presence of acute injury-activated microglia and astrocytes, that are believed important for boosting OPCs to differentiate into remyelinating oligodendrocytes (Glezer et al, 2006; Rhodes et al, 2006). To establish contact with the axon that will be remyelinated, OPCs express myelin genes, generating a myelin membrane, and finally wraps and compact the membranes to form the sheath around the axon. After multiple demyelination insults and in the progressive MS stage, remyelination fails (Franklin et al, 2008). Enhancing the remyelination process is therefore an important therapeutic goal, that may be combined with current immunomodulatory therapy, able to prevent the immune attack against self-myelin components (Rodgers et al, 2013).

4. Axonal pathology and neurodegeneration in MS

MRI and neuropathology studies show that the axonal pathology in MS start with the onset of disease and axonal degeneration is responsible for persistent neurological impairment (Friese et al, 2014). Functional decline in MS patients can be observed also in the absence of inflammation, suggesting that complex and dynamic mechanisms contribute to neurodegeneration (Filippi et al, 2018; Lassmann et al, 2018). Different forms of axonal degeneration exist in MS and related experimental models depending on the lesion type and time kinetics (Ferguson et al, 1997; Nikiè et al, 2011). Axonal damage is a consequence of

inflammatory demyelination (in acute lesions) or chronic demyelination (in chronic lesions) and axonal degeneration can occurr distal to the lesion without myelin loss *(Wallerian degeneration).* This is one histopathological correlate to normal appearing white matter alterations observed in MS patients. Moreover, characteristics of Wallerian degeneration can be also identified in the periplaque WM (Trapp et al, 2008; Dziedzie et al, 2010).

Approximately 85% of patients affected by MS begin with RRMS, which is characterised by reversible neurological deficits. Neurological disability in RRMS is caused by *acute inflammatory demyelination*, that is consequent to a direct inflammatory cells attack, release of inflammatory molecules by the innate immune system, including cytokines, oxidative products, free radicals and excitotoxic molecules, that lead to the oxidative damage to mitochondrial DNA, impaired activity of mitochondrial enzyme complexes, and axonal transection (Trapp et al, 1998; Trapp et al, 2009). Excessive glutamate release may play a major role in damaging oligodendrocytes and myelin, as revealed by the observation that glutamate receptor antagonists can be axon-protective under certain conditions (Li et al, 2000; Tekkok et al, 2001).

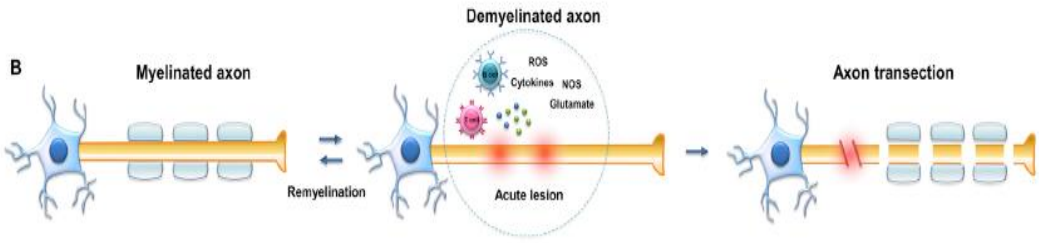

Figure 9. Acute inflammatory demyelination**.** Axonal damage induced by inflammatory demyelination is consequent to direct inflammatory cell attack and release of inflammatory molecules by the innate immune system. Boscia et al, 2020, *Cell Calcium*.

Axonal damage caused by *chronic demyelination* is consequent to the chronic lack of myelin-derived trophic support and involves an imbalance between energy demand and energy supply (Stys et al, 2005; Waxman et al, 2006; Trapp et al, 2008; Nave et al, 2008; Trapp et al, 2009). Following chronic demyelination, activation, dysfunction, and anomalous distribution of several ion channels and transporters along demyelinated axons play a central role in slowly progressing axonopathy, and suggests that MS may involve an acquired channelopathy (Waxman et al, 2001)

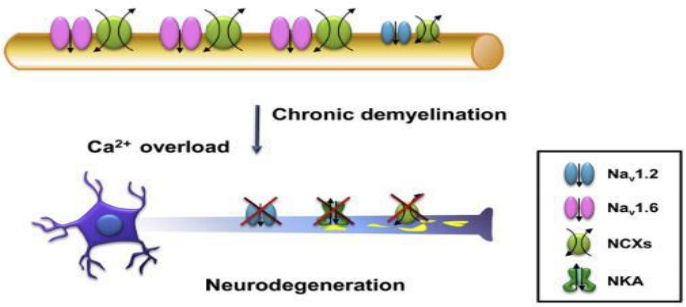

Figura 10. Axonal damage caused by chronic demyelination. It is consequent to the chronic lack of myelin and involves an imbalance between energy demand and energy supply, loss of ions channels and transporters along demyelinated axons that lead to neurodegeneration. Boscia et al, 2020, *Cell Calcium*.

More recently, it has been shown that, during acute inflammation in MS and EAE, an animal model of MS, myelinated axons may undergo to *focal axonal degeneration (FAD)*. FAD is a transient state of axonal dysfunction that can reverse or progress to irreversible damage which coincides with acute disease symptoms (Nikić et al, 2011). During this phase high levels of ROS and RNS lead to axonal swellings, dysmorphic mitochondria, and impaired axonal transport (Sorbara et al, 2014). These structural and functional changes can either progress to axonal fragmentation or resolve. Hence, FAD may be determined by the ability of individual axons to buffer $[Ca^{2+}]_i$ and favor its clearance (Witte et al, 2019)

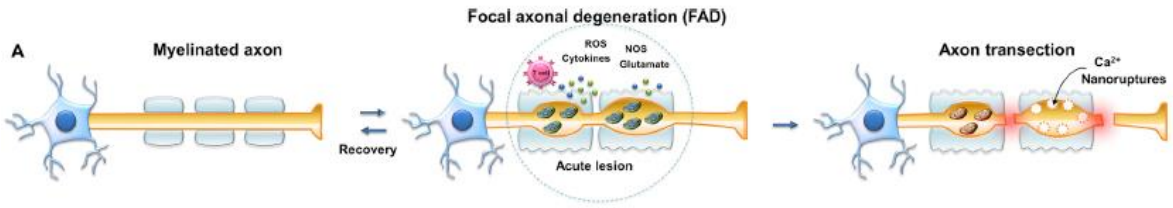

Figure 11. Focal axonal degeneration (FAD). In acute inflammatory lesions, myelinated axons undergo focal axonal degeneration (FAD), a transient state of axonal dysfunction that can reverse or progress to irreversible damage. In highly inflammatory lesions calcium influx may occur *via* membrane nanoruptures caused by the massive release of toxic mediators. Boscia et al, 2020, *Cell Calcium*.

The molecular mechanisms underlying axonal pathology have been mostly investigated in animal models of MS and ischemic/anoxic axon injury. The overexpression or dysfunction of ion channels and transporters regulates not only the adaptive response to demyelination but also the maladaptive sequel of events leading to persistent ionic imbalance in axons at progressive MS stages. The increased expression of Nav1.2 and the nodal Nav1.6, and the redistribution of the potassium channels Kv1.1 and Kv1.2 along denuded axons enable the propagation of the action potential and provide a substrate for remission of clinical deficits. Nonetheless, it also results in increased Na^+ influx during impulse conduction which lead to increase energy requirements during repolarization (Stys et al, 2005; Waxman et al, 2006; Smith et al, 2007; Nave et al, 2008; Trapp et al, 2009). Energy consumption and accumulating mitochondrial oxidative damage over time may contribute to reduction in ATP production and to Na^+/K^+ ATPase (NKA) pump failure, consequently generating a sustained Na^+ current, that reverse the Na^+/Ca^{2+} exchanger determining an intra-axonal calcium rise (Stys et al 1992, 1998). Ca^{2+} influx is not normally toxic in axons; however, due to increased energy demand and lack of ATP in axons, the energy-dependent Ca^{2+} buffering system inefficiently remove excess Ca^{2+} that consequently reaches toxic levels and drives a Ca^{2+} mediated degenerative response (Stys et al, 1998; Trapp et al, 2009). Indeed, the increased axonal Ca^{2+} activate proteolytic enzymes (proteases, phospholipases, calpains) ultimately leading to progressive proteolytic degradation of cytoskeletal proteins and axonal degeneration (Stys et al, 1998; 2005, Yang et al, 2013)

5. Current and emerging therapy in MS

There is no yet cure available for MS, but medicines and lifestyle changes can help to manage the disease. The clinical treatments are based on different strategies: 1) a rapid intervention immediately after the attack; 2) the attempt to slowdown the disease progression; 3) the managing of symptoms (for a review see Goldberg et al, 2012). The treatment of MS attacks includes the use of corticosteroids (i.e. prednisone given orally or methylprednisolone, given i.v.) and plasmapheresis, in case of inefficient steroids cure. Several pharmacological treatments are available for RRMS, including immunomodulators, immunosuppressants and monoclonal antibodies. Among *immunomodulators*, beta Interferon 1a and 1b (Avonex®, Rebif22®, Rebif44®, Betaferon®, Extavia®, Plegridy), injected under skin or intra-muscle, are the most prescribed drugs capable to reduce the frequency and the severity of relapses. Side effects include flu-like symptoms and local reaction in the site of injection. Applied to the first CIS, they are able to counteract the appearance of a new attack. Another old, but still used drug,

is the synthetic form of MBP (i.e. copolymer I or Copaxone). The *immunosuppressants* decrease the activation of the immune system in most severe form of MS, and include mitoxantrone, teriflunomide, dimethyl fumarate, and fingolimod. Specific *monoclonal antibodies*, i.e. Natalizumab and Alemtuzumab, selectively target cells or molecules, thus modifying the immune response. Despite their efficacy, the use of Natalizumab is associated with a progressive multifocal leukoencephalopathy, while the administration of Alemtuzumab is associated with the risk of infections and other autoimmune disorders. Finally, there a number of drugs for to relieve MS symptoms, in order to improve the quality of life. Uncontrollable spasms symptoms are cured with muscle relaxants; the neuropathic pain with topiramate, duloxetine, carbamazepine, amitriptyline; and emotional changes with benzodiazepines and antidepressants. The oromucosal spray *Sativex*, containing tetrahydrocannabinol and cannabidiol in 1:1 ratio, has been approved as add-on therapy for treatment of spasticity in adult MS patients who are not responding to conventional antispastic therapies. Fampridine (4-aminopyridine*)* is a potent inhibitor of voltage-gated potassium channels and improves symptoms in some patients. The beneficial effects have been attributed to the enhancement of neurotransmission in demyelinated neurons, translating into improved walking speed and muscle strength of the lower extremities. Side effects consist primarily of paraesthesia, dizziness, nausea/vomiting, falls/balance disorders, insomnia, urinary tract infections and asthenia.

Not less important is the research devoted to *rehabilitation*. In recent years several reports demonstrate the effectiveness of the rehabilitation treatment in MS patients. A typical physical therapy session may include stretching and strengthening exercises, useful to reduce weakness and other gait problems often associated with MS.

Emerging remyelination therapies

Treatments that enhance the speed of remyelination are predicted to protect neurons from axonal degeneration. Intervention to maintain and repair myelin should occur early as chronically demyelinated axons will degenerate precluding remyelination. Several studies have identified compounds that promote the recruitment, survival and differentiation of oligodendrocytes and, ultimately, may lead to improved remyelination. Several of these medications target either muscarinic acetylcholine receptors (such as M1) and/or histamine receptors (such as H1 and H3); they include benztropine, clemastine, quetiapine and GSK239512. Domperidone elevates prolactin levels, which improves remyelination through

prolactin receptor. Several medications also act through specific nuclear receptors: clobetasol activates glucocorticoid receptors, IRX4204 is a retinoid X like receptor (RXR) agonist, liothyronine stimulates thyroid hormone receptor (THR) and vitamin D activates vitamin D receptor. Several monoclonal antibodies may improve remyelination and are under investigation. Opicinumab targets LINGO1 and rHIgM22 may target the integrin αvβ3. Miconazole stimulates the mitogen-activated protein kinase (MAPK) pathway and extracellular-signal-regulated kinase 1 (ERK1) and ERK2 activity. XAV939 and indomethacin both attenuate inhibitory WNT–β-catenin signalling. (Plemel et al, 2017).

Opicinumab (BIIB033), is a monoclonal antibody directly against LINGO1 that enhance OPC differentiation and myelination. Phase 2 trial in patients with a first episode of optic neuritis showed an improvement on nerve impulse conduction along the affected optic nerve. Phase 2 trial in RRMS is ongoing.

Clemastine is a widely available first-generation antihistamine that exhibits M1 antimuscarinic properties. Clemastine has been validated in vitro and in vivo in several rodent models of demyelination to promote OPCs differentiation, with promising potential for remyelination therapies (Mei et al, 2016). *Quetiapine* is another M1 antagonist currently used as an atypical antipsychotic drug. It has been shown to stimulate OPCs differentiation through the ERK1/2 pathway. Further, quetiapine treatment was shown to prevent corpus callosum demyelination in the cuprizone model, suggesting a neuroprotective action. (Zhang et al, 2008; Chandran et al, 2012).

Olesoxime (TRO19622) is a cholesterol-like compound that accelerated oligodendrocyte maturation, enhanced myelination and the repair process, promoting myelin formation with consequent functional improvement. (Magalon et al, 2012). The beneficial effects were attributed to olesoxime's potential impact on oxidative stress, mitochondrial permeability transition or cholesterol homoeostasis. This drug is in clinical trial (Phase 1).

Liothyronine is used in Phase I for patient with MS. Thyroid hormone alleviated demyelination induced by CPZ by promoting the development of oligodendrocyte lineage cells and remyelination. (Zhang et al, 2016).

GSK239512 is a potent H_3 receptor antagonist/inverse agonist. Originally investigated for the treatment of cognitive impairment in Alzheimer's disease (AD) and schizophrenia GSK239512 promotes OPCs differentiation in vitro and enhances remyelination in the cuprizone mouse model of remyelination (Wang et al, 2014). It is in phase II as add-on therapy for patients treated with interferon-β1a or glatiramer acetate (Schwartzbach et al, 2017).

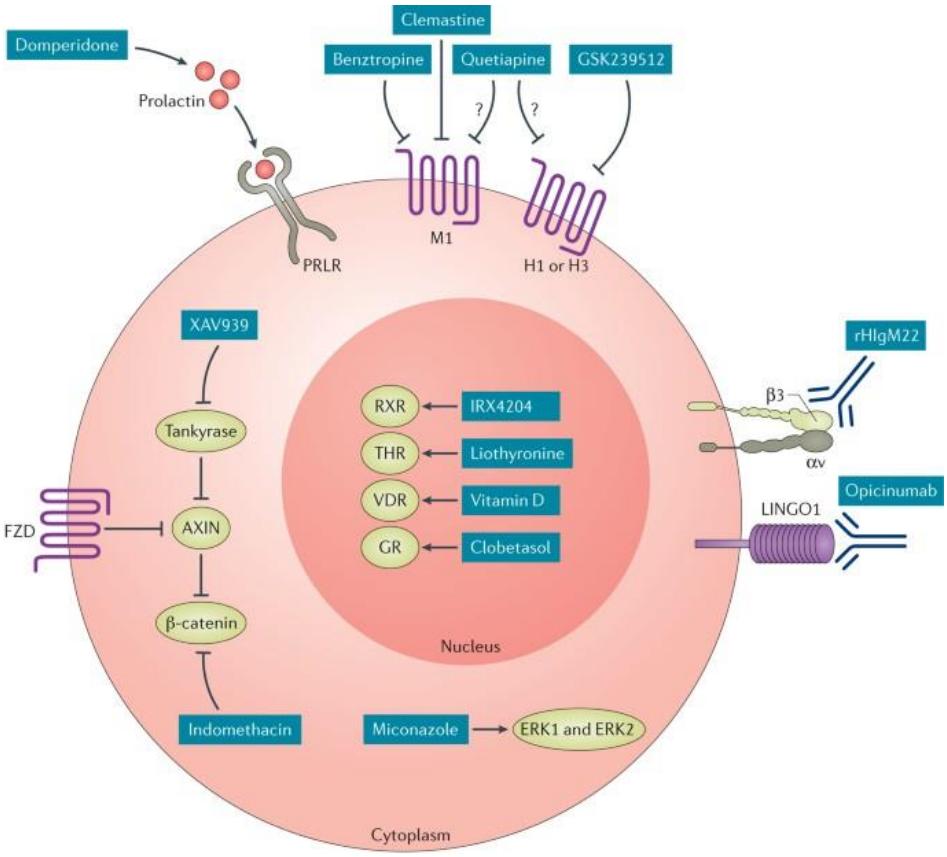

Figure 12. Drugs that affect myelin reformation and are prospective medications for repair in multiple sclerosis. Plemel et al, 2017, *Nature Reviews Drug Discovery*

6. The Na^+/Ca^{2+} exchangers in demyelinating diseases

The Na^+/Ca^{2+} exchangers (NCXs) are membrane proteins that belong to the superfamily of calcium-cation-antiporters. NCXs are encoded by three *ncx1 ncx2 ncx3* genes of *the Slc8* family located on human chromosomes 2, 9, 14, respectively (Li et al, 1994). The NCX exchangers have been found found in the plasmatic, mitochondrial and endoplasmic reticulum membranes of excitable cells (Kiedrowski et al, 1994; Patterson et al, 2007). The NCX1 gene is expressed in several tissues as brain, heart, skeletal muscle, smooth muscle, kidney, eye, secretory, and blood cells, whereas NCX2 and NCX3 genes have been found exclusively in neuronal and skeletal muscle tissues (Lee et al, 1994). In addition, NCX1 and NCX3 give rise to several splicing variants that appear to be selectively expressed in different regions and cellular populations of the brain (Quednau et al, 1997; Yu et al, 1997). NCX is composed of a ten transmembrane segments (TSM1-10) and a long cytosolic f-loop positioned between TM5 and TM6 arranged in two pseudo-symmetrical halves. The first six segments (TSM1-6) are the N-terminus hydrophobic domains while the TSM7-10, the C-terminus hydrophobic domains. NCX activity is regulated through a tandem of calcium-binding domains, CBD1 and CBD2, which are located within the cytosolic f-loop. CBD1 detect slight increases in cytosolic Ca^{2+} while CBD2 binds Ca^{2+} upon Ca^{2+} concentration increases (Annunziato et al, 2004; Gomez-Villafuertes et al, 2007). In addition, outside the CBD domains a sequence in the N-terminus domain of the f-loop, called exchanger inhibitory peptide (XIP) is a autoinhibitory region which is present in NCX1 and NCX3 and has been implicated in sodium-dependent inactivation probably activated by calmodulin (Matsuoka et al, 1997). Thus, to balance calcium and sodium homeostasis, NCXs cooperate with selective ion channels, transporters and ATP-dependent pumps. NCXs can operate either in the forward mode (Ca^{2+} extrusion) or in the reverse mode (Ca^{2+} entry) depending on the membrane potential and the transmembrane calcium and sodium gradients, participates in maintaining intracellular $[Na^+]_i$ and $[Ca^{2+}]_i$ homeostasis in physiological and pathophysiological conditions (Blaustein et al, 1999; Philipson et al, 2000). In order to be activated, NCX requires great changes in intracellular calcium amount, as occurs after the firing of action potentials in neurons (Annunziato et al, 2004).

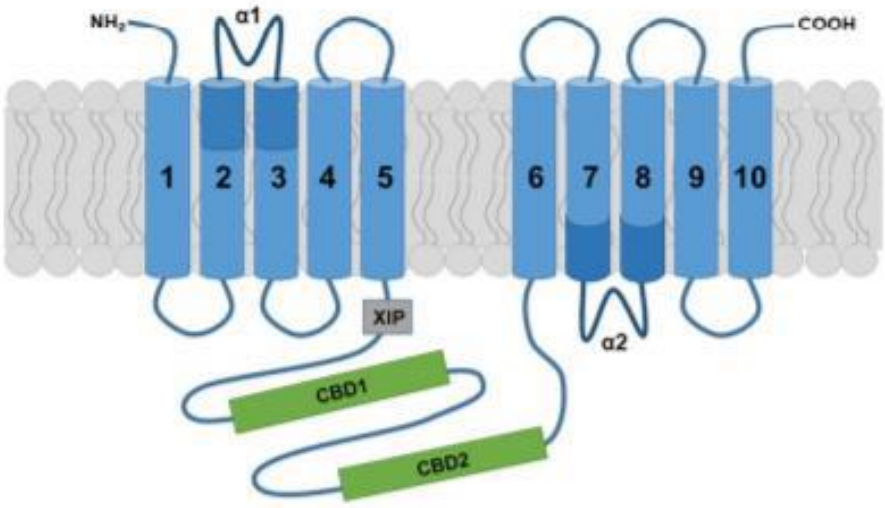

Figure 13. Structural architecture of NCX exchanger. Annunziato et al, 2004, *Pharmacological reviews*

Intracellular $[Na^+]_i$ and $[Ca^{2+}]_i$ imbalance significantly contribute not only to axonal dysfunctions but also maladaptive myelin repair or remyelination failure during SPMS. In line, brain sodium MRI demonstrated that the total tissue sodium concentration, a combined measure of the intracellular and extracellular sodium, increases in brain MS lesions and is higher in the brain of MS persons with greater disability and in progressive disease courses (Inglese et al, 2013; Brownlee et al, 2019). Several studies in recent years have demonstrated the importance of calcium transients in oligodendrocytes for remyelination of demyelinated axons (Dutta et al, 2014, Pan et al, 2017; Baraban et al, 2018). Hence, defining the relative contributions of each of NCX transporter in axon pathology and myelinating glia will constitute a major advance in understanding in detail the intricate mechanism of neurodegeneration and remyelination failure in demyelinating disease. It has been proposed that dysfunctional NCX exchangers may contribute to detrimental calcium overload and axonal degeneration in WM demyelinated axons. This suggests that blocking NCX activity under certain demyelinating conditions might be axon-protective. By contrast, a number of studies in the last decade highlight the protective function of NCX3 exchanger in brain ischemia and several neurodegenerative disease states, including demyelinating disorders (Molinaro et al, 2008; Molinaro et al, 2011; Boscia et al, 2012; Pannaccione et al, 2012; Secondo et al, 2015; Michel et al, 2015; Casamassa et al, 2016) and suggest an important functional role of this exchanger for myelin synthesis in oligodendroglia (Boscia et al, 2012; Friess et al, 2016; Hammann et al, 2018; de Rosa et al, 2019).

6.1 Role of NCXs in oligodendrocytes

The first characterization of NCXs in cells of the oligodendrocytes lineage was studied by Quednau et al (1997) which revealed the expression of all three mammalian genes in primary cultures of differentiating oligodendrocytes. While NCX2 exchanger remain poorly characterized in oligodendrocyte lineage, NCX1 was found to be predominantly expressed in OPCs. Tong et al (2009), demonstrated that the pharmacological inhibition of NCX1 or its silencing with selective siRNAs largely inhibits migration and GABA-induced Ca^{2+} signalling in cultured OPCs. Conversely, NCX3 increased at more mature stages of the oligodendrocytes lineage (Boscia et al, 2012). Indeed, Boscia et al, evidenced the important role of NCX3 in oligodendrocyte lineage progression from OPCs to mature myelinating oligodendrocyte, and demonstrate that NCX activity and NCX3 protein expression significantly increased when cells start to differentiate in rat primary OPCs. Immunohistochemical analysis performed in this study showed that the anti-NCX3 antibody depicted an intense and punctuate NCX3 immunoreactivity along MAG- positive areas in mature oligodendrocytes. One year later, Gopalakrishnan et al (2013) revealed that NCX3 protein is a myelin membrane component commonly expressed in human and murine myelin. Indeed, *ncx3* gene silencing in clonal human MO3.13 oligodendrocyte cell line significantly prevented the upregulation of CNPase and MBP during differentiation. By contrast, the overexpression of *ncx3* gene upregulated myelin marker expression, thus suggesting that an increased NCX activity may stimulate OPCs differentiation (Boscia et al, 2012; 2013). Later, Friess et al confirmed the importance of NCX function for myelin synthesis. By using a pharmacological approach, the authors demonstrated that NCX activity operating in the reverse mode is required for myelin synthesis in primary OPC cultures. Blocking NCX with KB-R7943, a nonselective NCX blocker, resulted in a significant increase in $[Na^+]_i$ and decrease in $[Ca^{2+}]_i$ in OPCs, and decreased MBP synthesis. In addition, they demonstrated that local $[Na^+]_i$ and membrane potential changes modulate Ca^{2+} influx through NCX and affected MBP synthesis. Indeed, a small depolarization, induced by a physiological rise of $[K^+]_e$-, or increasing $[Na^+]_i$ levels by partial inhibition of NKA with ouabain at 5DIV favour the reverse mode of NCX functioning, resulting in local $[Ca^{2+}]_i$ transients and stimulation of MBP synthesis. Also in these experimental conditions, the NCX blocker KB-R7943 significantly suppressed $[K^+]_{e-}$ and NKA-induced $[Ca^{2+}]_i$ transients and MBP production, thus further confirming the important role of NCX activity for myelin synthesis (Friess et al, 2016).

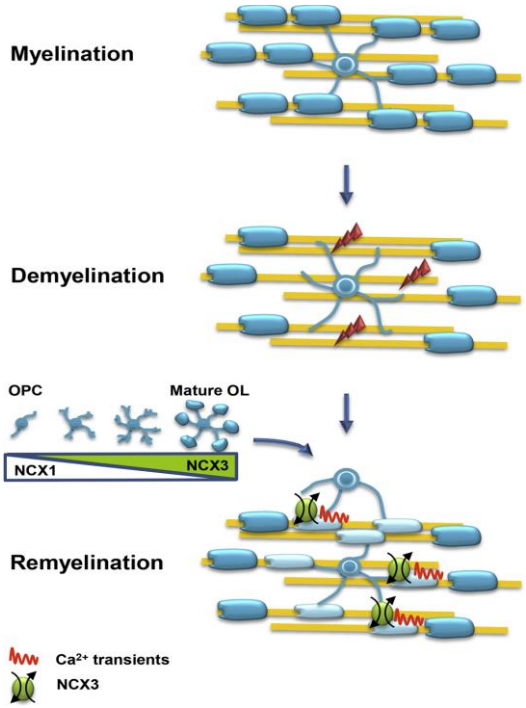

Figure 14. Schematic representation of NCXs expression and function in oligodendroglia. Axonal demyelination is followed by a spontaneous remyelination process in which existing or newly formed OPCs are recruited to the lesion, proliferate and remyelinate denuded axons. NCX1 and NCX3 exchangers are divergently modulated during oligodendrocyte development. NCX3 expression and activity significantly increased in developing OPCs and NCX3 activity is required for sustaining calcium transients and myelin synthesis in oligodendrocytes. Boscia et al, 2020, *Cell Calcium*.

The role of NCX3 exchanger in oligodendrocytes has been also studied in experimental models of MS, and by using *ncx3* knockout mice. Indeed, the experiments performed in experimental autoimmune encephalomyelitis (EAE), an animal model mimicking the pathophysiological features of MS, showed that the oligodendroglial NCX3 exchanger was involved both in early and late stages of OPCs response after a demyelinating insult. NCX3 expression was upregulated by CNPase-positive cells at the pre-onset and chronic stages of EAE disease, but not at the peak stage, during which it was significantly downregulated, suggesting that the exchanger may have a protective role at early stages and a regenerative function at later stages. Mice lacking ncx3 gene displayed increased susceptibility and developed more severe clinical symptoms after MOG35-55-induced EAE, an effect that was accompanied by a significant reduction in OPCs and premyelinating cells in the spinal cord during the chronic stage if compared to wild-type mice (Casamassa et al, 2016). In line with the beneficial role of this

exchanger, it has been demonstrated that NCX3-deficient mouse shows localized muscle fiber necrosis and impaired neuromuscular transmission (Sokolow et al, 2004) enhanced vulnerability to hypoxic-ischemic-insults (Secondo et al, 2007; Scorziello et al, 2013), impaired spatial learning and memory (Molinaro et al, 2011), and a reduced spinal cord size accompanied by a decreased expression of myelin markers and increased $NG2^{+}$ OPCs counts (Boscia et al, 2012).

6.2 Role of NCXs in axonal pathology

A number of studies highlight that $[Na^{+}]_i$ and $[Ca^{2+}]_i$ imbalance significantly contribute to neuro-axonal dysfunctions. An altered distribution of voltage-gated sodium and calcium channels, NCX and glutamate receptors has been observed in post-mortem human MS tissue, but a definitive understanding of axonal degeneration in MS is still unclear and the role of NCX subtypes in axonal pathology still need further investigation (Kurnellas et al, 2007; Kornek et al, 2001; Newcombe et al, 2008). It has been proposed that sodium influx into injured axons drives reverse operation of NCX with consequent accumulation of intra-axonal calcium levels (Stys et al, 1991, 1992a, Stys et al, 1998) (Banik et al, 1987, Young et al, 1992, Buki et al, 2000). By using anti-NCX antibodies Craner et al (2004), examined the correlation between the expression and distribution of Nav1.2, Nav1.6 channel with the expression of NCX, together with β-amyloid precursor protein (β-APP) a marker of axonal injury (Cochran et al, 1991, Trapp et al, 1998, Bitsch et al, 2000, Kuhlmann et al, 2002). The experiments performed in demyelinated axons of spinal cord sections of mice subjected to a chronic-relapsing myelin oligodendrocyte glycoprotein MOG35-55 –induced EAE showed that Nav1.2 and Nav1.6 channels were individually or concomitantly co-expressed by β- APP-positive axons. In particular, Nav1.6 subunits were found to be coexpressed in a large significant proportion (about 60 % for β-APP/ Nav1.6 > 38 % for β-APP/ Nav1.6/ Nav1.2 > 2 % for β-APP/Nav1.2), thus suggesting that Nav1.6 is preferentially associated with axonal injury in EAE. Analysis of confocal microscopy revealed that, while Nav1.6 and NCX were scarcely co-expressed by β-APP negative axons they were upregulated and largely co-localized in the majority of β-APP-positive axons (about 70 %). Interestingly, the expression of both Nav1.6 and NCX levels decreased in the remaining β-APP positive axons, thus possibly suggesting that, as axonal degeneration proceeds, they are degraded or downregulated. In line with this possibility, it has been proposed that many chronically demyelinated axons may be non-functional prior to

degeneration because they lack voltage-gated Na^+ channels (Black et al, 2007), NKA (Young et al, 2008), and, eventually, NCX (Bano et al, 2005; Black et al, 2007).

In accordance with this concept, the idea that mechanisms leading to axonal degeneration differ in different type of lesions (Craner et al 2004, Black et al, 2007) has been supported by findings showing that the expression of both Nav1.6 and NCX in demyelinated axons within chronic *versus* acute MS plaques substantially different. Indeed, Black et al (2007), demonstrated that, although it was expressed by astrocytes, NCX was not detected in demyelinated axons in chronic MS lesions obtained from post-mortem spinal cord sections of secondary progressive MS patients. In these lesions, only a low percentage of neurofilament-positive axons accumulated β-APP (about 2.9 %) and exhibited a detectable level of Nav1.6 channels immunoreactivity (about 15 %). By contrast, as observed in EAE model (Craner et al, 2004), in acute demyelinated lesions of spinal cord and optic nerves sections obtained from post-mortem patients with secondary progressive MS that the expression of Nav1.6 was about 80 % while the coexpression of Nav1.6 and NCX immunosignal was about 60 %. Then, the majority of demyelinated β-APP negative axons in acute lesions showed co-expression of Nav1.2 and NCX, and only a small percentage coexpressed Nav1.6/NCX (about 20 %) confirming that Nav1.6 coexpressed with NCX and associated with axonal injury. Recently we showed that not only NCX1, but also NCX3 subtype is abundantly expressed in white matter spinal cord axons and its expression is modulated at different stages of EAE (Casamassa et al, 2016). Hence, it will be important to investigate wether the redistribution of sodium channel subunits and different NCX subtypes in resilient (β-APP-negative) or vulnerable (β-APP-positive) demyelinated axons may contribute to functional recovery or axonal degeneration. Recently, Witte et al (2019) demonstrated that NCX inhibition with bepridil did not improve axonal fate in severe acute neuroinflammatory EAE lesions. By performing experiments using dye exclusion, they revealed that axonal membrane integrity is impaired in highly inflammatory EAE lesions and calcium influx from the extracellular space occurs *via* nanoruptures of the plasma membrane. These findings suggest that membrane damage can provide a persisting path for calcium entry during axonal damage in MS.

6.3 Pharmacological modulation of NCX3 exchanger

Currently, no positive modulators of NCX3 exchanger are still available, but many NCX blockers have been developed in the last decades. Recently, a new selective NCX3 inhibitor, the 5-amino-N-butyl-2-(4-ethoxyphenoxy)-benzamide hydrochloride (BED) was drawn taking into consideration the chemical structure of a well-known NCX inhibitor, SEA0400 (Secondo et al, 2015). If compared with the SEA0400 structure, the biphenyl ether moiety was maintained unaltered while an amino group and an amide group were inserted on one of the two benzene rings. These chemical modifications have produced dramatic changes in the biological activity of this compound, determining a high NCX3 isoform selectivity and potency never found in any other NCX inhibitor. The potency of this new compound BED is significantly higher (i.e., IC50 = 1nM) than that of the amiloride derivative 3-amino-6-chloro-5-[(4-chloro-benzyl)-amino]-N-[[(2,4dimethylbenzyl)amino]iminomethyl]-pyrazinecarboxamide (CB-DMB) and of the new isothyourea derivative YM-244769, which is the most potent available NCX3 inhibitor working in the nanomolar range. However, YM-244769 inhibits NCX3 only in the reverse mode of operation, whereas BED inhibits NCX3 when it acts bidirectionally. The region involved in BED inhibitory action was found outside the f-loop, at the level of both the α1 and α2 repeats of NCX3. In line with the observation that ncx3 knock-down or gene ablation lead to a worsening of brain damage in mice or rats subjected to focal ischemia, BED worsened the damage induced by oxygen/glucose deprivation (OGD) followed by reoxygenation in cortical neurons and hippocampal organotypic slices, and aggravated the infarct injury after transient middle cerebral artery occlusion in mice (Secondo et al, 2015). Previous studies showed that during ATP depletion, NCX1 and NCX2 isoform activities are reduced, whereas NCX3 is still operative. Moreover, *in vivo* studies showed that NCX3 mRNA is upregulated 24 hours after permanent middle cerebral artery occlusion in rats in brain regions belonging to the periinfarct area. This NCX3 upregulation may suggest a compensatory mechanism that counterbalances the reduced activity of NCX2 protein, thus counteracting the dysregulation of $[Ca^{2+}]_i$ homeostasis in the surviving neurons of the penumbra zone (Boscia et al, 2006). BED is one of the most potent inhibitor of NCX3 so far identified, representing a useful tool to dissect the role played by NCX3 in the control of Ca^{2+} homeostasis under physiological and pathological conditions.

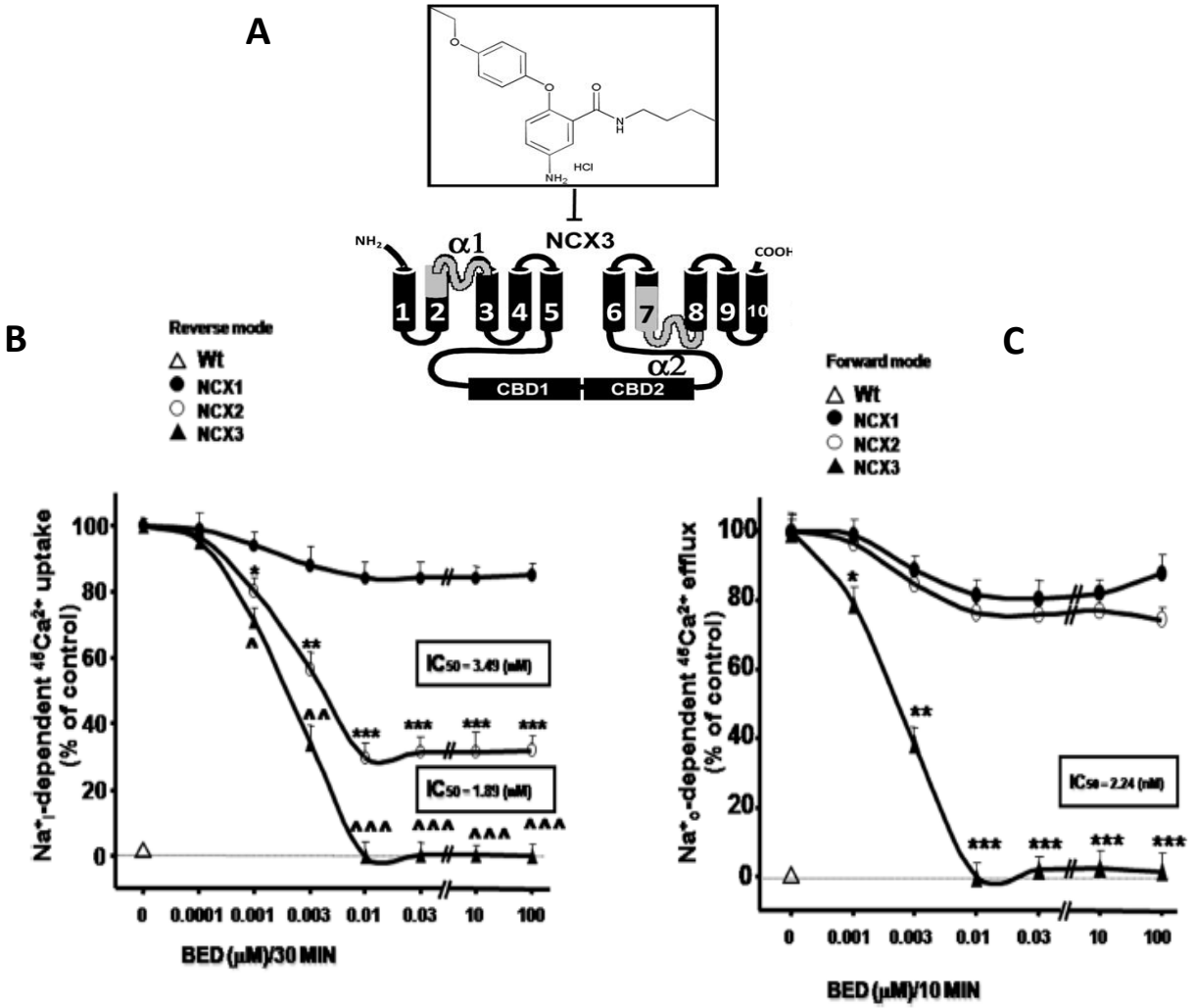

Figure 15. Structure of the new synthesized compound 5-amino-Nbutyl- 2-(4-ethoxyphenoxy)-benzamide hydrochloride (BED) and NCX3 exchanger. Dose response curves of BED on NCX working in the reveerse and forward mode of operation in BHK cells expressing distinctly the three NCX isoforms. Secondo el al, 2015, *ASC Chemical Neuroscience*

7. The Endocannabinoid (EC) system

The EC system was identified in the early 1990. This system involves three major components: endocannabinoids (ECs), endocannabinoid receptors, and their corresponding ligands and proteins. The ECs are derivatives of long chain polyunsaturated fatty acids, specifically of the lipid arachidonic acid (AA). The most important ECs are N-arachidonoylethanolamine (anandamide, AEA) and 2-arachidonoylglycerol (2-AG), but also oleoylethanolamide (OEA) and palmitoylethanolamide (PEA) that may bind cannabinoid receptors CB1 and CB2, metabotropic, nuclear and ionotropic receptors as G-protein receptor 55 (GPR55), peroxisome proliferator-activated receptor (PPAR), and transient receptor potential vanilloid 1 (TRPV1). ECs are produced "*on demand* " under different biological stimuli and act paracrinally or autocrinally. AEA is synthesized from membrane precursors via N-acylphosphatidyl-ethanolamine (NAPE)-specific phospholipase D (NAPE-PLD) (Di Marzo et al, 1994, Leung et al, 2006, Liu et al, 2006, Okamoto et al, 2004) and is cleaved into AA and ethanolamine by the fatty acid amide hydrolase (FAAH) located postsynaptically (Gulyas et al, 2004). On the other hand, 2-AG is formed by the action of two diacylglycerol lipases, DAGLa and DAGLb and is primarily degraded into AA and glycerol by monoacylglycerol lipase (MAGL) located at presynaptic neuronal level (Gulyas et al, 2004). Endocannabinoids act as retrograde messengers; indeed, when the neurotransmitter is released from vesicles within the presynaptic neuron, it activates the postsynaptic neuron that lead to the synthesis and releases of endocannabinoids. Once they are released, the endocannabinoids may bind the cannabinoid CB1 receptors at presynaptic sites. ECs suppress the presynaptic release of GABA and glutamate through a process termed depolarization-induced suppression of inhibition or excitation (DSI, DSE) that requires activation of cannabinoid CB1 receptors. CB1 and CB2 receptors are coupled to Gi/o proteins inhibiting the activity of adenylate cyclases (cAMP), stimulate mitogen-activated protein kinases (MAPK) and, in the case of CB1 receptors, inhibit voltage-activated Ca^{2+} channels and stimulate inwardly rectifying K^{+} channels, to transduce the binding of agonists into biological responses. A large number of evidence in the last decade demonstrated that the EC system regulates important CNS functions, including learning, memory, cognition, motor control, analgesia, synaptic plasticity, and exert immunomodulant and neuroprotective actions in models of neurodegeneration and inflammation (Shenglong et al, 2018). CB1 are found in the CNS, mostly in neuronal cells, but it is also expressed in many non-neuronal tissues. Conversely, CB2 are mostly expressed in the peripheral organs especially

cells associated with the immune system, but also in adipocytes, liver, and, in the CNS, is mostly found in microglia, astrocytes and selective neuronal populations (Di Marzo et al, 2015). ECs are also taken up by cells through a mechanism that is not yet fully elucidated but likely involves membrane carriers, intracellular carrier proteins and/or possibly endocytosis. ECs play an important role in the treatment of CNS disorders, and compounds enhancing the endocannabinoid tone are regarded as potential new CNS drugs in several neurological conditions.

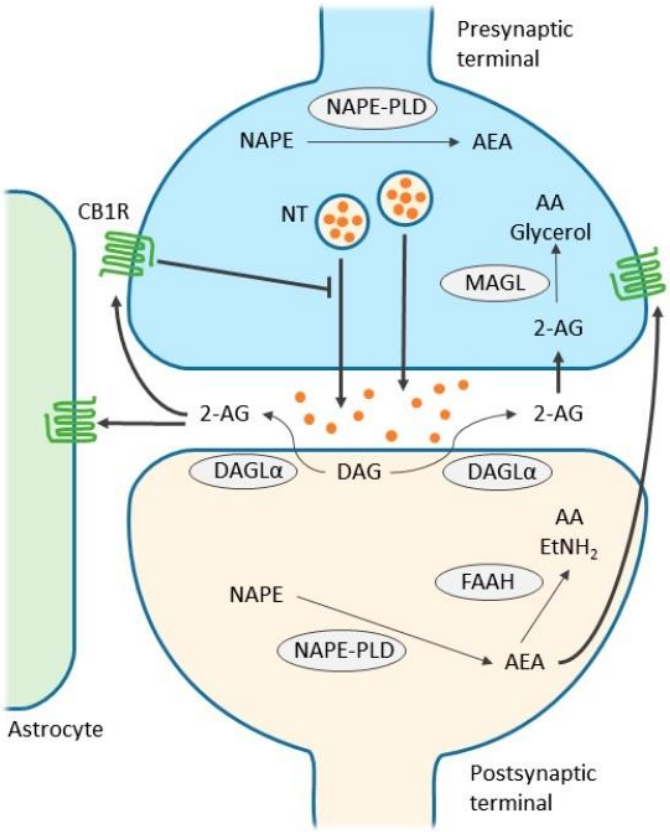

Figure 16. A schematic diagram illustrating the endocannabinoid EC system. CB1 receptors are expressed in presynaptic terminals and astroglial cells. 2-AG is synthesized in postsynaptic neurons from phosphatidylinositol (PI) lipid precursors through enzymatic activities of phospholipase C (PLC) and the DAGLα and DAGLβ enzymes, and inactivated in presynaptic terminals by monoacylglycerol lipase (MAGL). AEA is mainly synthesized from phosphatidylethanolamine (PE) and N-acyl phosphatidylethanolamine (NAPE) by the enzymes calcium-dependent transacylase (CDTA) and phospholipase D (PLD) and inactivated by the enzyme fatty acid amide hydrolase (FAAH). Mastinu et al, 2018, *Molecular Biology and Clinical Investigation*

7.1 Neuroprotective and immunomodulatory effects of ECs during neuroinflammation

Neuroinflammation is a process related with the onset and progression of several neurodegenerative disorders, including MS, traumatic brain injur (TBI), parkinson's disease (PD), AD, and amyotrophic lateral sclerosis (ALS).

The large interest in ECs and in the cannabimimetic activity of many natural products is due to their beneficial pharmacological actions as they may provide antioxidant, neuroprotective, anti-inflammatory, immunomodulatory and cardio-protective functions. The ECs signaling involves both cannabinoid receptor-dependent effects, such as the activation of CB1 receptors to normalize glutamate homeostasis or to activate autophagy, the activation of CB2 receptors and PPARγ, or the modulation of GPR55 to reduce local inflammatory events, and/or antioxidant likely cannabinoid receptor-independent properties of cannabinoids that have been demonstrated to operate against acute or chronic neurodegeneration (see Fernández-Ruiz et al, 2005, 2007, for review). Indeed, the activation of CB2 receptors might control the production of different cytotoxic factors such as cytokines, nitric oxide (NO) or reactive oxygen species (ROS), in particular, by reactive microglia, thereby increasing neuronal survival (Fernandez-Ruiz Julian et al, 2007).

CB1 receptors are found throughout the nervous system and in the periphery and their activation modulate the presynaptic release of neurotransmitters (Scotter et al, 2010). The CB2 receptors are highly localized on immune cells and their stimulation with either endogenous or exogenous cannabinoids is associated with immunomodulatory effects (De Petrocellis et al, 2009, Tanasescu et al, 2010). Astrocytes express low levels of CB1 receptors, but upon activation, they may modify the expression of either CB1 or CB2 receptor. The different cell types have the machinery for endocannabinoid biosynthesis, 2-AG, or AEA, thus contributing to the endocannabinoid tone in the brain. Accordingly, the pharmacological and/or genetic inhibition of ECs degrading enzymes restrained neuroinflammation and prevented neurodegeneration in various animal models of neuroinflammatory conditions suggesting that enhancing endogenously-released cannabinoid ligands in the brain may provide therapeutic effects more safely and effectively than administering drugs directly acting at the cannabinoid receptor, which, instead may mediate psychotropic effects.

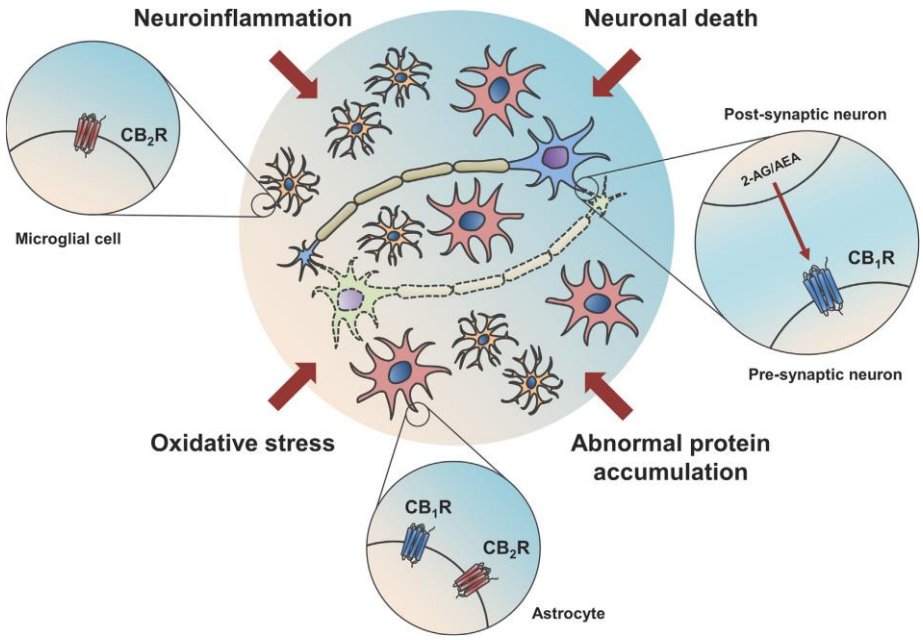

Figure 17. The EC system modulates common traits of neurodegeneration counteracting neuronal death, oxidative stress, neuroinflammation, or abnormal protein accumulation. The key location of the different ECs elements within the brain enables modulation of crucial processes for the correct balance between neuron survival and degeneration. Aymerich et al, 2018, *Biochemical Pharmacology*

7.2 Pharmacological modulation of ECs with inhibition of FAAH enzymes

FAAH represents the primary degradation enzyme of the ECs AEA, OEA and PEA (Guy et al, 2018). FAAH inhibition prevents the breakdown of endogenous ligands for CB receptors and PPAR, including AEA, and PEA, producing potentially therapeutic effects, some through CB receptors and some through PPAR. Recently, a renewed interest for FAAH inhibitors as therapeutic treatment strategy in several neurological conditions emerged following the identification of the off-target proteins of the FAAH inhibitor BIA10-2474 that lead to the death of one volunteer and produced mild-to-severe neurological symptoms in four other. During these years several studies demonstrated that mice lacking FAAH develop a less severe EAE and prevents sEPSC alterations, and result in a better clinical EAE remission in mice (Rossi et al, 200; Lopez et al, 2009). Further studies supported that, silencing FAAH suppressed PGE2 production and pro-inflammatory gene expression in BV2 microglial cell exposed to LPS

(Tanaka et al, 2019) and that knocking out FAAH or FAAH inhibition benefit spasticity during EAE in Biozzi ABH mice (Pryce et al, 2013).

The clinical safety profile of other tested FAAH inhibitors (van Esbroeck et al, 2017*)* suggests that pharmacological agents targeting FAAH represent a valuable treatment option for pain, cognition, depression, anxiety, spasticity and inflammation-related neurodegeneration. (Centonze et al, 2007; Gregus et al, 2020). FAAH inhibitors are currently under clinical evaluation for treatment of cannabis use disorder, Tourette syndrome, and chronic pain (Egmond et al, 2020). FAAH inhibition also contribute to the pharmacological effects of the non-psycoactive compound cannabidiol, which is currently approved in a 1:1 tetrahydrocannabinol/cannabidiol formulation for treatment of spasticity in MS patients (Syed et al, 2014). A number of FAAH inhibitors have been described, but some of these compounds lack, however, the target selectivity and/or biological availability needed in a therapeutic drug. An emerging second generation of FAAH inhibitors comprises several structurally diverse groups of compounds, in particular, the compound URB-597 (KDS-4103) that has been characterized both *in vitro* and *in vivo*. URB-597 has a remarkable selectivity for FAAH with no activity on other cannabinoid-related targets, including cannabinoid receptors, anandamide transport and monoglycerol lipase (the enzyme involved in the deactivation of the endocannabinoid ester 2-AG). Such target discrimination is matched by a lack of overt cannabimimetic effects in vivo (Piomelli et al, 2006). Further studies have been performed mediated the new LC/MS-MS method, combined with measurements of FAAH activity, to determine the tissue distribution of URB-597 after oral administration in rats. The results confirm that URB-597 is orally available and does not enter the CNS at doses that effectively inhibit FAAH activity, elevate peripheral OEA levels, and substantially reduce nociceptive responses (Sasso et al, 2012) suggest that these compounds display marked analgesic properties in rodent models (Clapper et al, 2010, Sasso et al, 2015) and that peripheral FAAH blockade may offer a new approach to pain therapy. URB-597 is orally available, peripherally restricted and well-tolerated after acute and chronic oral administration. As such, our results encourage further development of this promising analgesic drug candidate.

8. Melatonin

Melatonin is a neurohormone primarily produced by the pineal gland, and the precursors of its biosynthesis are the amino acid L-tryptophan and serotonin. The L-tryptophan is taken up from the circulation and is hydroxylated by the enzyme tryptophan hydroxylase to produce 5-hydroxytryptophan (5-HTP). The 5-HTP is decarboxylated by pyridoxal phosphate and 5-hydroxytryptophan decarboxylase to produce serotonin (5-HT). Serotonin is then converted into N-acetyl-serotonin (NAS) by the enzyme aryl-alkyl-amine-N-acetyl transferase (AANAT) while NAS is converted into melatonin by the enzyme hydroxy-indole-O-methyltransferase (HIOMT). Once synthetized, melatonin is released into the circulation, and its high lipid and water solubility enable it to penetrate the cell membrane and reach various body fluids such as saliva, urine, milk, and cerebrospinal fluid (CSF) through the blood brain barrier (BBB) (Bars et al, 1991; Claustrat et al, 2015).

Melatonin levels increase during the night and fall in the daytime and regulates multiple physiological functions such as sleep wake cycle, appetite, body temperature, mood, motor activity (Cecon et al, 2018). Melatonin exerts antioxidant, immunomodulatory, and neuroprotective effects, that are mediated by its binding to two specific melatonin G protein-coupled receptors MT1 and MT2, the nuclear orphan receptors RZR/ROR, and the cytosolic MT3 receptor quinone reductase (QR2). The MT1 receptor is present in different brain areas such as, hippocampus, amygdala, hypothalamus, and cerebellum, as well as in peripheral tissues such as retina, pancreatic cells and immune system (Ren et al, 2017). The MT2 receptor is expressed primarily in peripheral tissues such as the retina, and secondarily in the brain (Wu et al, 2013).

Once melatonin binds to the MT1 receptors three different signaling pathways can be triggered: (1) inhibition of forskolin-stimulated cAMP, (2) inhibition of protein kinase A (PKA) and phosphorylation of the cAMP-responsive element binding, and (3) increased phosphorylation of the mitogen-activated protein kinase kinases 1 and 2 (MEK1 and MEK2), the extracellular signal-regulated kinases 1 and 2 (ERK1 and ERK2) and c-Jun N-terminal kinase (c-JNK). Melatonin MT2 receptor activation inhibits both forskolin stimulated cAMP production and cGMP formation, while activates protein kinase C (PKC) in the peripheral nervous system (DubocovichM et al, 2010). Currently, melatonin is used as dietary supplement for the short-term treatment of insomnia, and is candidate in clinical evaluation in MS not only to regulate sleep and fatigue but also for neuroprotective effects and disability progression (Skarlis et al, 2020)

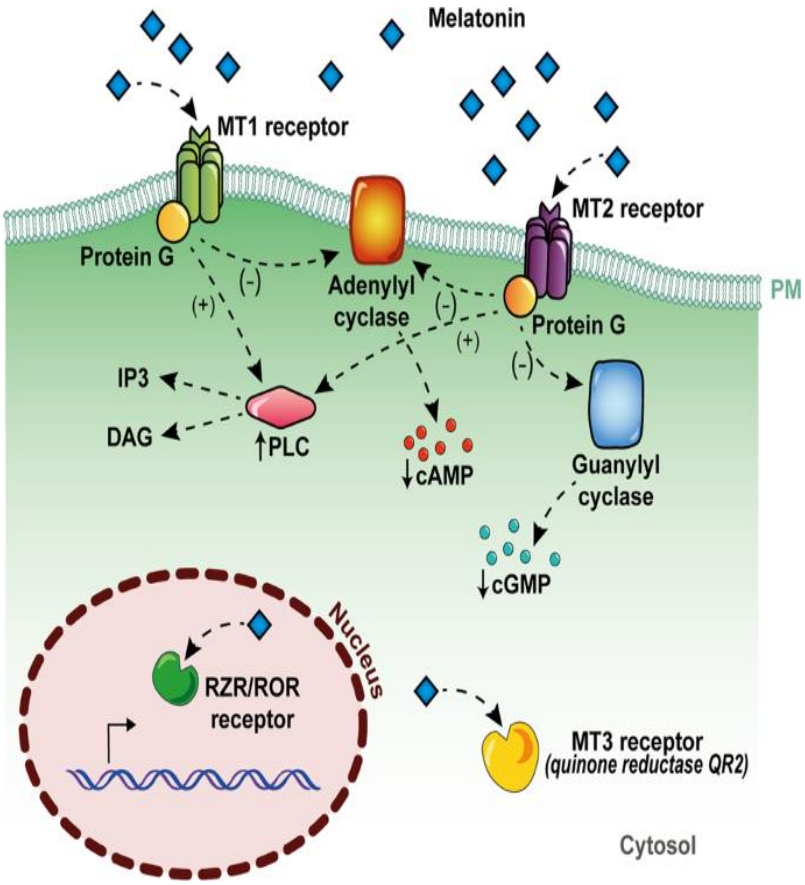

Figure 18. Mechanisms of action of melatonin. Melatonin can exert its effects by acting through receptor-independent mechanisms, which involve the direct interaction of melatonin and other molecules, and they are mainly related to its antioxidant and radical scavenging action. As any other hormone, melatonin can also act through specific cellular receptors, by membrane melatonin receptors, called MT1 and MT2, which are seven transmembrane-spanning proteins belonging to the G-protein-coupled receptor (GPCR) superfamily, and through the cytosolic enzyme QR2 (also called MT3), or through the nuclear receptors RZR/ROR. Tarocco et al, 2019, *Cell Death*

8.1 Neuroprotective and immunomodulatory effects of melatonin during neuroinflammation

The ability of melatonin to cross the BBB and its short life with no significant side effects has made melatonin a promising neuroprotective and anti-inflammatory agent. Melatonin may modulate the apoptotic pathway because decreases the expression of proapoptotic genes (Bax and caspase3) and mitochondrial noxious enzymes, while increases the level of the anti-apoptotic gene Bcl-2. Melatonin structure is composed of an indole ring with an alkyl amide side chain and a methoxy side chain on a benzene ring (Kim et al, 2019) as a potent free-radical scavenger which also stimulates activity of the antioxidant enzymes and has an influence on the immune system (Mercolini et al, 2012). In experimental models of MS, melatonin prevented demyelination, oligodendrocyte loss and axonal injury in EAE mice (Wen et al, 2016). In the cuprizone model of myelin damage and repair, it stimulated OPC differentiation and accelerated remyelination (Ghareghani et al, 2017, 2019, Alghamdi et al, 2020). Oxidative stress and inflammation are important factors underlying the process of demyelination. Many studies have confirmed that melatonin has significant protective effects against redox signaling in both MS animal models and clinical studies and suggest that melatonin may reduce behavioural deficits in animal models of MS and the severity of clinical MS symptoms (Chen et al, 2020). In fact, melatonin reduces CNS infiltrates, peripheral and central Th1/Th17 responses, while enhances Treg frequency and IL-10 synthesis (Álvarez-Sánchez et al, 2015) increases the anti-inflammatory IL-4 cytokine levels, and reduces the IFN-γ, IL-1β and TNF-α levels in brain lysates from EAE mice (Mathes et al, 2008). Based on these large number of beneficial pharmacological effect, a detailed screening of the molecular mechanisms mediating the neuroprotective effects of melatonin in both animal and human subjects is needed. Melatonin is currently in clinical evaluation in MS not only to regulate sleep and fatigue but also for neuroprotective effects and disability progression.

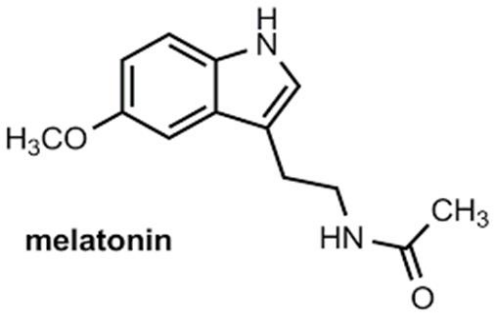

melatonin

Registration number/ reference	Medication	Type of study	Status	Primary outcome	Study duration	Primary outcome fulfilled
NCT01279876/Roostaei et al., 2015 [134]	Interferon 1-b/ 3 mg melatonin before sleep	Randomized, placebo-controlled trial, phase II	Completed	Changes in number of relapses, EDSS, PASAT-3 score,T2 and gadolinium-enhancing brain lesions	12 months	Failed
NCT01718678	3 mg once a month	Randomized, parallel assignment, phase II	Terminated	Modified fatigue impact scale (MFIS)	12 months	NA
NCT02463318/Emamgholipour et al., 2016 [122]	One millimolar, one micromolar, one nanomolar, 12-h treatment	Randomized, open label, single group assignment	Completed	Relative gene expression of SIRT1 pathway in PBMCs derived from MS patients	12 h	Yes
NCT03498131	3 mg melatonin/once a day	Randomized parallel assignment	Recruiting	Changes in 24-h urinary 6-sulfatoxymelatonin and serum morning melatonin over time	12 months	NA
NCT03540485	300 mg melatonin daily between 10 p.m. and 11 p.m.	Randomized, single-blind, placebo-controlled trial	Not yet recruiting	Rates of neurological impairment, rates of disability	24 months	NA
NCT04035889	0.5-mg tablets of melatonin with the option of switching to an "escalation dose" of 3 mg if no relief after 3 days	Randomized, cross-over, placebo-controlled, pilot trial	Recruiting	Changes in total sleep time, sleep quality, sleep disturbances assessed by the Pittsburgh sleep quality index and insomnia severity index	4 weeks	NA

Figure 19. Clinical trials with melatonin in MS. Skarlis et al, 2020, *Neurological Sciences*

8.2 Pharmacological modulation of endocannabinoids and melatoninergic systems

By combining the pharmacophore elements required for activation of melatonergic receptors with those for FAAH inhibition, such as the N-anilinoethylamide melatonergic ligands and N-alkyl-Oarylcarbamate of FAAH inhibitors, Spadoni et al, synthetized bivalent ligands provided by melatonin receptor agonism and FAAH inhibitory activity, that were tested in experimental models of glaucoma. These compounds, applied topically, were highly effective in reducing the intraocular pressure in rabbits and exhibited a longer action and improved efficacy compared to the reference compounds melatonin and URB-597 (Spadoni et al, 2018). These compounds may represent a potential alternative therapeutic approach for the treatment of ocular hypertension and might offer a promising option for others diseases in light of their neuroprotective and immunomodulatory actions.

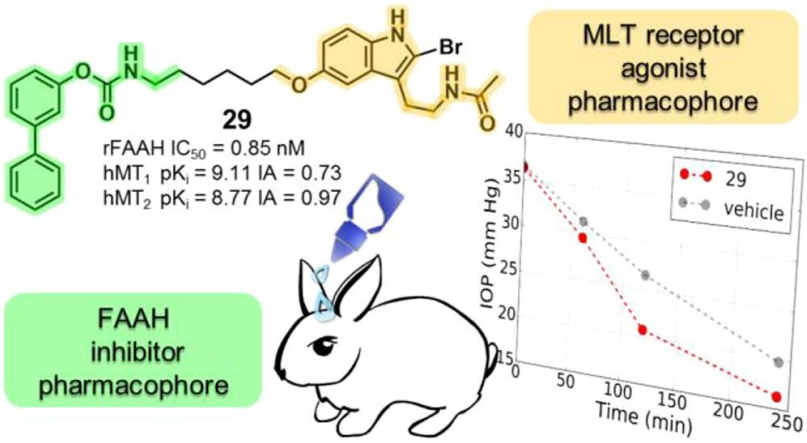

Figure 20. A bivalent ligand with melatonin receptor agonism and fatty acid amide hydrolase (FAAH) inhibitory activity. Spadoni et al, 2018 *Journal Medicinal Chemistry*

II. AIM OF THE STUDY

Oligodendrocytes, the myelin-forming cells in the CNS are the main target of the aberrant auto-immune attack occurring in MS, which chronically leads to persistent demyelination and axonal damage. Astrocytes, resident microglia, and infiltrating macrophages orchestrate the degenerative as well as the protective and remyelinating response after a neuroinflammatory injury (Franklin et al, 2017, Lloyd et al, 2019, Rawji et al, 2020). MS therapies are primarily immunomodulatory and aim at reducing disease activity and relapses in RR-MS, but no neuroprotective or remyelinating therapies are still available to prevent the accumulation of disability and disease progression. Hence, a significant effort is underway to develop molecules with the potential to halt the neurodegenerative and demyelination processes, modulate the microglia/macrophage response to neuroinflammation and stimulate myelin repair, particularly for the treatment of progressive MS forms, for which current therapies are relatively ineffective.
In the present thesis we investigated the neuroprotective potential and remyelinating properties of novel pharmacological compounds targeting the Na^+/Ca^{2+} exchanger NCX3 and the EC system, two distinct key signaling pathways contributing to oligodendrocyte differentiation and neuroprotection.
It has been proposed that dysfunctional NCX exchangers may contribute to detrimental calcium overload and axonal degeneration in white matter demyelinated axons. Although more studies are required to better define the role of each NCX isoform in axon pathology during MS, current knowledge suggest that stimulating NCX3 activity may drive pro-differentiative effects in myelinating glia. Currently, no positive modulators of NCX3 exchanger are still available, but many NCX blockers have been developed in the last decades. Given that the pharmacological effects of NCX blockers rely on what mode of NCX operation is more specifically blocked and which isoform is selectively inhibited, divergent effects on cell survival have been reported in physiological and pathophysiological conditions. Furthermore, since any change in NCX activity dynamically affect Na^+ and Ca^{2+} fluxes and Na^+ and Ca^{2+} gradients tightly control the kinetics and directionality of NCX operation, more studies are required to understand the pharmacological effects of selective NCX3 blockers in oligodendroglia and neuronal cells under demyelinating conditions. These studies will be instrumental to develop and identify novel neurorepair strategies targeting NCX exchangers. Among NCX blockers, the 5–amino-N-butyl-2–(4-ethoxyphenoxy) benzamide hydrochloride (BED), a compound recently synthesized by our research group, is a potent NCX3 inhibitor that blocks both the forward and reverse mode of operation in the nanomolar range.

In the first part of the study we investigated the pharmacological effects of the NCX3 blocker BED in oligodendroglia.
To this aim, the specific objectives of our study were:

1. to investigate the effects of NCX3 inhibition on oligodendrocyte viability and NCXs expression at different time points after BED exposure and following drug-free washout by performing MTT assay, confocal microscopy and Western blotting analyses both in human MO3.13 oligodendrocytes and rat primary OPCs.

2. to explore the dose-dependent effects of BED during chronic exposure and after drug-free washout on NCX activity and intracellular sodium and calcium levels by means of patch-clamp electrophysiology and single-cell Fura-2AM and sodium-binding benzofuran isophthalate (SBFI) video-imaging in human MO3.13 oligodendrocytes.

3. to study the effects of BED exposure and drug-free washout on rat primary OPCs. By employing biochemical analysis, confocal double immunofluorescence with oligodendrocyte lineage markers and patch-clamp electrophysiology we investigated the BED effects on OPCs proliferation and differentiation, as well as on NCX3 expression and I_{NCX} activity.

4. to investigate the effects of BED-free washout on myelin sheet formation and calcium response by means of confocal colocalization analyses and microfluorimetry in rat primary oligodendrocytes.

In the second part of the thesis we investigated the neuroprotective potential of a novel pharmacological compound targeting the EC and the melatoninergic system. Regulating ECs levels by inhibiting FAAH hydrolysing enzymes is an attractive therapeutic perspective in several neuroinflammatory and neurodegenerative conditions. Similarly, melatonin, more commonly known as the sleep hormone is provided by potent immunomodulatory, antioxidant, and protective roles, although the physicochemical properties may limit its clinical efficacy in neurodegenerative conditions. Recently, the novel bivalent ligand UCM-1341, provided of FAAH inhibitory activity and melatonin receptor agonism, has been developed with improved

physicochemical properties and increased metabolic stability if compared to the reference compounds, URB-597 and melatonin.

To investigate the neuroprotective actions of UCM-1341 under neuroinflammatory conditions the specific objectives of our study were:

1. to set up a novel model of neuroinflammatory damage in hippocampal organotypic explants. To this aim we characterized the time-dependent effects of combined Lipopolysaccharide (LPS) and gamma Interferon (IFN-γ) on cell death, inflammation, and demyelination in hippocampal subfileds, by means of confocal microscopy and biochemical studies.

2. to characterize the expression of FAAH enzymes and melatonin MT1 and MT2 receptors at different time points after the neuroinflammatory insults in rat hippocampal organotypic slice cultures. In addition, by performing colocalization analyses, we explored FAAH distribution in neurons, astrocytes and microglia under LPS + IFN-γ exposure.

3. to evaluate the dose-dependent effects of UCM-1341 and references compounds against LPS+IFN-γ induced neuroinflammatory insult and N-Methyl-D-Aspartate (NMDA) - induced excitotoxic damage in rat hippocampal organotypic slices.

4. to evaluate the effect of UCM-1341 on neuronal damage, myelin loss and inflammation, by performing biochemical and quantitative colocalization studies in hippocampal organotypic slice cultures following LPS+IFN-γ exposure.

III. MATERIALS AND METHODS

1. Drugs and materials

The compound BED (Secondo et al, 2015) was kindly provided by Prof. Federico Fiorino and Prof. Beatrice Severino (Department of Pharmacy, University of Naples, Italy). Melatonin was from Sigma, URB-597 and UCM-1341 (Spadoni et al, 2018) were synthetized and kindly provided by Prof. Marco Mor from (University of Parma and Urbino). Propidium iodite (PI), N-methyl-D-aspartate (NMDA), Lipopolysaccharides (LPS), recombinant human interferon-gamma (INF-γ) were from Sigma (Merk). All other drugs or chemicals not mentioned otherwise were from Sigma. All media and serum for MO3.13 cells, OPCs and organotypic hippocampal slice cultures were purchased from Gibco (Milan, Italy). Experimental solutions were prepared daily by appropriate dilutions from stock solution. UCM-1341, URB-597 and melatonin were dissolved in dimethylsulfoxide (DMSO; stock solutions of 25 mM), aliquoted and kept frozen at -20°C. NMDA, was dissolved directly in serum-free medium (stock solutions of 10 mM), LPS was dissolved in D-PBS, and IFN–γ was dissolved directly in BSA 0,1% (stock solutions of 100ug/ml) and then diluted to the desired concentrations.

2. Animals

All animal experiments and animal handling and care were in accordance with the ARRIVE guidelines and the Guide for the Care and Use of Laboratory Animals (EU Directive 2010/63/EU), and the experimental protocol was approved by the Animal Care and Use Committee of "Federico II" University of Naples, Italy, and Ministry of Health, Italy (#515/2019-PR). Female Wistar rats (14-days timed pregnant) were obtained from Charles River Laboratories (Italy) and maintained at a constant temperature (22 -1°C) on a 12-h light/dark cycle (lights on at 7 AM) with food and water *ad libitum*. The pregnant dams were allowed to deliver their pups naturally; 1-3 postpartum littermates were used for OPCs isolation, while 7-9 days postpartum littermates were used for the preparation of organotypic explants. All efforts were made to minimize animal suffering and to reduce the number of animals used.

3. The human oligodendrocyte MO3.13 cell line and drugs exposure

MO3.13 cells at passage 8 were maintained in Dulbecco's modified Eagle's medium (DMEM) supplemented with 10% fetal bovine serum (FBS), 100 U/ml penicillin, 10 lg/ml streptomycin, and 2 mmol/l glutamine (normal medium) (Boscia et al, 2012). During BED treatment and after its suspension, human MO3.13 cells were maintained in a serum-free chemically defined medium composed of DMEM supplemented with 500 μg/l insulin, 100 μg/ml human transferrin, 0.52 μg/l sodium selenite, 0.63 μg/ml progesterone, 16.2 μg/ml putrescine, 100 U/ml penicillin, 100 μg/ml streptomycin, 2 mM glutamine, 5 mg/ml N-acetyl-L-cysteine, and 10 μM D-biotin (OPC medium). 30-300nM BED was incubated for 2, 4, or 6 days. Fresh drug was added to the cultures every 48 hours in fresh medium. The calpain inhibitor, 300nM calpeptin, was incubated at 1 day after BED washout for 15-17 hours. Control cultures were kept in OPC medium.

4. Rat primary OPCs cultures and drugs exposure

OPCs cultures were prepared as previously described (Boscia et al, 2012). OPCs were plated onto poly-D-lysine coated plates in OPC medium supplemented with 10 ng/ml recombinant human platelet-derived growth factor-AA (PDGF-AA) and 10 ng/ml basic fibroblast growth factor (bFGF) each day for 3-4 days to maintain the undifferentiated state at 37°C in a humidified, 5% CO_2 incubator. BED was added to OPCs cultures the day after plating and kept in OPC medium supplemented with mitotic factors for 4 days. Fresh drug was added every 2 days. Control cultures were kept in OPC medium.

5. Rat hippocampal organotypic explants

Organotypic slice cultures were prepared as previously described (Boscia et al, 2006, 2008; de Rosa et al., 2019). Briefly, 400-μm-thick parasagittal slices were obtained from hippocampi of P7- to P9-day-old Wistar rat pups (Charles River Laboratories, Calco, Italy) using a McIlwain tissue chopper (Campden Instruments, Leicester, UK) and placed into ice-cold Hank's balanced salt solution (HBSS, Gibco, Italy) supplemented with 5 mg/ml glucose and 1.5% (v/v) Fungizone. Cultures were then transferred to a humidified semiporous membrane (30-mm Millicell tissue culture plate inserts of 0.4 mm pore size from Millipore, Italy) in six-well tissue culture plates (4 slices per membrane). Each well contained 1.2 ml of tissue culture medium consisting of 50% minimal essential medium (MEM, Gibco, Monza, Italy), 25% HBSS, 25% heat-inactivated horse serum, 6.5 mg/ml glucose, 1 mM glutamine, and 1.5% Fungizone.

Cultures were maintained at a 37°C and 5% CO2-conditioned atmosphere. All experiments were performed on cultures kept in vitro for 12-13 days (DIV).

6. Lipopolysaccharide (LPS) plus gamma interferon (INF-γ) induced neurodegeneration and drug exposure

Hippocampal explants were removed from normal serum-containing medium (NM), washed in and exposed to a combined application of 10μg/ml LPS plus 100ng/ml INF−γ for 96 hours in serum-free medium SFM containing HS (SFM, consisting of NM with serum replaced with MEM). This model, by mimicking the microglia interaction with infiltrating peripheral immune T cells, triggers the release of massive proinflammatory and cytotoxic factors, and promotes an inflammatory neurodegeneration (Papageorgiou et al, 2010). Appropriate concentrations of UCM-1314, (01-1-10μM), URB-597, (10μM) and melatonin (10μM), or vehicle dimethyl sulfoxide solution (DMSO ≤0.1%) were added to the medium at the beginning of the insult, and were kept in the culture medium during the entire duration of the experiment. Control culture explants, in the absence or in the presence of compounds, were kept in SFM.

7. NMDA induced neurodegeneration and drugs exposure

N-Methyl-D-aspartate (NMDA) exposure was performed in hippocampal cultures as previously described (Boscia et al, 2006). Organotypic hippocampal slice cultures were removed from normal serum-containing (Boscia et al, 2006) NM, washed in SFM and exposed to 10-30μM NMDA (with or with-out additional compounds) for 24-48 hours in fresh SFM. Control hippocampal cultures were kept in SFM.

Assessment of cell death and image analysis

Cell injury was assessed in explants by live incorporation of a marker of compromised membrane integrity, propidium iodide (PI, 5 μg/ml, Molecular Probes), that emits a bright red fluorescence when exposed to blue-green light. For densitometric measurements, the digital pictures were analyzed with the Image Pro-Plus software (Media Cybernetics), after freehand outlining of the CA neuronal layer, as previously described (Boscia et al, 2006, 2008).

8. MTT assay

The MTT analyses were performed by incubating cells with (3- (4, 5-dimethylthiazol-2-yl)-2, 5-diphenyltetrazolium bromide (MTT, 0.5 mg/ml) and incubated at 37°C in a 5 % CO_2, 95 % air atmosphere for 30 minutes. Then, the MTT solution was replaced with DMSO, 1 ml to each well, and the MTT absorbance was measured at 590 nm using a spectrophotometer (Eppendorf BioPhotometer).

9. Western blotting

Lysates from human MO3.13 progenitors, OPCs and rat hippocampal organotypic slice cultures were separated on 8 or 14% sodium dodecyl sulphate polyacrylamide gel and electrophoretically transferred onto nitrocellulose membranes, as described (Esposito et al, 2012; Boscia et al, 2015). Filters were probed with the indicated primary antibodies: rabbit polyclonal anti-NCX3 (1:500, Abcam), mouse monoclonal anti-NCX1 (Swant, 1:1000 dilution), rabbit polyclonal anti-NCX2 (Alpha Diagnostics International, 1:1000 dilution), rabbit polyclonal anti-sodium/potassium-transporting ATPase subunit alpha-2 (α_2-NKA, 1:1000, Proteintech), anti-β−actin (1:1000, Sigma, Italy), anti-α-tubulin (1:1,000; #T5168, Sigma, Milan, Italy) rabbit polyclonal anti- fatty acid amide hydrolase (1:5000, Cayman) polyclonal anti-glial fibrillary acidic protein GFAP (1:1000, Sigma), monoclonal mouse anti-Iba1 (1:2000, Dako), monoclonal mouse anti-MEL-1A/B-R (1:1000, Santa Cruz) rat monoclonal anti-myelin basic protein (1:1000, Merk), rabbit polyclonal anti-mannose receptor CD206 (1:5000, Abcam). Proteins were visualized with peroxidase-conjugated secondary antibodies, using the enhanced chemiluminescence system (Amersham-Pharmacia Biosciences LTD, Uppsala, Sweden). Films were scanned and the signal ratio protein of interest/housekeeping protein was quantified densitometrically.

10. In vitro NCX3 silencing

Silencing of NCX3 in MO3.13 cells was performed by using the HiPerFect Transfection Kit (Qiagen, Milan, Italy), by using the following FlexiTube siRNAs for NCX3, Hs_Slc8A3(#8) 50- CACCACGCTCTTGCTTCCTAA-30, and a validated irrelevant AllStars siRNA as a negative control (siCtl), as previously described (Boscia et al 2012, de Rosa et al 2019). Following BED treatment for 4 days, cells were incubated with Opti-MEM (Invitrogen)

supplemented with the RNAiFect Transfection Reagent (Qiagen) and 20 nM of the siRNA duplex for 6 h. Cells were incubated in BED-free OPC medium for 48 hours before performing electrophysiological recordings.

11. Confocal immunofluorescence analysis

Confocal immunofluorescence procedures in cells or slices were performed as previously described (Boscia et al 2008, 2009, 2015). Cell cultures or slices were fixed in 4% wt/vol. paraformaldehyde in phosphate buffer for 30-60 minutes. After blocking with 3% BSA, cells or slices were incubated with the following primary antibodies for 24 hours. The primary antibodies used were the following: rabbit polyclonal anti-NCX3 (1:4000, Swant), rabbit polyclonal anti-α_2-NKA (1:1000, Proteintech), mouse monoclonal anti-CNPase (1:1000, Millipore), rat monoclonal anti-myelin basic protein MBP (1:1000, Merk), mouse monoclonal anti-calcium/calmodulin-dependent protein kinase IIβ (CAMKIIβ, 1:2000, Life-techonlogies), mouse monoclonal anti-ki67 (1:500, eBioscence). Then, cells were incubated with corresponding fluorescence- labeled secondary antibodies (Alexa488- or Alexa594-conjugated anti-mouse or anti-rabbit IgGs). Dapi was used to stain nuclei. Images were observed using a Zeiss LSM 700 laser (Carl Zeiss) scanning confocal microscope. Single images were taken with an optical thickness of 0.7 μm and a resolution of 1,024 × 1,024. All staining and morphological analyses were blindly conducted. Confocal immunofluorescence procedures in slices were fixed in 4% wt/vol paraformaldehyde in phosphate buffer (PB) for 1 h, blocked with 3% bovine serum albumin (BSA) and 0.05% Triton X (Sigma, Milan, Italy) for 40 minutes, and then incubated with rabbit polyclonal anti- fatty acid amide hydrolase (1:1500, Cayman), rabbit polyclonal anti-GFAP (1:1000, Sigma), mouse monoclonal anti-Iba1 (1:2000, Dako), mouse monoclonal anti- microtubule-associated proteins MAP2 (1:2000, Millipore), rabbit polyclonal anti- neurofilament-200 (anti-NF200; 1:500, Sigma), monoclonal anti-myelin basic protein (1:1000, Covance), rabbit polyclonal anti-mannose receptor CD206 (1:13000, Abcam), polyclonal anti-Gaba (1:400, Merk.) primary antibodies for 48 hours at 4°C. Then, cells o slices were incubated with the corresponding secondary antibodies overnight at 4°C, and finally mounted on glass slides and imaged with Zeiss LSM 700 laser (Carl Zeiss) scanning confocal microscope.

Quantitative analysis

Images were processed and analyzed with the public domain Java-based image processing software ImageJ (National Institutes of Health, Bethesda, Maryland, USA).

The number of NG2+ cells displaying no NCX3 immunoreactivity (NCX3-negative cells) and NCX3 immunoreactivity only in the soma (S) or both in the soma and proximal processes (S+P), as well as the number of $NG2^+$ cells displaying α2-NKA immunoreactivity, Ki67 signal in the nucleus, and the number of double-labelled $NCX3^+/MBP^+$ cells was determined by manual counting at × 40 magnification. In NG2/NCX3 colocalization studies, all cells with bipolar or multipolar morphology showing a clearly visible punctate NCX3 labeling were counted. Quantification of CAMKIIβ and α2-NKA fluorescence intensities were quantified in terms of pixel intensity by using the NIH image software, as described previously (Boscia et al, 2012, de Rosa et, 2019). Briefly, digital images were taken with 63 × objective and identical laser power settings and exposure times were applied to all the photographs from each experimental set. Oligodendroglial cell morphology *in vitro* was evaluated with Alexa594–phalloidin (Thermo Fisher Scientific, Milan, Italy), as previously described (Zuchero et al, 2015; de Rosa et al, 2019). Individual phalloidin-positive oligodendrocytes were scored according to their morphological complexity in four categories: (i) *bipolar/stellate,* defined as cells having from two to four processes; *multipolar*, including cells having more than four radially oriented processes, (ii) *arborized*, including cells with radially oriented arborization pattern containing intersections (iii) *partial ring,* including cells with arborized morphology but also containing ring-like regions; and (iv) *ring*, including oligodendrocytes with fully ring-like morphology. Quantification of relative cell surface area occupied by MBP protein was performed with ImageJ using the application: threshold from background, followed by manually defining the area, and finally measuring the area fraction above the threshold.

Quantification of colocalization studies in hippocampal slices

The quantification of co-localization between FAAH and MAP2, GFAP, Iba1, MBP and NF200 immunostaining was assessed by using the 'co-localization highlighter' plug-in for the ImageJ software (NIH, Bethesda, MA, USA). Before co-localization analysis, images were first thresholder to identify the positive signal, subsequently, the pixels expressing both FAAH and MAP2, GFAP and Iba1 and MBP, NF200 were identified. Finally, the number of pixels positive

for FAAH/MAP, GFAP/Iba1 and MBP/NF200 was measured per microscope field, as previously described (de Rosa et al, 2019). This value, expressed as percentage of co-localization, represents the extent of FAAH/MAP2, FAAH/GFAP, FAAH/IBA1 and MBP/NF200 coexpression. Four to five independent slices were analysed per condition.

12. Microfluorimetric $[Ca^{2+}]_i$ and $[Na^+]_i$ measurements

Intracellular changes in $[Ca^{2+}]_i$ and $[Na^+]_i$ were measured by means of single-cell Fura-2 AM and sodium-binding benzofuran isophthalate (SBFI) video-imaging technique, in oligodendrocyte MO3.13 progenitors and rat primary OPCs plated on 10 μg/ml poly-D-lysine-coated glass coverslips, as previously described (Secondo et al, 2015).

Fura-2 calcium imaging. Cells were incubated with 6 mM Fura-2 AM for 30 minutes at 37°C in normal Krebs solution containing 5.5 mM KCl, 160 mM NaCl, 1.2 mM $MgCl_2$, 1.5 mM $CaCl_2$, 10 mM glucose, and 10 mM HEPES-NaOH (pH 7.4). Then, the coverslips were placed into a perfusion chamber (Medical System Co., Greenvale, NY, USA), mounted onto the stage of an inverted Zeiss Axiovert 200 microscope (Carl Zeiss, Milan, Italy), equipped with a FLUAR 40× oil objective lens. The experiments were carried out with a digital imaging system composed of a MicroMax 512BFT cooled CCD camera (Princeton Instruments), LAMBDA10–2 filter wheeler (Sutter Instruments), and Meta-Morph/MetaFluor Imaging System software (Universal Imaging). Cells were alternatively illuminated at wavelengths of 340 and 380 nm by a Xenon lamp. The emitted light was passed through a 512 nm barrier filter. Fura-2 fluorescence intensity was measured every 3 s. Fura-2 ratiometric values were automatically converted by Meta-Morph/MetaFluor Imaging System software (Universal Imaging) to $[Ca^{2+}]_i$ by using a preloaded calibration curve obtained in preliminary experiments, as described (Grynkiewicz et al 1985). Both sodium-free induced calcium response and intracellular Ca^{2+} transients after 100μM D-Aspartate stimulation were recorded in primary oligodendrocyte cultures by using the Meta-Morph/MetaFluor Imaging System software (Universal Imaging). $[Ca^{2+}]_i$ was analyzed within the traced rows at the cell soma and proximal processes, as indicated in Figure 7B. For each cell, 3-4 proximal processes were recorded. The effect of D-Asp was quantified as Δ% of peak-basal values of $[Ca^{2+}]_i$. The mean value of the last 10 seconds of acquisition was considered the peak useful for the quantification.

SBFI sodium imaging. To load SBFI, coverslips plated with cells were placed in standard perfusion medium containing 10 μM SBFI-AM and 0.1% Pluronic F-127 in the presence of 5 mg/ml bovine serum albumin, and incubated for 120–180 min at 37°C. Then, coverslips were placed in standard medium for 20 min to ensure de-esterification of the dye and then mounted in the chamber. Cells were excited alternately at 334 and 380 nm via a ×40 LD Achroplan objective, by using the same apparatus described above for Fura-2 experiments. The *in vitro* calibration of SBFI was accomplished by using the in situ procedure, according to Diarra et al, 2001. Specifically, SBFI ratios measured during the course of experiments were transformed into $[Na^+]_i$ values by a "one-point" procedure in which, at the end of an experiment, SBFI-loaded cells were exposed to a pH 7.3 medium containing 10 mM Na^+ and 4 μM gramicidin D.

13. Electrophysiology

NCX currents (I_{NCX}) in human MO3.13 oligodendrocytes were recorded by the patch-clamp technique in whole-cell configuration using the amplifier Axopatch200B and Digidata1322A interface (Molecular Devices), as previously described (Molinaro et al, 2008, Pannaccione et al 2007, Boscia et al, 2007). I_{NCX} were recorded starting from a holding potential of -60 mV up to a short-step depolarization at +60 mV (60ms). A descending voltage ramp from +60 mV to -120 mV was applied. I_{NCX} recorded in the descending portion of the ramp (from +60 mV to -120 mV) were used to plot the current-voltage (I–V) relation curve. The I_{NCX} magnitude was measured at the end of +60 mV (reverse mode) and at the end of -120 mV (forward mode), respectively. The Ni^{2+}-insensitive component was subtracted from total currents to isolate I_{NCX}. The MO3.13 cells were perfused with the external Ringer's solution containing the following (in mM): 126 NaCl, 1.2 $NaHPO_4$, 2.4 KCl, 2.4 $CaCl_2$, 1.2 $MgCl_2$, 10 glucose, and 18 NaHCO3, pH 7.4. Twenty millimolar tetraethylammonium (TEA), and 10mM nimodipine were added to Ringer's solution to abolish potassium and calcium currents. The dialyzing pipette solution contained the following (in mM): 100 Cs-gluconate, 10 TEA, 20 NaCl, 1 Mg-ATP, 0.1 $CaCl_2$, $2MgCl_2$, 0.75 EGTA, and 10 HEPES, adjusted to pH 7.2 with CsOH. Possible changes in cell size occurring after specific treatments were calculated by monitoring the capacitance of each cell membrane, which is directly related to the membrane surface area and by expressing the current amplitude data as current densities (pA/pF). Capacitive currents were estimated from the decay of the capacitive transient induced by 5 mV depolarizing pulses from a holding potential of –80 mV and acquired at a sampling rate of 50 kHz. The capacitance of the membrane was calculated according to the following equation: Cm=tc·Io/DEm(1-I¥/Io), where

Cm is membrane capacitance, tc is the time constant of the membrane capacitance, Io is the maximum capacitance current value, DEm is the amplitude of the voltage step, and I¥ is the amplitude of the steady-state current. I_{NCX} in the different experimental conditions were expressed as percentage of internal controls.

14. Statistical analysis

In results I, statistical analysis was performed by using two-tailed Student's *t-test*, one-way ANOVA followed by Bonferroni or Tukey *post-hoc test* as indicated in the legends of figures. Analysis was done using the software Graph Pad Prism 6. Values represent the mean ± SEM of at least three independent experiments. Differences were considered statistically significant at * $p < 0.05$. In results II, statistical analysis was performed by using one-way ANOVA followed by Bonferroni post-hoc test as indicated in the legends of figures. Analysis was done using the software GraphPad Prism 5. Values represent the mean ± SEM of at least three independent experiments. Differences were considered statistically significant at * p < 0.05.

IV. RESULTS

Results I

1. Time and dose-depending effects of BED exposure on cell viability in human MO3.13 oligodendrocyte progenitors.

To test the effects of NCX3 blocking on cell viability, human MO3.13 oligodendrocyte cells were incubated with different concentrations of the NCX3 inhibitor 30-100-300 nM BED for 4 or 6 days. BED treatment did not significantly affected cell viability at any of the concentrations used or time points analysed, as revealed by MTT assay (Fig. 1A). Next, to evaluate whether prolonged BED exposure may influence NCX3 expression levels, human MO3.13 oligodendrocytes were incubated in the absence or in the presence of 30-100-300nM BED for 6 days and cell lysates were analysed. In line with previous studies, the anti-NCX3 antibody revealed 3 main chemiluminescent bands in human MO3.13 lysates: a doublet of ~105 kDa corresponding to the full-length NCX3, a band of ~70 kDa and a cluster of bands of 58-60 kDa, referred as NCX3 calpain-cleaved fragments provided by exchanger activity (Pannaccione et al, 2012) (Fig. 1B). Densitometric analysis of NCX3 immunoreactive bands showed that BED exposure for 2-4 days (data not shown) or 6 days did not significantly affected NCX3 protein levels at neither of the concentration used (30-300nM), if compared to untreated cultures (Fig. 1C).

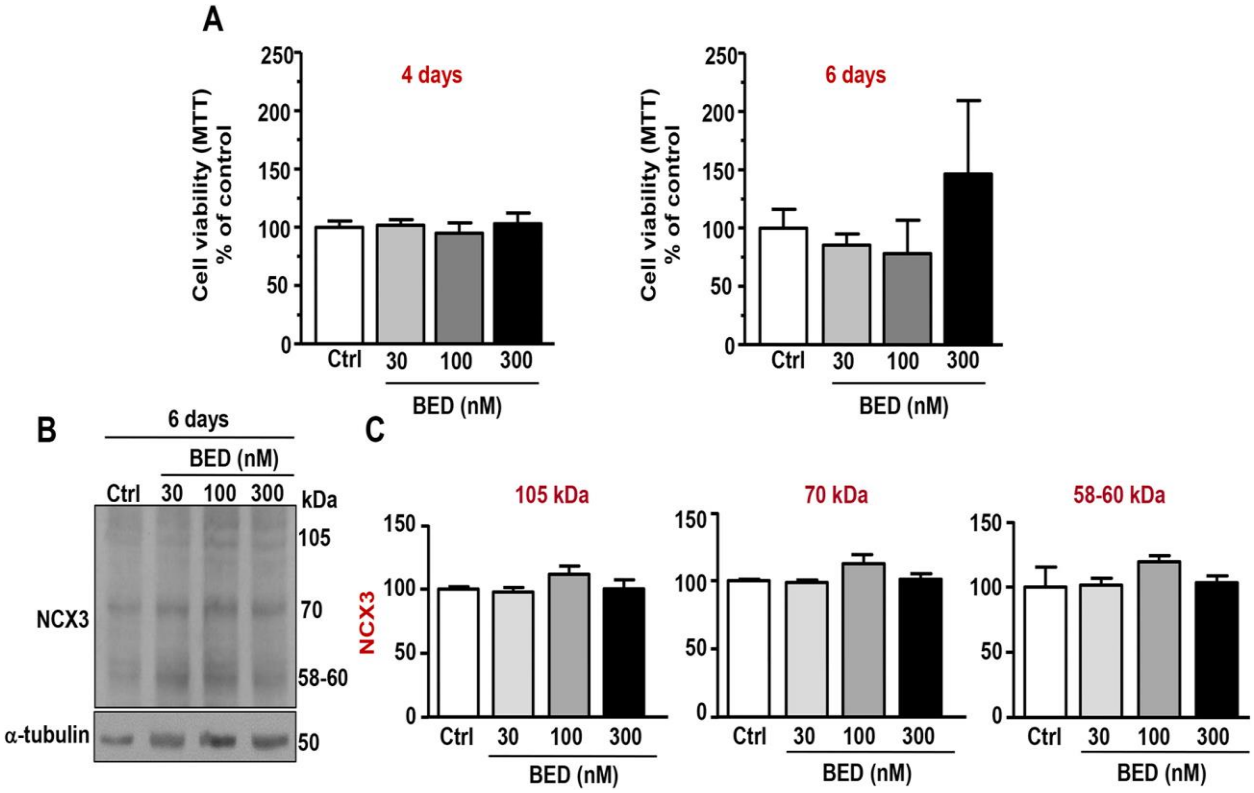

Figure 1. Time and dose-depending effects of BED exposure on cell viability and NCX3 expression in human MO3.13 oligodendrocytes. **A**, Cell viability measured by MTT assay in M03.13 cells exposed to 10, 100, or 300 nM BED for 4 days (left) or 6 days (right). Data are expressed as percentage of control. The values represent the mean±S.E.M. (n = 3). **B**, Western blotting analysis of NCX3 protein levels from homogenates of MO3.13 oligodendrocytes cultured in the absence or in the presence of 30, 100, or 300 nM BED for 6 days; **C**, Densitometric analysis of the three major NCX3-specific enhanced chemiluminescence bands at ~105 kDa (left), 70 kDa (middle), and 58–60 kDa (right). Data were normalized on the basis of α-tubulin levels and expressed as percentage of control. The values represent the means±S.E.M (n = 3).

2. Effects of BED exposure for 6 days on NCX3 expression and I_{NCX} activity in human MO3.13 oligodendrocytes.

Then, we tested the effects of BED exposure for 6 days plus 2 days of washout on NCX3 protein distribution and expression in human MO3.13 oligodendrocytes. Confocal analysis performed with anti-NCX3 antibodies depicted a moderate NCX3 immunosignal in the cytosolic compartment after 6 days of BED exposure. One day after BED-free washout, a pronounced plasma membrane NCX3 immunoreactivity was observed only in cells exposed to BED for 6 days (Fig. 2A). In MO3.13 oligodendrocytes exposed to BED for 6 days a more intense NCX3 immunostaining was observed both in the cytosol and plasma membrane compartments if compared to untreated cells. Twenty percent of stained NCX3-positive cells with a rounded morphology were observed only in MO3.13 cultures exposed to BED for 6 days + 2 days of washout (Fig. 2A, c). Nevertheless, the NCX3 inhibitor, 100nM BED, did not significantly affected cell viability after 6 days of BED treatment + 2 days of washout, as revealed by MTT assay (Fig. 2D). Western blot and quantitative densitometric analyses revealed that when cells were exposed to 100nM BED for 6 days + 2 days of drug washout a significant upregulation of NCX3 bands at 58-60kDa was observed.

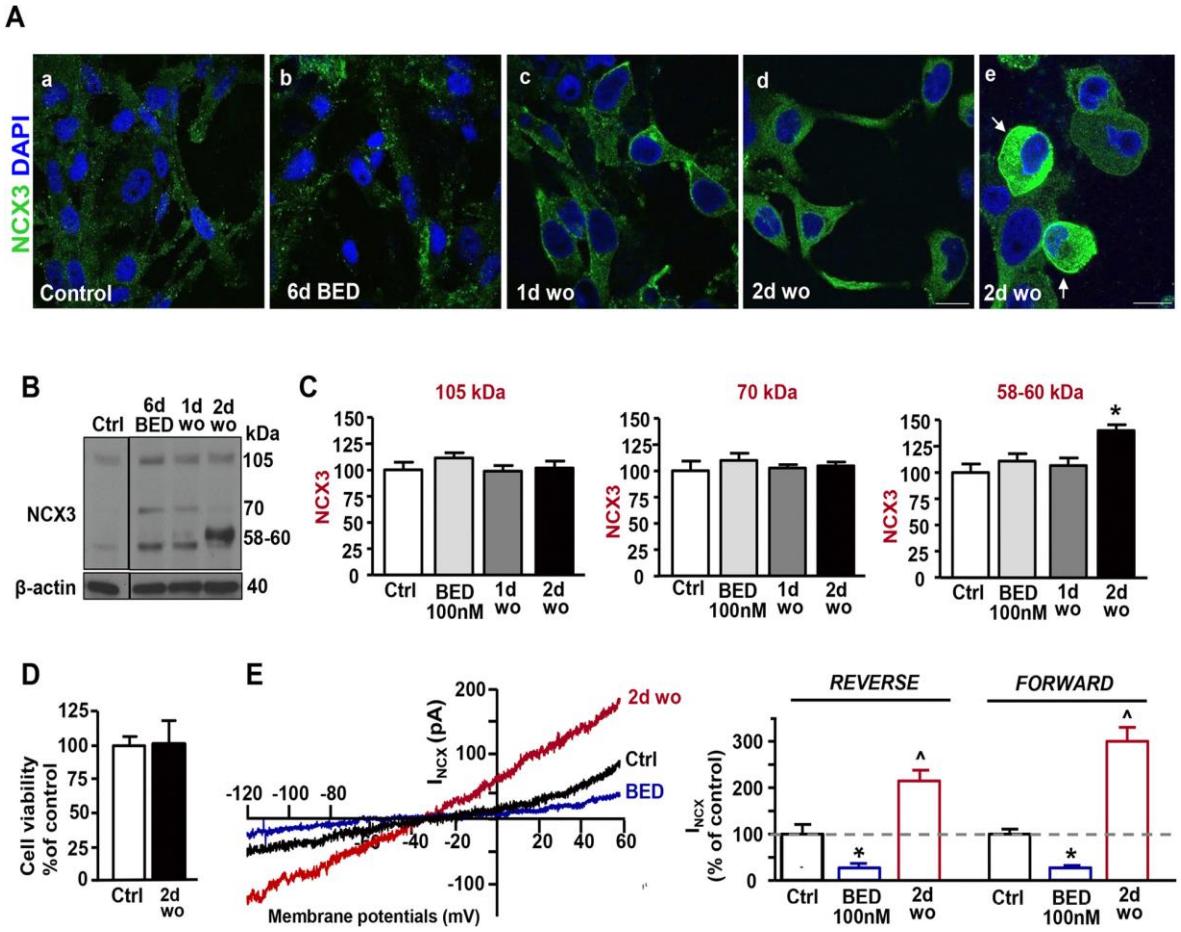

Figure 2. Effect of 6-days BED treatment and washout on NCX3 expression and I_{NCX} in human MO3.13 oligodendrocytes. A, Representative confocal microscopic images showing NCX3 immunoreactivity in MO3.13 oligodendrocytes under control conditions (a), in the presence of 100 nM BED for 6 days (b), and after drug-free washout for 1 (c) or 2 days (d-e). Panel e shows a representative MO3.13 cells with rounded morphology displaying an intense NCX3 immunoreactivity within the soma and along plasma membrane (arrows). Scale bar: a-e: 20 μm. **B**, Western blotting analysis of NCX3 protein levels from homogenates of MO3.13 oligodendrocytes cultured under control conditions, in the presence of 100 nM BED for 6 days, and after drug-free washout for 1–2 days. **C**, Densitometric analysis of the three major NCX3-specific enhanced chemiluminescence bands of ~105 kDa (*left*), 70 kDa (*middle*), and 58–60 kDa (*right*). The data were normalized on the basis of *β*-actin levels and expressed as percentage of control. The values represent the means±S.E.M. (n = 3). *p < 0.05 versus control. **D**, Cell viability measured by MTT assay in untreated or M03.13-treated cells exposed to 100 nM BED for 6 days + 2 days after BED-washout. Data were expressed as percentage of control. The values represent the means±S.E.M. (n = 3). **E**, *left*. Representative I_{NCX}-superimposed traces recorded from MO3.13 oligodendrocytes under control conditions (black), in the presence of 100 nM BED for 6 days (blue), and 2 days after BED washout (red). E, *right*, I_{NCX} quantification is expressed as % of control in conditions, in the presence of 100 nM BED for 6 days and 2 days after BED washout. Each bar represents the mean±S.E.M. of the data obtained from 20 cells per group in three independent experimental sessions. *p < 0.05 versus control.

3. Effects of BED exposure for 4 days on NCX3 expression and I_{NCX} activity in human MO3.13 oligodendrocytes.

Then, we tested the effects of BED exposure for 4 days plus 2 days washout on NCX3 protein distribution and expression in human MO3.13 oligodendrocytes. Confocal analysis performed with anti-NCX3 antibodies depicted a moderate NCX3 immunosignal in the cytosolic compartment after 4 days of BED exposure. In MO3.13 oligodendrocytes exposed to BED for 4 days + 2 days after BED washout, a more intense NCX3 immunostaining was observed both in the cytosol and plasma membrane compartments if compared to untreated cells (Fig. 3A). The NCX3 inhibitor 100nM BED did not significantly affected cell viability after 4 days of BED treatment + 2 days of washout, as revealed by MTT assay (Fig. 3D). Western blot and quantitative densitometric analyses revealed that BED treatment for 4 days + 2 days washout significantly upregulated both the 75kDa and 58-60kDa NCX3 bands. (Fig. 3B-C). Next, to investigate whether the increased NCX3 protein levels observed after BED treatment + drug washout was accompanied by an upregulation of NCX currents (I_{NCX}), we performed patch-clamp electrophysiology in MO3.13 oligodendrocytes. As expected, 100nM BED treatment significantly reduced $I_{NCX,}$ both in the forward and reverse mode of operation (Fig. 3D). By contrast, I_{NCX}, recorded after 2 days of BED washout, significantly increased in cells exposed to 100nM BED for 4 days. Interestingly, a selective enhancement of *reverse* NCX *operational mode was recorded* in MO3.13 oligodendrocytes exposed to BED for 4 days + 2 days of washout. Dose-dependent electrophysiological responses showed that 30nM BED was less effective to block I_{NCX} after 4 days of treatment, while it has no significant effect on I_{NCX} currents after drug washout (Fig. 3E).

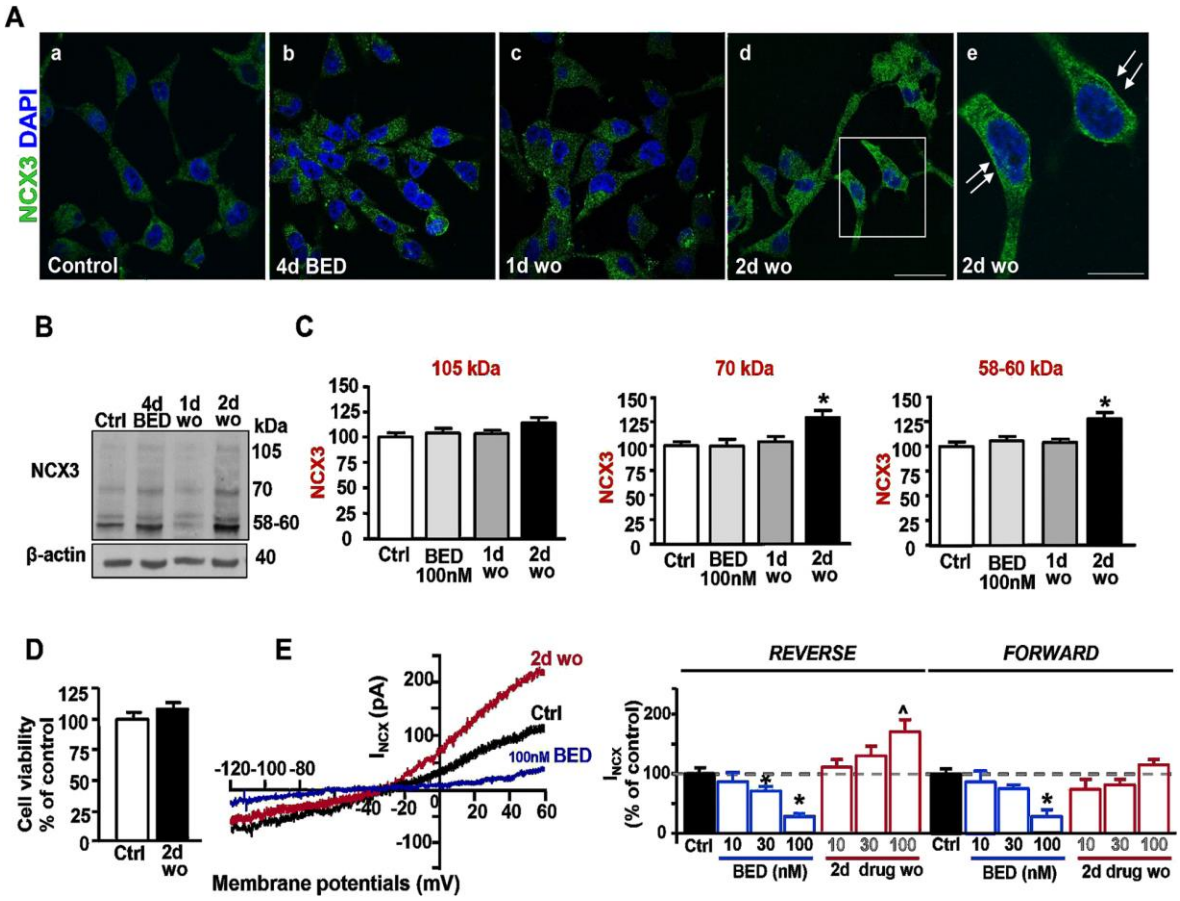

Figure 3. Effect of 4-days BED treatment and washout on NCX3 expression and I_{NCX} in human MO3.13 oligodendrocytes. A, Representative confocal microscopic images showing NCX3 immunoreactivity in MO3.13 oligodendrocytes cultures under control conditions (a), in the presence of 100 nM BED for 4 days (b) and after drug-free washout for 1 (c) or 2 days (d-e). Panel e shows higher magnification image of the frame depicted in panel d. Arrows point to NCX3 immunoreactivity along cell plasma membrane. Scale bars in a-d: 50 μm; in e: 20 μm. **B**, Western blotting analysis of NCX3 protein levels from homogenates of MO3.13 oligodendrocytes cultured under control conditions, in the presence of 100 nM BED for 4 days, and after drug-free washout for 1–2 days. **C**, Densitometric analysis of the three major NCX3-specific enhanced chemiluminescence bands of ~105 kDa (*left*), 70 kDa (*middle*), 58–60 kDa (*right*). The data were normalized on the basis of *β*-actin levels and expressed as percentage of control. The values represent the means±S.E.M. (n = 3). *p < 0.05 versus control. **D**, Cell viability measured by MTT assay in untreated or M03.13 cells exposed to 100 nM BED for 4 days + 2 days after BED-washout. Data were expressed as percentage of control. The values represent the means±S.E.M. (n = 3). **E**, *left*. Representative I_{NCX}-superimposed traces recorded from MO3.13 cells under control conditions (black), in the presence of 100 nM BED for 4 days (blue), and 2 days after BED washout (red). E, *right*, I_{NCX} quantification is expressed as % of control in control conditions, in the presence of 30–100 nM BED for 4 days and after 2 days of BED washout. Each bar represents the mean±S.E.M. of the data obtained from 20 cells per group in three independent experimental sessions. *p < 0.05 versus control.

Conversely, 10nM BED was ineffective to inhibit I_{NCX} during drug treatment or enhance I_{NCX} and NCX3 protein levels after drug washout.

To further confirm the specificity of BED for NCX3 we evaluated the expression levels of NCX1 and NCX2 exchangers in response to 4- and 6-days 100nM BED treatment and subsequent drug-free washout. To this aim, filters were stripped and probed with anti-NCX1 and anti-NCX2 antibodies. Densitometric analysis of NCX1 major bands revealed that NCX1 protein levels were significantly upregulated by BED treatment after both 4 or 6 days. During BED-free washout NCX1 levels remained significantly higher in the 6-days protocol, while they returned to basal levels in the 4-days protocol. The 102 kDa band of NCX2 was not altered by BED treatment neither after 4 or 6 days (Fig. 4A-B). During BED-free washout NCX2 protein levels significantly increased after 2 days in the 6-days protocol, while they were only transiently upregulated after one day in the 4-days protocol (Fig. 4C-D). These results suggest that BED suspension after 4 days of exposure selectively enhanced reverse I_{NCX} activity and selectively affected NCX3 levels 2 days after drug washout.

Finally, to further to further verify the involvement of NCX3 in BED-induced pharmacological effects, we silenced ncx3 gene in MO3.13 cells after 4 days of BED treatment. Then, cells were kept in BED-free OPC medium for 48 hours before performing electrophysiological analyses. As shown in Fig. 4E-F, silencing ncx3 gene during drug washout significantly prevented the upregulation reverse I_{NCX} activity. These results suggest that NCX3 significantly contributed to the reverse I_{NCX} activity recorded after 4 days of BED treatment + 2 days of BED-free washout.

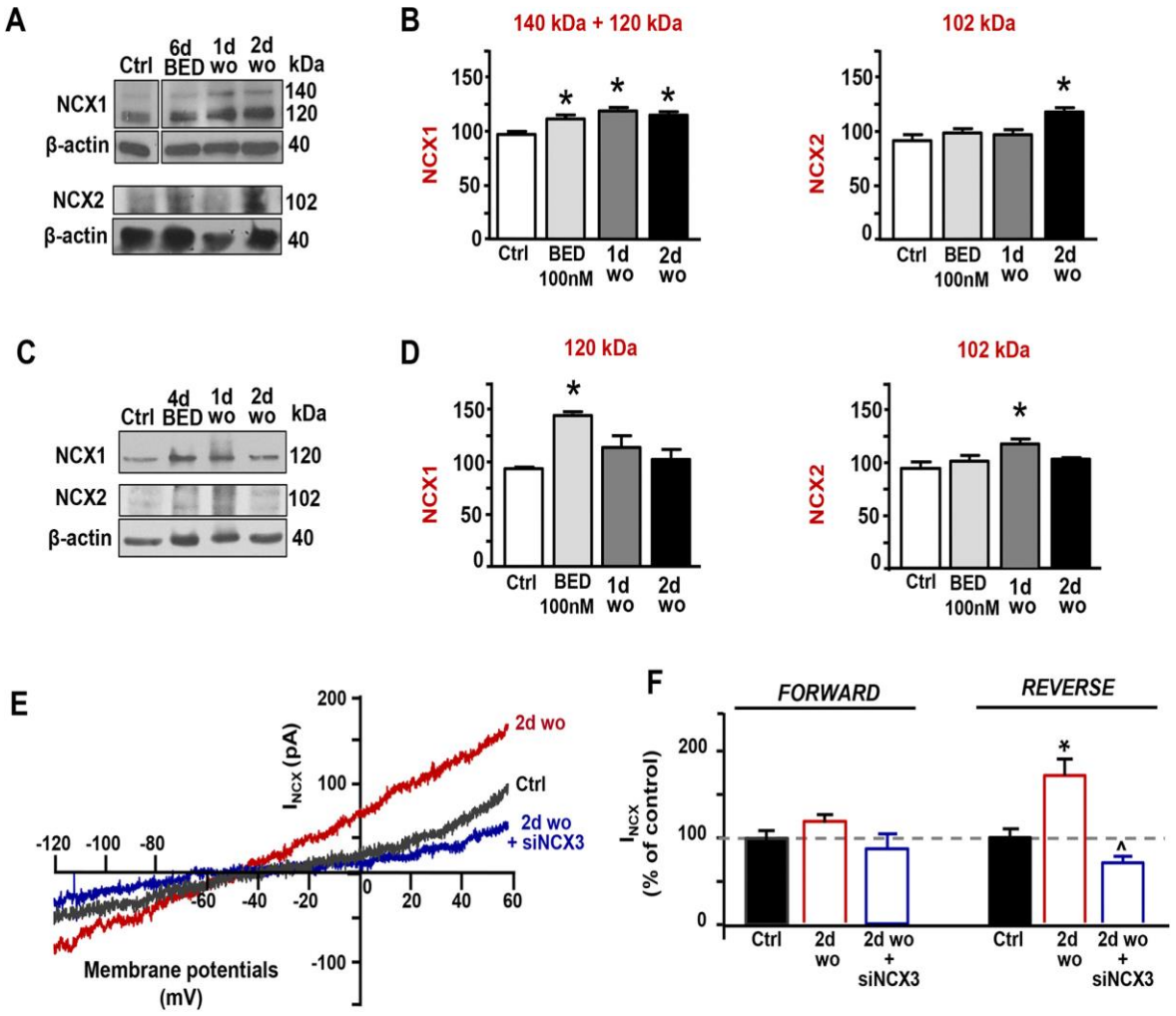

Figure 4. Effect of BED treatment on NCX1 and NCX2 protein levels and of *ncx3* gene silencing on I_{NCX} in human MO3.13 oligodendrocytes. A-B, Western blot and densitometric analysis of NCX1 and NCX2 protein levels from homogenates of MO3.13 oligodendrocytes cultured under control conditions, in the presence of 100 nM BED for 6 days, and after drug-free washout for 1–2 days. The filter showed in Fig. 2B was stripped and blotted with anti-NCX1 antibody. **C-D**, Western blot and densitometric analysis of NCX1 and NCX2 protein levels from homogenates of MO3.13 oligodendrocytes cultured under control conditions, in the presence of 100 nM BED for 4 days, and after drug-free washout for 1–2 days. The filter showed in Fig.2E was stripped and blotted with anti-NCX1 or anti-NCX2 antibodies. The values represent the means±S.E.M. (n = 3). *p < 0.05 versus control. **E**, Representative I_{NCX}-superimposed traces recorded from MO3.13 cells days after 4 days of 100 nM BED treatment + 2 days of BED washout under control conditions (black) and in absence (red) or in presence of siNCX3 (blue). **F**, I_{NCX} quantification is expressed as % of control. Each bar represents the mean±S.E.M. of the data obtained from 20 cells per group in three independent experimental sessions. *p < 0.05 versus control.

4. BED exposure induced $[Na^+]_i$ accumulation, and modulate α_2-NKA protein expression and $[Ca^{+2}]_i$ levels after drug washout in human MO3.13 oligodendrocytes.

Next, considering that $[Na^+]_i$ is the main regulator of exchange mode and activity of NCX (Annunziato et al, 2013; Boscia et al, 2016), we speculated that the NCX3 inhibitor BED would partly occlude Na^+ extrusion and may induce $[Na^+]_i$ accumulation during prolonged exposure, consequently driving Ca^{2+} influx after drug washout. (Fig. 5A). To test this hypothesis, by means of SBFI- and Fura-2 video-imaging, we first recorded intracellular $[Na^+]_i$ at 4 days after BED exposure, and then intracellular $[Ca^{2+}]_i$ after BED washout in human MO3.13 oligodendrocytes (Fig. 5B). As shown, $[Na^+]_i$ levels significantly increased in MO3.13 cells exposed to 100nM BED for 4 days if compared to untreated cells. Fura-2 video imaging showed that 3 hours after BED washout a significant $[Ca^{2+}]_i$ rise was recorded in cultures exposed to 100nM BED for 4 days if compared to untreated cells or BED-treated cells. The reverse NCX3 inhibitor, 100nM YM-24476, applied 2,5 hours after BED washout, significantly prevented $[Ca^{2+}]_i$ rise in MO3.13 cells thus suggesting that NCX3 activity contributes to BED washout-induced calcium increase. Previous studies showed that a sustained increase in $[Ca^{2+}]_i$ may generate calpain-cleaved forms of NCX3 (Iwamoto et al, 2006), that may lead to increased functional activity of the antiporter in the reverse mode of operation (Pannaccione et al, 2012) or exchanger inactivation (Iwamoto et al, 2006). Hence, we investigated whether the increased NCX3 protein levels observed during BED washout in MO3.13 cells might be attributed to the exchanger cleavage mediated by calpains. To this aim, MO3.13 cultures were first incubated with BED for 4 days, and then with the calpain inhibitor, calpeptin, during drug washout. Western blots analysis showed that 300nM calpeptin significantly prevented the upregulation of both 75 kDa and 58-60 kDa NCX3 bands if compared to untreated cultures, thus suggesting that the upregulation of NCX3 minor bands is associated with increased fragmentation of NCX3 exchanger mediated by a calcium-dependent activation of calpains (Fig. 5C-D). Then, based on the observation that the Na^+/K^+-ATPase (NKA), a major regulator of $[Na^+]_i$, and cell volume, is functionally coupled to NCX (Bano et al, 2005), and that the α_2-NKA isoform can modulate NCX-mediated Ca^{2+} influx in oligodendrocytes (Hamman et al, 2018), we investigated the effects of BED exposure and washout on α_2-NKA protein levels. Densitometric analysis of Western blot experiments revealed that α_2-NKA protein levels remained unchanged after 4 days of BED exposure if compared to untreated cells, significantly decreased at 1 day of BED washout, and subsequently increased over the basal levels at 2 days of BED washout (Fig. 5E). Conversely, the α_2-NKA protein levels remained unchanged when human MO3.13

oligodendrocytes were exposed to BED for 2 days + 1 or 2 days of drug washout (Fig. 5F). Based on recent findings showing that silencing α_2-NKA expression in oligodendrocytes not only stimulated NCX-mediated $[Ca^{2+}]_i$ rise but also boosted myelin marker expression, we explored the localization of the myelin marker CNPase in human MO3.13 oligodendrocytes during BED washout. Confocal double-labeling experiments and line profiling the CNPase (red) and NCX3 (green) fluorescence intensities showed an enhanced coexpression of NCX3 and CNPase immunoreactivities along plasma membrane domains of cell exposed to BED for 4 days + 2 days of drug washout (Fig. 5G).

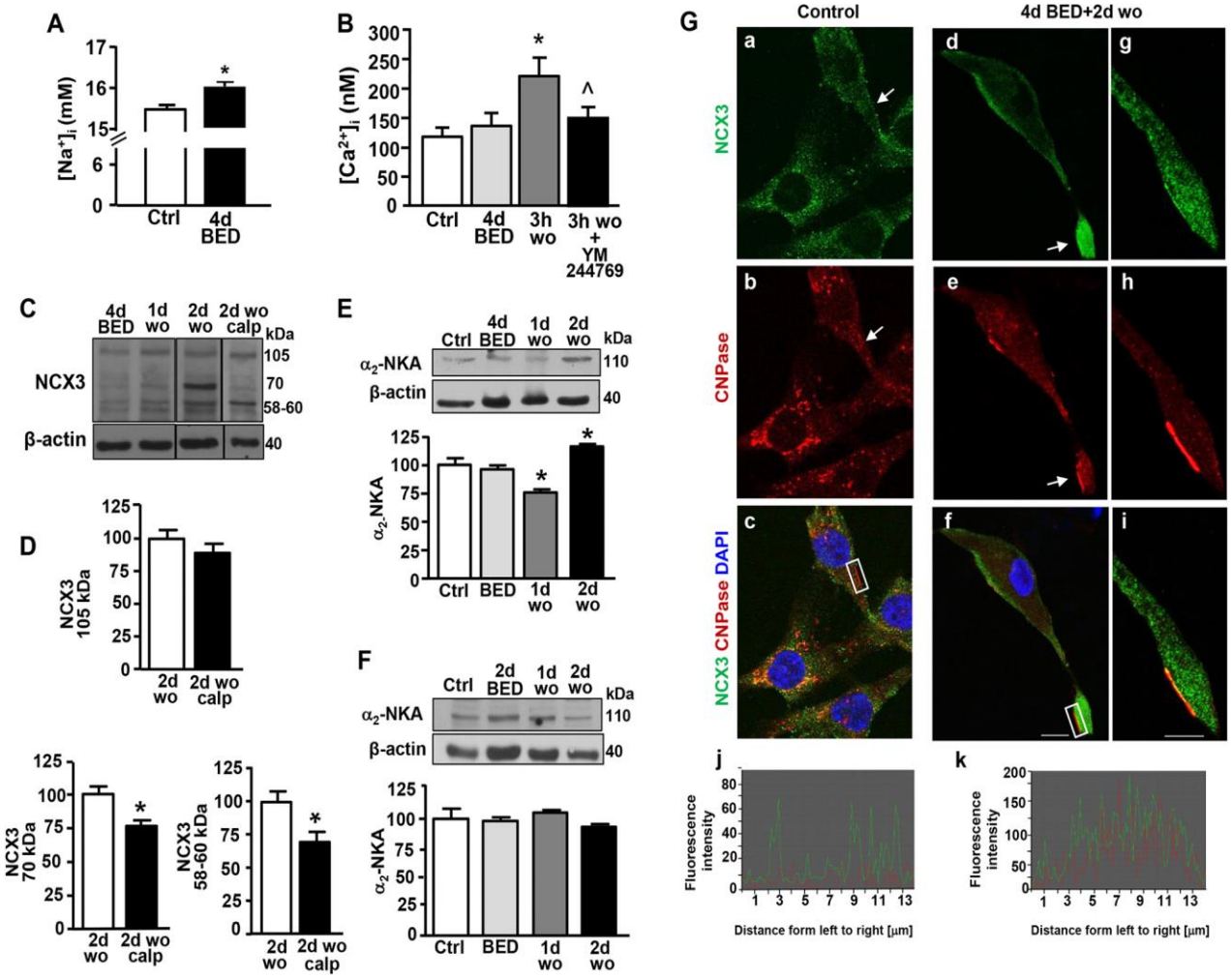

Figure 5. Effects of 4-days BED treatment and washout on $[Na^+]_i$ and $[Ca^{2+}]_i$ levels, α2-NKA and CNPase expression in human MO3.13 oligodendrocytes. A, Quantification of $[Na^+]_i$ detected with SBFI in MO3.13 oligodendrocytes under control conditions, and exposed to 100 nM BED for 4 days. Each bar represents the mean±S.E.M. of the data obtained from 30 cells per group in three independent experimental sessions. *p < 0.05 versus control. **B**, Quantification of $[Ca^{2+}]_i$ recorded with Fura-2 in MO3.13 cells under control conditions, after 100 nM BED for 4 days, and after 3 hours of BED washout (3 hours wo), in absence or in the presence of the NCX3 inhibitor 100 nM YM-24476. Each bar represents the mean±S.E.M. of the data obtained from 30 cells per group in three independent experimental sessions. *p < 0.05 versus control. and BED 4 days; ^p < 0.05 versus 3 hours wo. **C**, Western blotting analysis of NCX3 protein levels from homogenates of MO3.13 oligodendrocytes cultured in the presence of 100 nM BED for 4 days, and after drug-free washout for 1–2 days, in the absence or in the presence of 300 nM calpeptin. **D**, Densitometric analysis of the three major NCX3-specific enhanced chemiluminescence bands of ~105 kDa, 70 kDa, 58–60 kDa. The data were normalized on the basis of β-actin levels and expressed as percentage of 2-days-washout. The values represent the means±S.E.M (*n* = 3). * *p* < 0.05 versus control. **E-F**, Western blotting and densitometric analysis of α2-NKA protein levels from homogenates of MO3.13 oligodendrocytes cultured under control conditions, in the presence of 100 nM BED for 4 days (E) or 2 days (F) and after 1 or 2 days of drug-washout. The data were normalized on the basis of β-actin levels and expressed as percentage of control. The values represent the means±S.E.M. (*n* = 4). **G**, Confocal microscopic images displaying NCX3 (green) and CNPase (red) immunoreactivities in untreated (a-c) and MO3.13 oligodendrocytes treated with BED for 4 days + 2 days of drug-free-washout (d-i). Arrows in panels d-f point to the intense NCX3 and CNPase immunolabeling along plasma membrane. *j-k*, line profiling of NCX3 (green) and CNPase (red) fluorescence intensities along the line selected on the plasma membrane of both control (c) and BED-treated cell (f). Scale bars: a- f: 20 μm; g-i: 10 μm.

5. Drug washout following BED exposure reduced OPCs proliferation and upregulated NCX3 expression and I_{NCX} activity in rat primary OPCs.

To explore the pharmacological actions of BED exposure in rat primary OPCs, we first analysed the effects of 4 days BED exposure + drug-free washout on OPCs proliferation and on calcium/calmodulin-dependent kinase type IIβ (CaMKIIβ) expression, a critical component of the molecular mechanism regulating oligodendrocyte maturation (Swift et al, 2010, Waggener et al, 2013). Based on the findings showing that blocking NCX activity prevented OPCs differentiation (Boscia et al, 2012, Friess et al, 2016, de Rosa et al, 2019), we exposed OPCs in the presence of BED for 4 days during the proliferation stage, and then analyzed the effects on OPCs development after drug washout.

Quantitative confocal immunofluorescence analysis revealed that the number of $NG2^+$ cells coexpressing the nuclear proliferation marker Ki67 was significantly higher in cultures exposed to 100nM BED for 2 days if compared to untreated cultures. After 4 days of BED treatment, the number of double-labelled $NG2^+/Ki67^+$ OPCs significantly increased in the control group, while no difference was observed among control and BED-treated cultures. One day after BED washout, the number of double-labelled $NG2^+/Ki67^+$ cells significantly decreased in BED-treated if compared to untreated cultures (Fig. 6A). In addition, one day after BED washout, $NG2^+$ cells displayed a significant upregulation of CAMKIIβ fluorescence intensity if compared to untreated OPCs (Fig. 6B). Quantitative confocal studies showed that the α_2-NKA immunofluorescence intensity in oligodendrocyte $NG2^+$ precursors were globally and significantly reduced 1 day after BED washout if compared to untreated cultures. Quantitative analysis showed that the number of double-labelled $NG2^+/\alpha_2\text{-NKA}^+$ cells with bipolar morphology was significantly reduced if compared to untreated cells. Conversely, a significant number of $NG2^+/\alpha_2\text{-NKA}^+$ cells with multipolar morphology was detected, suggesting that the α_2-NKA immunoreactivity is re-established in cells progressing to a more mature phenotype (Fig. 6C).

Next, we investigated the effects of BED exposure + drug-free washout on NCX3 expression and activity in primary OPCs cultures. Confocal double immunofluorescence analysis showed that the number of $NG2^+$ cells coexpressing NCX3 was significantly higher in OPCs exposed to BED for 4 days if compared to untreated cells. In undifferentiated OPCs, NCX3 immunoreactivity was moderately detected in the somatic compartment (Fig. 7A).

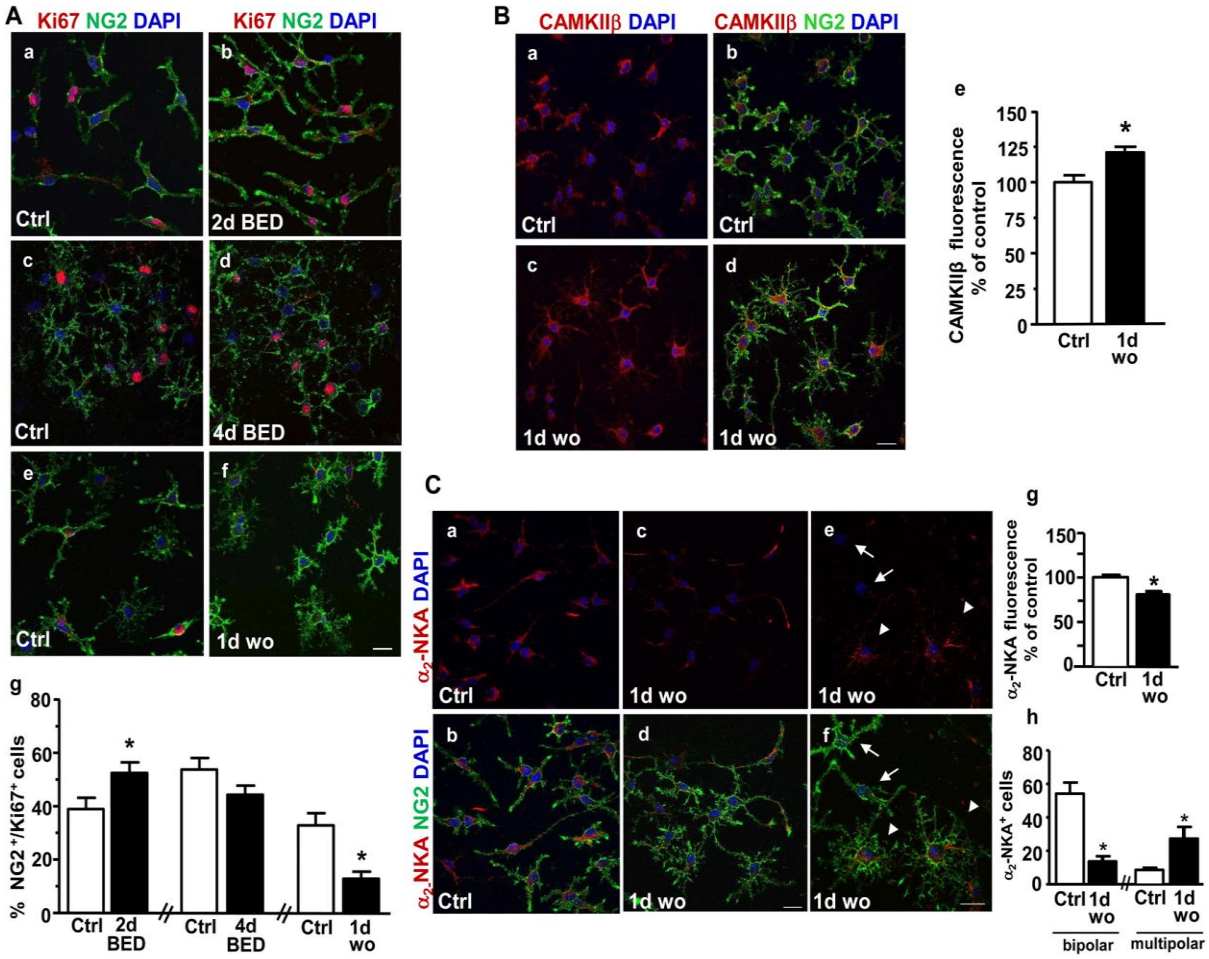

Figure 6. Effects of 4-days BED treatment and washout on Ki67, CAMKIIβ, and α2-NKA expression in rat primary OPCs. A, Representative confocal double immunofluorescence images (a-l) and quantitative analysis (g) of the number of NG2+ cells (green) coexpressing the nuclear proliferation marker Ki67 (red) in rat primary OPCs under control conditions, after 2 or 4 days of BED treatment (a-b and c-d, respectively), and after 4 days of BED treatment + 1 day of drug-free-washout (e-f). Nuclei were counterstained with dapi (blue). Scale bars in a–f: 20 μm. **B**, Confocal double immunofluorescence images displaying the distribution of CAMKIIβ immunosignal (red) and NG2 (green) in rat primary OPCs under control conditions (a-b) and after 4 days of BED treatment + 1 day of drug-washout (c-d). e; quantitative analysis of CAMKIIβ fluorescence intensity in rat primary OPCs under control conditions and after 4 days of BED treatment + 1 day of drug-washout. Nuclei were counterstained with dapi (blue). Data were normalized to the total number NG2+ cells. The values represent the means±S.E.M. (n = 3). * $p < 0.05$ versus control. Scale bars: a–d: 20 μm. **C**, Representative confocal images displaying the distribution of α2-NKA (red) and NG2 (green) immunosignals in rat primary OPCs cultured under control conditions (a-b) and after 4 days of BED treatment + 1 day of drug-washout (c-f). Arrows in e-f point to bipolar NG2+ cells showing a negligible α2-NKA immunosignal; arrowheads in e-f point to multipolar NG2+ cells displaying an α2-NKA immunosignal along cell processes. Nuclei were counterstained with dapi (blue). g; quantitative analysis of α2-NKA fluorescence intensity in rat primary OPCs under control conditions and after 4 days of BED treatment + 1 day of drug-washout. h, quantitative analysis of the number of bipolar and multipolar oligodendrocytes displaying α2-NKA immunoreactivity after 1 day of BED-free washout. Data were normalized on to the total number of $NG2^+$ cells. The values represent the means±S.E.M. (n = 3). * $p < 0.05$ versus control. Scale bars: a–f: 20 μm.

Conversely, 2 days after BED washout, a significant increase in the number of multipolar $NG2^+$ cells displaying a punctuated NCX3 immunoreactivity both in the soma and along processes was observed, if compared to untreated cultures. In line, an upregulated chemiluminescence signal of NCX3 immunoreactive bands was revealed by Western blot analysis performed on OPCs lysates from cultures exposed to BED for 4 days + 2 days washout cultures (Fig. 7B). Furthermore, NCX activity, recorded by Fura-2-video imaging at 2 days after BED washout, significantly increased both in oligodendrocyte soma and processes if compared to untreated cultures (Fig. 7C).

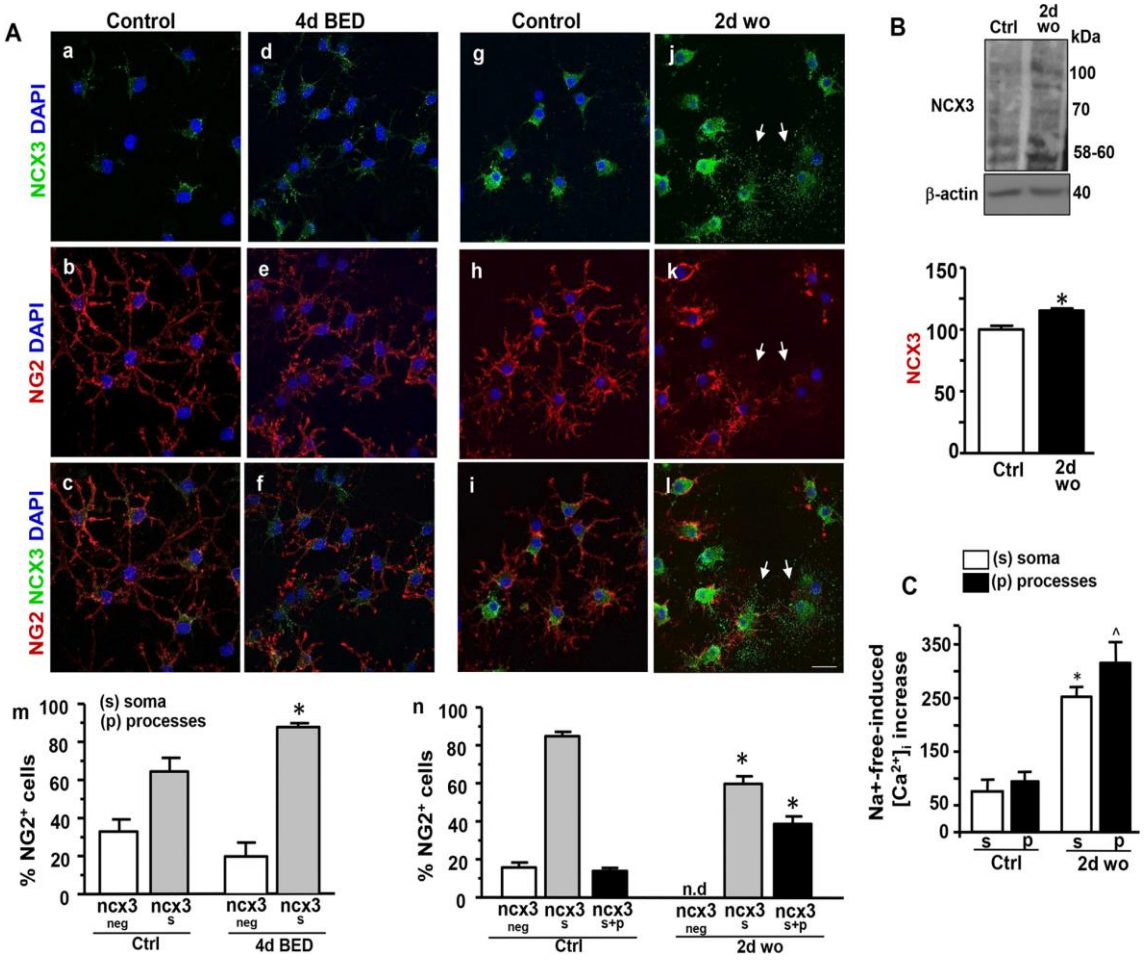

Figure 7. Effects of 4-days BED treatment and washout on NCX3 expression and NCX activity in rat primary OPCs. A, Confocal microscopic images displaying NCX3 (green) and NG2 (red) immunoreactivities in rat primary OPCs in absence or in presence of BED for 4 days (a-c and d-f, respectively) and in OPCs under control conditions or exposed to BED treatment for 4 days + 2 days of drug-washout (g-i and j-l, respectively). Nuclei were counterstained with dapi (blue). Arrows in j-l point to multipolar NG2+ cells displaying NCX3 immunosignal in soma and along cell processes. Scale bars in a-l: 20 μm. (m); quantitative analysis of the number of $NG2^+/NCX3^-$ and double-labelled $NG2^+/NCX3^+$ cells displaying NCX3 immunoreactivity in the soma (s) or along processes (p) under control conditions and 4 days after BED exposure; (n), quantitative analysis of the number of $NG2^+/NCX3^-$ and double-labelled $NG2^+/NCX3^+$ cells displaying NCX3 immunoreactivity in the soma (s) or along processes (p) under control conditions and 4 days after BED exposure + 2 days of BED-washout. Data

were normalized on the total number of $NG2^+$ cells and expressed as percentage of control. The values represent the means±S.E.M. (n = 3). * $p < 0.05$ versus control. **B**, Western blotting and densitometric analysis of NCX3 protein levels from homogenates of rat primary OPCs under control conditions, and after 4 days of BED treatment + 2 days of drug-washout. The data were normalized on the basis of β-actin levels and expressed as percentage of control. The values represent the means±S.E.M. (n = 3). *p < 0.05 versus control. **C**, Quantification of NCX activity measured as Na^+-free-induced $[Ca^{2+}]_i$ increase, quantified as Δ% of peak versus basal values, in the soma (s) and processes (p) of rat primary OPCs cultured under control conditions, and after 4 days of BED treatment + 2 days of BED washout (2d wo). Each bar represents the mean±S.E.M. of the data obtained from 20 cells per group in three independent experimental sessions. *p < 0.05 versus respective control; ^p < 0.05 versus soma at 2d wo.

6. Drug washout following BED exposure enhanced D-Aspartate-induced calcium response and accelerated myelin sheet formation in rat primary oligodendrocytes.

We recently showed that D-Aspartate (D-Asp) exposure evoked a calcium response in OPCs that involve the activation of AMPA and NMDA receptors and NCX3 and stimulated oligodendrocyte differentiation (de Rosa et al, 2019). Based on this observation we explored the effects of acute D-Asp treatment on calcium response in OPCs exposed to BED for 4 days + 2 days of BED washout and untreated cultures. As shown in Figure 8, acute application of D-Asp induced a greater calcium response both in the soma and processes of immature oligodendrocytes of BED-treated, if compared to untreated cultures.

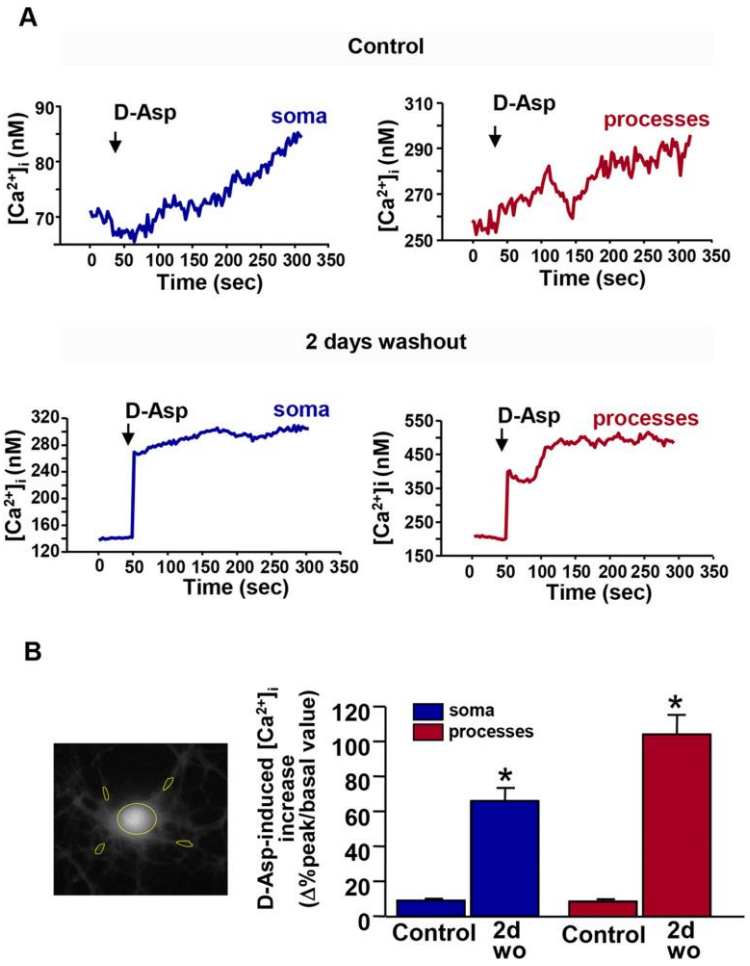

Figure 8. D-Aspartate-induced calcium response in rat primary OPCs exposed to 4- days BED treatment þ 2 days of drug-free washout. A, Superimposed single-cell traces representative of the effect of 100 μM acute D-Asp exposure on $[Ca^{2+}]_i$ detected in the soma (left panels) or processes (right panels) of rat primary OPCs under control conditions and after 4-days of BED treatment + 2 days of drug-free washout. **B**, Quantification of $[Ca^{2+}]_i$ increase showed in A, measured as Δ% of peak versus basal values. A representative cell with traced rows at the soma and proximal processes is showed on the left. Each bar represents the mean±S.E.M. of the data obtained from 10 cells per group in three independent experimental sessions. * $p < 0.05$ versus respective control.

To explore the consequence of the augmented reversal NCX activity and calcium response on differentiation and myelin formation in oligodendrocytes, the BED-free washout was prolonged for 4 days (Fig. 9A). Analysis of oligodendrocyte morphology with phalloidin staining showed that a higher number of cells with partial or fully ring-like morphology (myelinating oligodendrocytes) was detected in cultures treated with BED for 4 days + 4 days of washout if compared to untreated cells. A punctuated distribution of NCX3 immunoreactivity was detected in the soma and along processes of MBP-stained of cells in both treated and untreated cultures (Fig. 9B). Quantitative colocalization experiments performed with anti-NCX3 and anti-MBP

antibodies revealed that the percentage of MBP^+ cells coexpressing NCX3 and the quantification of MBP-stained area were significantly higher in BED-treated if compared to untreated cells.

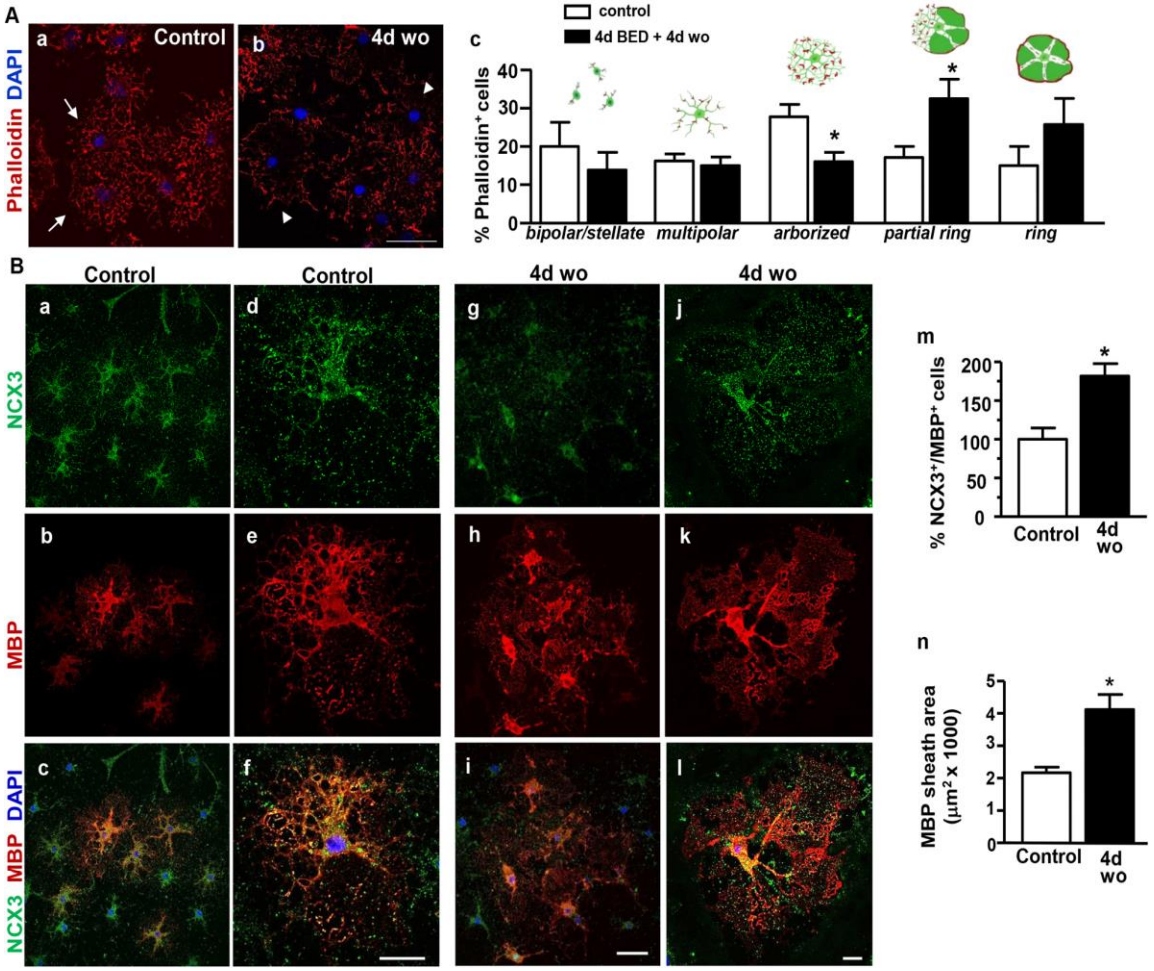

Figure 9. Distribution of NCX3 and MBP immunoreactivities in rat primary OPCs exposed to 4-days BED treatment 4 days of drug-free-washout. A, Representative confocal images displaying the distribution of phalloidin in OPCs under control conditions (a) or after 4-days of BED treatment + 4 days of drug-free washout (b). Arrows and arrowheads in a-b point to phalloidin-stained cells with arborized or ring morphology, respectively. Scale bars in a-b 20 µm. (c), quantitative analysis of the number of phalloidin + cells with bipolar/stellate, multipolar, arborized, partial ring, ring morphology. Data were normalized on the number of total number of phalloidin+ cells. The values represent the means±S.E.M. (n = 3). * $p < 0.05$ versus control. **B**, Representative confocal images displaying the distribution of NCX3 (green) and MBP (red) immunosignals in oligodendrocyte cultures under control conditions (a-f) and after 4 days of BED treatment + 4 days of drug-free-washout (g-l). Panels d-f and j-l show higher magnification images of a single representative $NCX3^+/MBP^+$ under control conditions and after 4 days of BED treatment + 4 days of drug-free-washout, respectively. (m); quantitative analysis of the number of $NCX3^+/MBP^+$ cells in control cultures and in cultures exposed to 4 days of BED treatment + 4 days of drug-free-washout. Data were normalized on the number of total $NCX3^+$ cells and expressed as percentage of control. The values represent the means±S.E.M. (n = 3). * $p < 0.05$ versus control. (n), quantitative analysis of the MBP-positive area from partial ring and ring cells. Nuclei were counterstained with dapi (blue). Scale bars in a-c and g-i: 50 µm; in d-f-i: 20 µm; in j-l: 20 µm.

Results II

1. Neuroprotective effects of UCM-1341 against NMDA-induced excitotoxicity in organotypic brain explants.

To study the neuroprotective potential of UCM-1341, we first investigated the protective effects of 0.1-10μM UCM-1341 against a milder and more severe excitotoxic insult induced by 10μM or 30μM NMDA exposure for 48 hours (Boscia et al, 2006, 2009). When hippocampal explants were exposed for 48 hours to 10μM NMDA, cell death selectively occurred in the CA1 pyramidal cell layer and, to a lesser degree, in the CA3. By contrast, higher NMDA concentrations (30μM) caused more marked neurodegenerative effects which involved both CA1 and CA3 (Fig. 10B). When slices were incubated with 10μM NMDA in presence of 0.1-10μM UCM-1341, a significant prevention of PI uptake was observed both in the CA1 region with 1μM and 10μM UCM-1341. Conversely, UCM-1341 was less effective in counteract CA degeneration induced by 30μM NMDA, and a significant neuroprotective effect was observed only with 10μM UCM-1341 in the CA1 region (Fig. 10A). Then, we investigated the neuroprotective potential of the reference compounds, melatonin and URB-597, against NMDA-induced neurodegeneration. To this aim hippocampal explants were exposed to 10μM NMDA in the absence or in the presence of the reference compounds melatonin or URB-597, alone or in combination (all at 10μM), and compared the effects with those afforded by the bivalent ligand UCM-1341 (at 10μM). As shown in Figure 1C, 10μM melatonin, but not 10μM URB-597, exerted a significant neuroprotection in the CA1 against NMDA-induced excitotoxicity. When melatonin and URB-597 were applied in combination, a significant neuroprotection, but comparable with that of UCM-1341, was observed in the CA1 region.

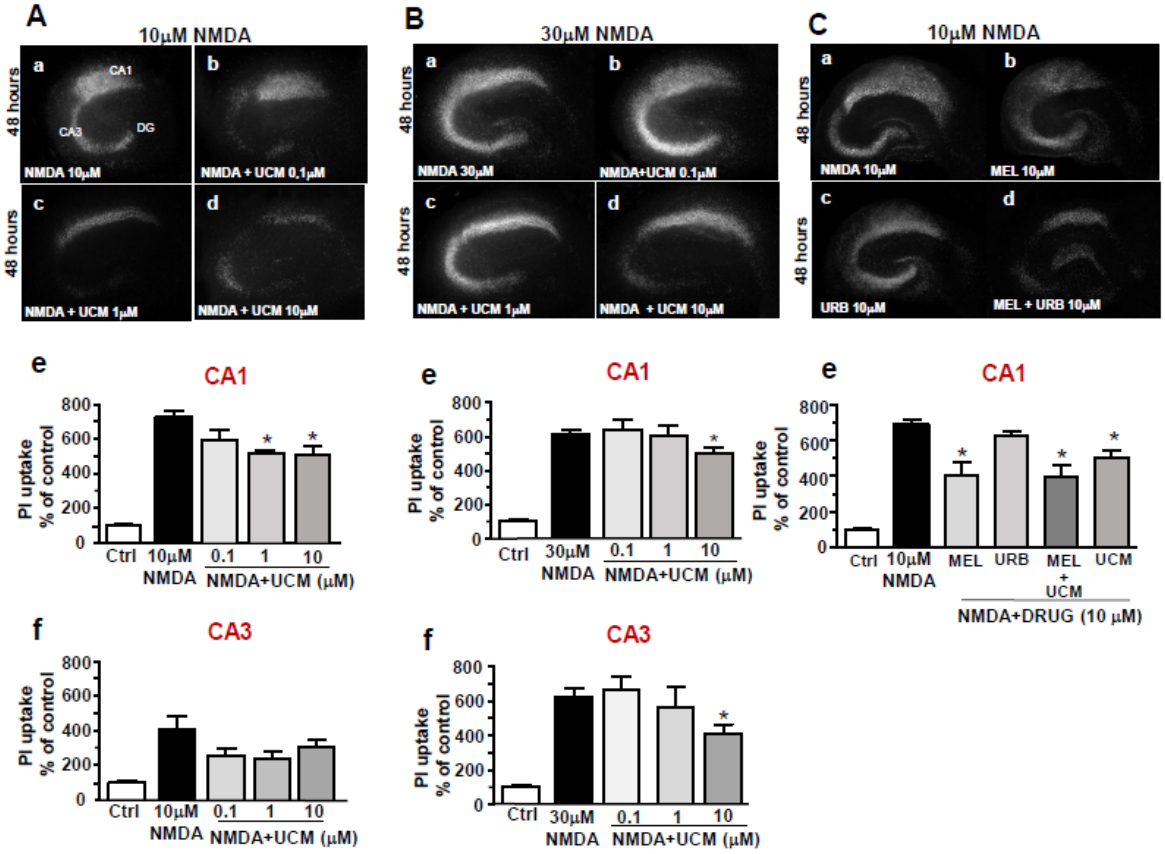

Figure 1. Dose-dependent effects of UCM-1341 and reference compounds, melatonin and URB-597, against NMDA-induced cell death in hippocampal organotypic slices. A-C, a-d; PI fluorescence staining patterns observed in representative slices 48 hours following 10μM NMDA (A, C) or 30μM NMDA (B) exposure in presence of UCM-1341 or URB-597 or melatonin, at the indicated concentrations. Scale bar: 400 mm. **A-C e-f;** Quantification of PI uptake in hippocampal CA1 and CA3 subregions by densitometric analysis. Data are expressed as percentage of control. Each data point is the mean S.E.M. of the data obtained from 20-25 hippocampal slices in three separate experiments. *p < 0.05 versus NMDA.

2. LPS+IFN-γ exposure preferentially induced inflammatory degeneration in the CA1 region of hippocampal explants and modulated FAAH enzymes and melatonin receptors in brain cells.

Next, to study the neuroprotective actions of UCM-1341 on neuroinflammatory damage, organotypic explants were exposed to a combined application of 10 μg/mL LPS and human recombinant 100 ng/mL IFN-γ for 3 days, a model that, by mimicking the microglia interaction with infiltrating peripheral immune T cells, triggers the release of massive proinflammatory and cytotoxic factors, and promotes an inflammatory neurodegeneration (Papageorgiou et al, 2010). Here, we show that the cell degeneration induced by LPS+INF-γ exposure can be monitored in hippocampal explant cultures by PI uptake (Fig. 11A). Quantitative densitometric analysis showed that LPS + IFN-γ treatment for 24 or 48 hours did not significantly affected cell viability in the CA and DG subfields. Conversely, 72 hours after LPS + IFN-γ incubation, a significant upregulation of PI uptake was recorded in the CA1 region, while the CA3 and DG subregions were less affected (Fig. 11B). As expected, LPS+IFN-γ exposure induced a significant increase in the expression levels of the GFAP and Iba1 markers after 24 and 48 hours (Fig. 11C-D), indicating that microglia and astrocytes activated after the insult. The pro-inflammatory insult significantly and intensely downregulated MBP protein levels in the CA1 region after 72 hours (Fig. 11F), as revealed by Western blotting analysis (Fig. 11F). To investigate whether the pro-inflammatory demyelinating insult affected melatonin MT receptors and the endocannabinoid hydrolyzing FAAH enzyme protein levels we performed biochemical analyses in lysates from hippocampal explants. FAAH protein levels were upregulated 24 hours after LPS+IFN-γ exposure, then they return to basal levels (Fig. 11E). The nonselective anti-MT receptor antibody revealed a divergent modulation of MT1 and MT2 protein levels. In fact, while the 40 kDa band of MT1 protein was upregulated at 48-72 hours after the neuroinflammatory insult, the 38 kDa band of MT1 protein was, instead, downregulated after a transient increase (Fig. 11G).

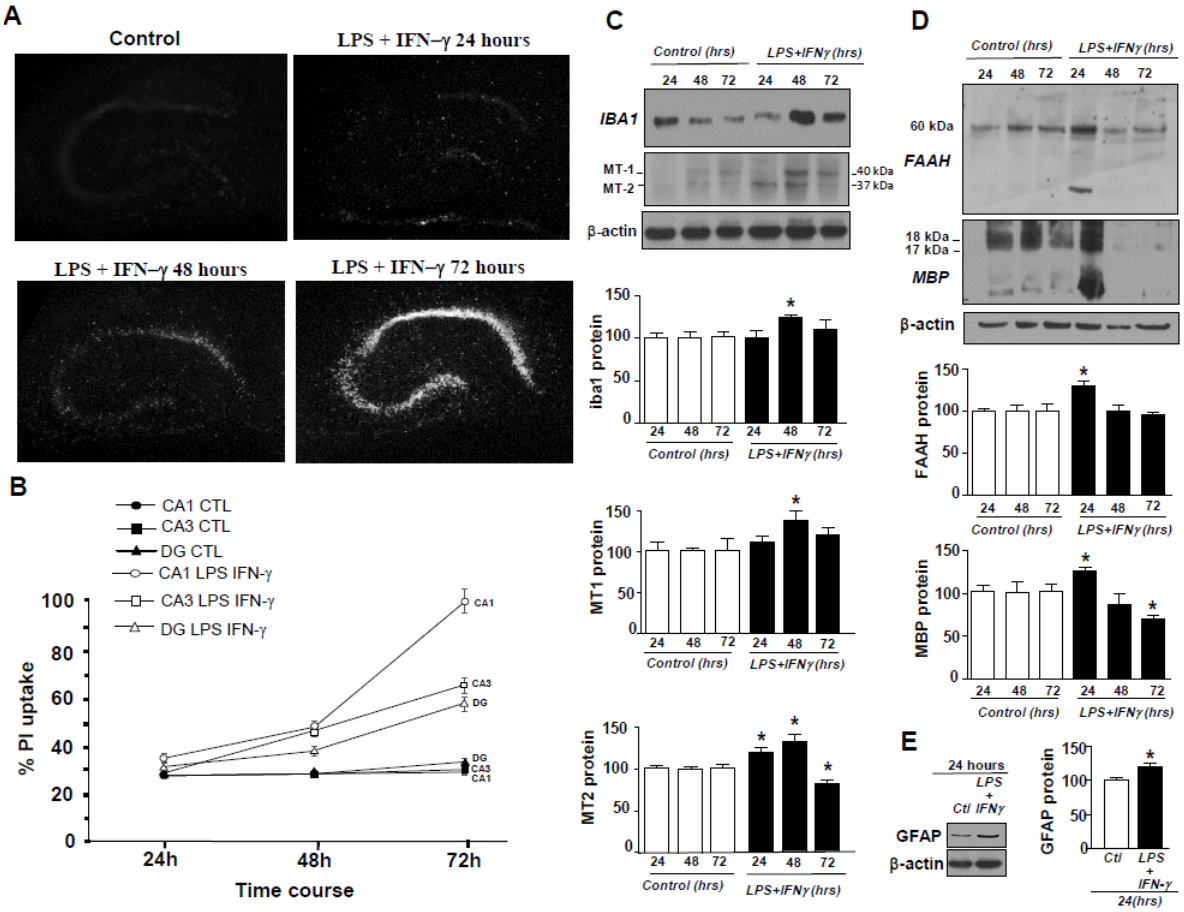

Figure 2. Time-dependent effects of LPS+IFN-γ exposure on PI uptake, glia activation, MBP, FAAH and melatonin receptor protein levels in rat hippocampal organotypic slices. A-B, Representative images (A) and quantitative densitometric analysis (B) of PI fluorescence uptake recorded after 24-72 hours of LPS + IFN-γ exposure in the CA and DG subfields. The values represent the mean±S.E.M. (n = 3). **C**, Western blotting analysis of Iba1 and MT1/MT2 protein levels in hippocampal slices under control conditions and after LPS + IFN–γ exposure for 24-72 hours. **D** Western blotting analysis of FAAH, MBP, protein levels in hippocampal slices under control conditions and after LPS + IFN–γ exposure for 24-72 hours. **E**, Western blotting analysis of GFAP protein levels in hippocampal slices under control conditions and 24 hours after LPS + IFN–γ exposure. Data were normalized on the basis of β-actin levels and expressed as percentage of control. The values represent the means±S.E.M. (n = 3) * p < 0.05 versus controls.

In line with previous studies (Gulyas et al, 2004), confocal analysis performed with the anti-FAAH antibodies in hippocampal slice cultures showed the predominant distribution of FAAH enzymes in somata and dendrites of principal cells (Fig. 12). Quantitative confocal analysis revealed that the fluorescence intensities of FAAH, GFAP but not MAP2 and CD11b significantly increased 24 after LPS+IFN-γ exposure, if compared to untreated controls. At this time point, quantitative colocalization analyses revealed that FAAH immunofluorescence intensity significantly and largely increased in both MAP-positive neurons and GFAP-positive astrocytes of the CA1 region. After 48 hours, FAAH immunofluorescence returned to basal level, while GFAP and CD11b immunofluorescences were upregulated. Nevertheless, quantitative coexpression analysis revealed a significant upregulation of FAAH in microglia and astrocytes, but not in neuronal cells (Fig. 12H).

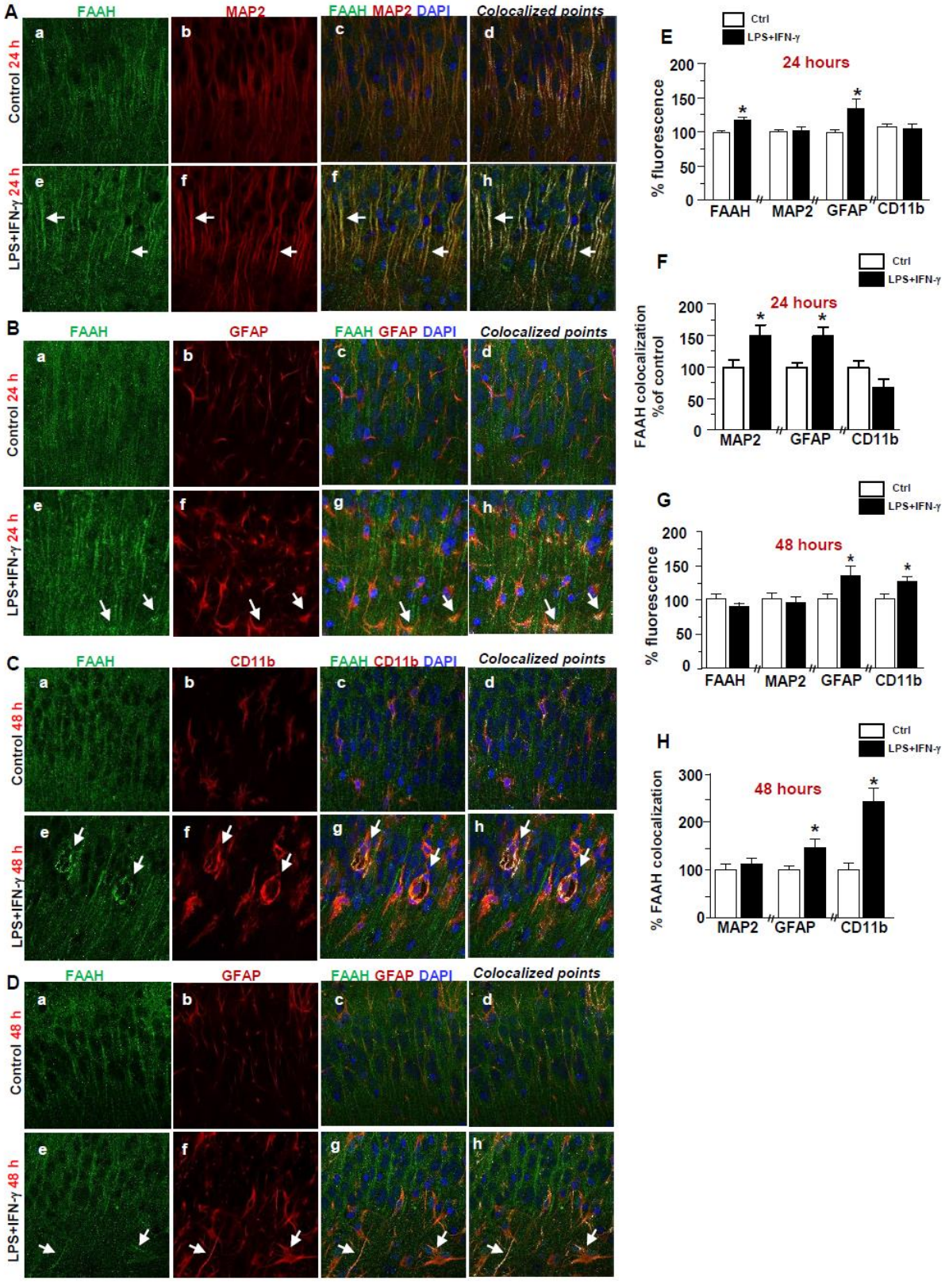
A
FAAH
MAP2
FAAH MAP2 DAPI
Colocalized points
Control 24 h
LPS+IFN-γ 24 h
B
FAAH
GFAP
FAAH GFAP DAPI
Colocalized points
Control 24 h
LPS+IFN-γ 24 h
C
FAAH
CD11b
FAAH CD11b DAPI
Colocalized points
Control 48 h
LPS+IFN-γ 48 h
D
FAAH
GFAP
FAAH GFAP DAPI
Colocalized points
Control 48 h
LPS+IFN-γ 48 h
E
Ctrl
LPS+IFN-γ
24 hours
% fluorescence
FAAH
MAP2
GFAP
CD11b
F
Ctrl
LPS+IFN-γ
24 hours
FAAH colocalization %of control
MAP2
GFAP
CD11b
G
Ctrl
LPS+IFN-γ
48 hours
% fluorescence
FAAH
MAP2
GFAP
CD11b
H
Ctrl
LPS+IFN-γ
48 hours
% FAAH colocalization
MAP2
GFAP
CD11b

Figure 3. Distribution of FAAH immunoreactivity in neurons, astrocytes and microglia in hippocampal organotypic slices during LPS+IFN–γ exposure. A-B, Confocal images displaying the colocalization of FAAH with MAP2 (A) or GFAP (B) immunoreactivities in the CA1 hippocampal region, in the absence (a–d) or in the presence of LPS+IFN-γ (e–h) for 24 hours. Panels d and h display the colocalized points (white). **C-D**, Confocal images displaying colocalization of FAAH with GFAP (C) and CD11b (D) immunoreactivities in the CA1 hippocampal region, in the absence (a–d) or in the presence of LPS+IFN-γ (e–h) for 48 hours. Panels d and h display the colocalized points (white). **E-F**, Quantitative analysis of FAAH, MAP2, GFAP, and CD11b immunofluorescence intensities (E) and FAAH coexpression with MAP2, GFAP, and CD11b immunosignals (F) in the CA1 hippocampal region, in the absence or in the presence of LPS+IFN-γ for 24 hours **G-H,** Quantitative analysis of FAAH, MAP2, GFAP, and CD11b immunofluorescence intensities (G) and FAAH coexpression with MAP2, GFAP, and CD11b immunosignals (H) in the absence or in the presence of LPS+IFN-γ for 48 hours. The values represent the means + S.E.M. (N = 12-15 slices per group). Level of significance was determined by using two-tailed Student's t-test, *$p < 0.05$ versus control

3. Effect of UCM-1341 on Iba1 and GFAP expression following LPS+IFN-γ-exposure in the CA1 region of hippocampal organotypic slices.

UCM-1341 significantly prevented the loss of microglia and astrocytes 72 hours after the inflammatory injury, as revealed by the significant higher number of Iba1-positive cells and $GFAP^+$ area measured in the CA1 region if compared to untreated cultures (Fig. 13). Morphological assessment of Iba1-positive cells showed that dystrophic microglia dominate in the CA1 subfield of LPS+IFN-γ-exposed explants after 72 hours, while the foamy phenotype was clearly prevalent in slices treated with 10μM UCM-1341 during the inflammatory insult (Fig. 13A)

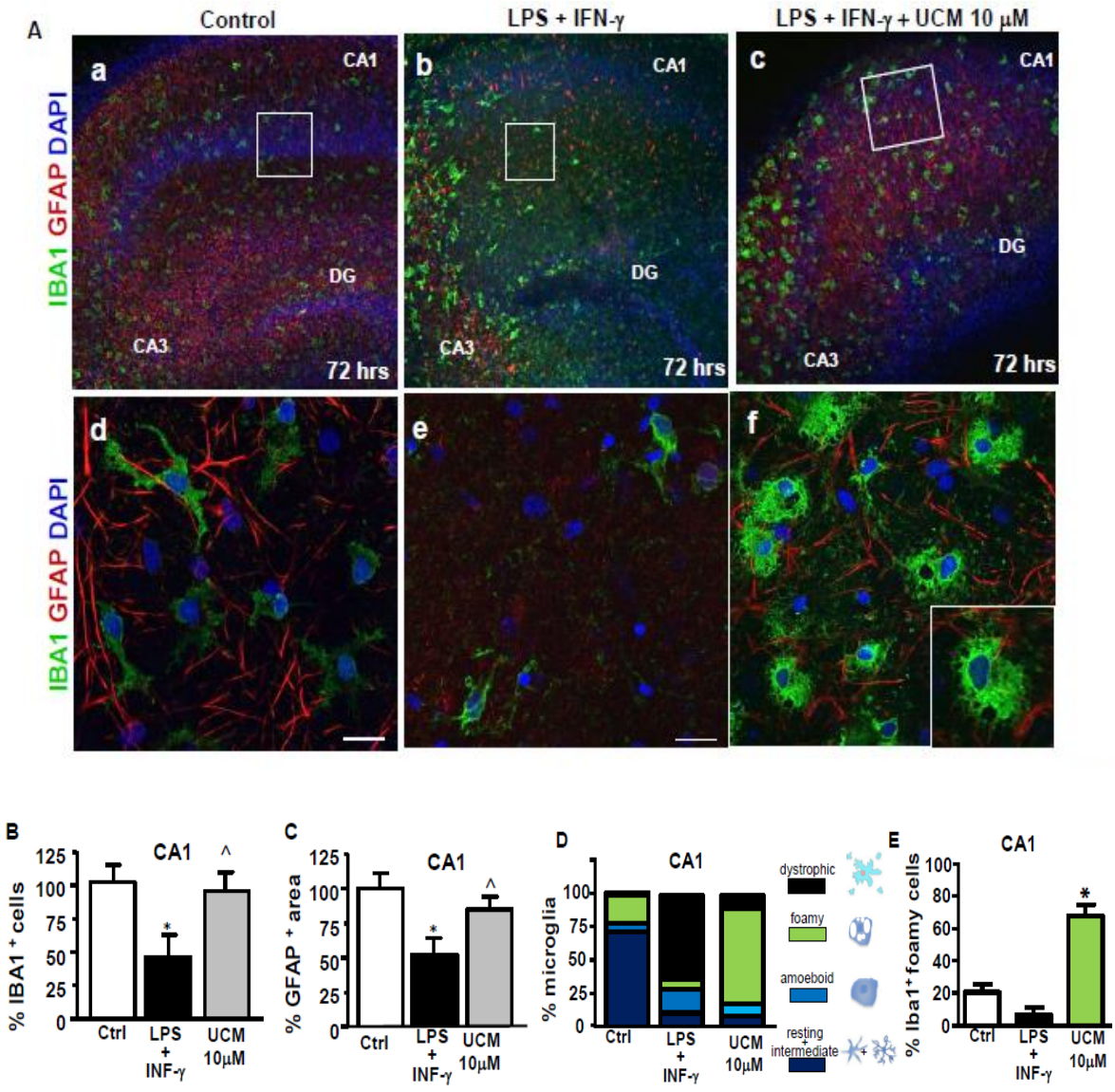

Figure 4. Effect of UCM-1341 on Iba1 and GFAP immunoreactivities following 72 hours after LPS+IFN-γ exposure. A, Representative confocal microscopic images showing Iba1 and GFAP immunoreactivities in the CA1 hippocampal region under control conditions (a), in the presence of LPS+IFN-γ (b), and in the presence of LPS+IFN-γ + UCM-1341 (c). Panels d-f show higher magnification images of Iba1 and GFAP under control conditions (a), in the presence of LPS+IFN-γ (b) or LPS+IFN-γ + UCM-1341 (c). **B-C**, Quantitative analysis of Iba1$^+$ cells (B) and GFAP$^+$ area (C) in control cultures, in LPS+IFN-γ–treated cultures, in the absence or in the presence of 10μM UCM–1341. **D,** Quantitative analysis of resting + intermediate (dark blue), amoeboid (light blue), foamy (green), dystrophic (black) microglia phenotypes, in control cultures, LPS+IFN-γ–treated cultures, and in the absence or in the presence of 10μM UCM-1341.

4. UCM-1341 prevented LPS+IFN-γ-induced damage, benefit microglia M2 polarization and exerted a greater neuroprotection against the neuroinflammatory insult if compared to the reference compounds melatonin and URB-597.

To investigate the effects of UCM-1341 on inflammation-mediated neurodegeneration, slices were exposed to LPS + IFN-γ in absence in presence of 0.1-10μM UCM-1341 for 3 days. Densitometric analysis of PI uptake revealed that UCM-1341 exerted a marked and dose-dependent neuroprotective actions in the more-vulnerable CA1 region as well as in the less affected CA3 hippocampal subregion (Fig. 14A). At 10μM, UCM-1341 fully counteracted cell death occurring 3 days after LPS + IFN-γ exposure. Confocal analysis showed that the neuronal NF200 immunofluorescence loss observed in the CA1 region of LPS+IFN-γ-treated slices was significantly prevented by UCM-1341 (Fig. 14B-d). Nevertheless, coexpression analysis of NF200 with MBP revealed that UCM-1341 only partially attenuated demyelination, as revealed by the quantitative analysis of the myelination index (Fig.14B, e). Immunoblotting revealed that the *protein* levels of the *mannose receptor CD206*, an M2 macrophage marker, were significantly higher in slices exposed to LPS+IFN-γ for 48 hours in presence of UCM-1341, if compared to untreated slices. In line, confocal double immunofluorescence staining showed significant higher number of intensely stained CD206 positive macrophages in drug-exposed slices after 48 hours (Fig. 14C).

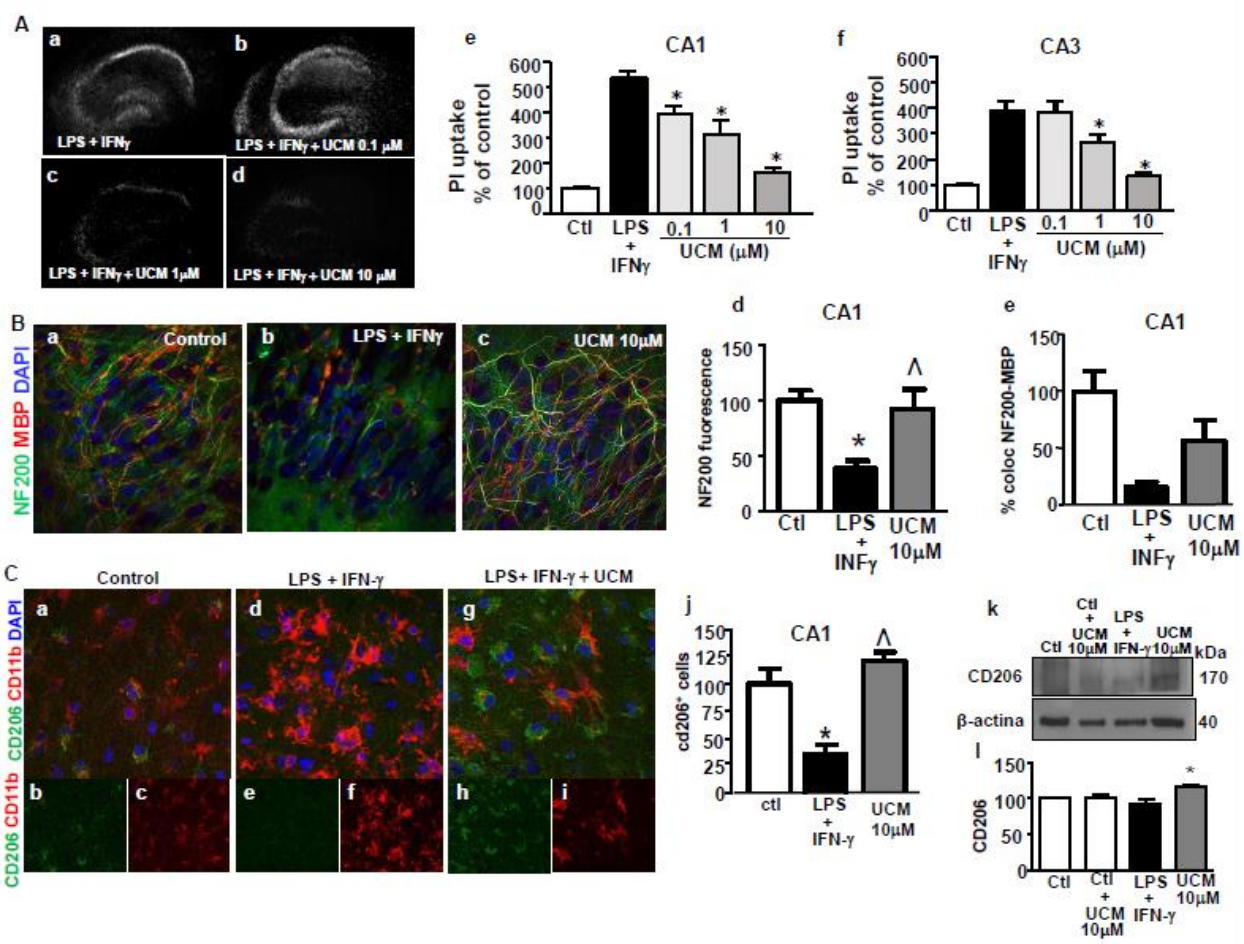

Figure 5. Effect of UCM-1341 against LPS+IFN-γ–induced neuroinflammatory damage and microglia polarization. A, a-d; PI fluorescence staining patterns observed in representative slices 72 hours following LPS+IFN-γ in presence of UCM-1341 at the indicated concentrations. **A, e-f;** Quantitative densitometric analysis of PI fluorescence uptake recorded in slices under control conditions, in the presence of LPS+IFN-γ, and in the presence of LPS+IFN-γ + UCM-1341 for 72 hours. The values represent the mean±S.E.M. (n=3). **B, a-c;** Representative confocal microscopic images showing NF200 and MBP immunoreactivity in the CA1 hippocampal region under control conditions, and LPS+IFN-γ exposure, in the presence of 10μM UCM−1341 (c). Panel d-e show a quantitative analysis of NF200 and MBP immunofluorescence intensities in control conditions, LPS+IFN-γ , and in the presence of 10μM UCM−1341. The values represent the means + S.E.M. (N = 12-15 slices per group). Level of significance was determined by using two-tailed Student's t-test, *p < 0.05 versus control. **C, a-i;** Representative confocal microscopic images showing CD206 and CD11b immunoreactivity in the CA1 hippocampal region under control conditions, LPS+IFN-γ, and in the presence of 10μM UCM1341. **C, j;** Quantitative analysis of $CD206^+$ cells in slices under control conditions, LPS+IFN-γ, and in the presence of 10μM UCM−1341. **C, k-l;** Western blotting analysis (k) and densitometric analysis (l) of CD206 protein levels in hippocampal slices under control conditions and after LPS+ IFN−γ exposure for 72 hours in the absence or in the presence of 10μM UCM−1341. Data were normalized on the basis of β-actin levels and expressed as percentage of control. The values represent the means±S.E.M. (n = 3) * p < 0.05 versus controls.

Next, to explore the synergistic neuroprotective potential of melatonin and URB-597, hippocampal explants were exposed to LPS+IFN-γ in the absence or in the presence of 10 μM melatonin or 10μM URB-597, alone or in combination. Both melatonin or URB-597 exerted a significant neuroprotection against LPS+IFN-γ- induced neurodegeneration, as recorded by PI uptake after 72 hours (Fig. 15A). When drugs were used in combination (both at 10μM), they fully counteracted cell death in the CA1 region, thus demonstrating the synergistic neuroprotective effects of melatonin and URB-597 against LPS+IFN-γ-induced inflammatory damage.

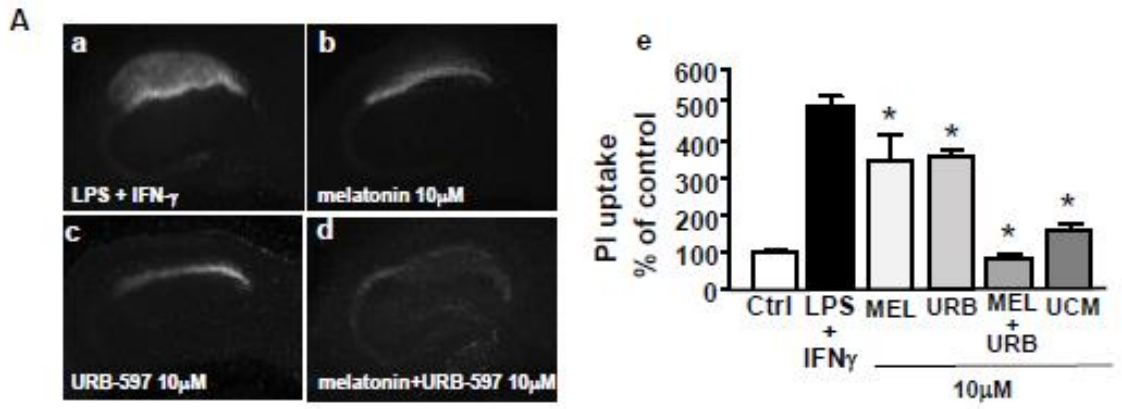

Figure 6. Effect of melatonin and URB-597 against LPS+IFN-γ-induced inflammatory damage in the CA1 region of hippocampal slices. A, a-d; Quantitative densitometric analysis of PI fluorescence uptake recorded 72 hours after LPS + IFN–γ exposure in the absence or in the presence of melatonin, URB-597, melatonin + URB-597, and UCM-1341, all at 10μM. The values represent the mean±S.E.M. (n = 3). **A, e**; Quantitative densitometric analysis of PI fluorescence uptake recorded after 72 hours in slices under control conditions, in the presence of LPS+IFN-γ, and in the presence of LPS+IFN-γ + melatonin, or URB-597 or - melatonin + URB-597, or UCM-1341 (all at 10μM) The values represent the mean±S.E.M. (n=3). * $p < 0.05$ versus controls.

V. DISCUSSION

Rebound activation of NCX3 exchanger following its pharmacological inhibition wit BED blocker stimulated oligodendrocyte development.

In the first part of the present study we demonstrated that drug-free washout after a prolonged blocking of NCX3 exchanger with the pharmacological inhibitor BED enhanced NCX3 expression, stimulated reversal I_{NCX} activity, and accelerated myelin sheet formation in oligodendrocytes.

Our survival and biochemical studies showed that NCX3 inhibition with the BED blocker did not significantly affected oligodendrocyte survival and NCX3 expression levels, although some increase can be detected after prolonged drug exposure (6 days). In this regard, it should be considered that the increased MTT reduction may also reflect an increased cell proliferation following BED exposure, as supported by our findings showing that BED exposure increased the number of OPCs coexpressing the nuclear proliferation marker Ki67.

Recently, it has been pointed out that prolonged exposure to NCX blockers differentially affected intracellular $[Na^+]_i$ and $[Ca^{2+}]_i$ and, consequently, may alter cell viability (Hu et al, 2019). Indeed, pharmacological compounds blocking the forward, but not reverse mode of NCX, by increasing intracellular $[Ca^{2+}]_i$ are toxic to glioblastoma cells (Hu et al, 2019). Our functional analysis showed that 4 days exposure to 100nM BED significantly inhibited both the forward and reverse NCX operational modes and increased $[Na^+]_i$ in oligodendrocytes. We previously showed that 10-100nM BED dose-dependently inhibited both the forward and reverse NCX3 mode of operation, moderately inhibited the reverse mode of NCX2, while failed to modulate NCX1 in BHK cell line stably transfected with each of the NCX isoforms (Secondo et al, 2015). In our MO3.13 oligodendrocyte cultures, 10nM BED treatment failed to significantly block I_{NCX} after 4 days of treatment, possibly suggesting that the prolonged incubation time may affect the potency of BED inhibitor in oligodendrocytes. Although further studies are needed to clarify the mechanisms underlying the $[Na^+]_i$ increase during BED exposure, it is plausible that the inhibition of both NCX3 and NCX2 exchangers activities may contribute. More interestingly, we found that drug suspension after 4 days of continuous 100nM BED exposure promoted a significant $[Ca^{2+}]_i$ rise in oligodendrocytes, suggesting that reversal NCX activity, driven by sodium accumulation, contributed to such increase. Accordingly, several evidence demonstrated that NCX can reverse upon increase in $[Na^+]_i$ and function as a Ca^{2+} loader in brain cells under physiological and pathophysiological conditions (Kirischuk et al, 1997, Floyd et al, 2005, Boscia et al, 2016, Gerkau et al, 2019). More interestingly, we found that drug suspension after 4 or 6 days of BED exposure differentially modulated NCXs

expression and NCX activity. BED-free washout after NCX3 inhibition for 6 days significantly upregulated the 58-60kDa protein of NCX3, an effect that was accompanied by the concomitant upregulation of both NCX1 and NCX2 proteins, and increased NCX activity in the reverse and forward mode. Early data have hypothesized that, under pathophysiological conditions, calpain cleaves and inactivates NCX3, and this inactivation prevented the extrusion of excess neuronal Ca^{2+} contributing to Ca^{2+} dysregulation and death (Iwamoto et al, 2006, Bano et al, 2007, Araújo et al, 2007, Brustovetsky et al, 2010, Atherton et al, 2014). This observation may suggest that NCX1 and NCX2 levels may increase in response to the proteolytic NCX3 cleavage contributing to the upregulated NCX currents recorded in oligodendrocytes during drug-free washout after 6 days of drug treatment. More intriguingly, BED-free washout after 4 days of drug treatment transiently increased NCX2 proteins at 1 day, while selectively upregulated the 70kDa and 58-60kDa NCX3 proteins at 2 days, an effect that was accompanied by a selective increase in reversal NCX activity. Previous findings showed that calpain-mediated NCX3 cleavage in neuronal cultures may generate the appearance of a 75kDa and 58-60kDa proteolytic NCX3 bands that are NCX3 hyperfunctional forms contributing to ER Ca^{2+} refilling, helping neurons to mitigate ER stress during Aβ exposure (Pannaccione et al, 2012, Verkhratsky et al, 2003). The calpain proteolysis of NCX3 sequence may generate three products (Iwamoto et al, 2006) and site-directed mutagenesis showed that the removal of two lysine residues (370–371) in the consensus site for calpain cleavage in the f-loop of NCX3 sequence prevented the formation of the hyperfunctional fragment, and abolished the $A\beta_{1-42}$ stimulatory effect on NCX3 (Pannaccione et al, 2012). These findings, together with our results showing that ncx3 gene silencing significantly prevented the upregulation of reversal I_{NCX}, support our hypothesis that it is NCX3 that predominantly contribute to the increased NCX reversal activity in the 4-days BED treatment protocol.

Moreover, $[Ca^{2+}]_i$ levels recorded after 3 hours of BED washout were significantly higher than that measured after 2 days of washout, a time point in which only the NCX reverse mode significantly increased. In this regard, our biochemical studies showed that NCX2 levels were slightly and transiently upregulated one day after drug washout, indicating that, at this early time point, its activity may also contribute to $[Ca^{2+}]_i$ increase. On the other hand, due to the persistent Ca^{2+} entrance, it is also possible to hypothesize that a compensatory refilling of calcium into intracellular organelles may occur after 2 days of BED washout. Accordingly, a functional coupling between NCX3 reverse mode and ER Ca^{2+} store has been already demonstrated by our research group (Pannaccione et al, 2012). In this regard, although a

detailed analysis of the subcellular localization of low molecular weight forms of NCX3 is lacking, our immunocytochemical studies showed that NCX3 immunoreactivity increased not only along some plasma membrane domains but also in the cytosolic compartment.

Beside the important role in delaying neuronal death, the activation of reversal NCX3 plays a more physiological function in oligodendroglia as it is required for myelin synthesis (Boscia et al, 2012, Friess et al, 2016). In fact, NCX-mediated Ca^{2+} influx sustains both spontaneous and D-Aspartate triggered $[Ca^{2+}]_i$ oscillations in differentiating oligodendrocytes and blocking NCX3 pharmacologically or silencing ncx3 gene prevented myelin formation (Boscia et al, 2012, Hammann et al, 2018, de Rosa et al, 2019, Boscia et al, 2020). In agreement with these observations, we found that 4-days of BED treatment was associated with increased OPCs proliferation, while BED washout reduced proliferation, elevated CaMKIIβ, a critical regulator of oligodendrocyte maturation (Swift et al, 2010, Martinez-Lozada et al, 2014) and upregulated reversal I_{NCX} and NCX3 immunoreactivity in the soma and processes of differentiating oligodendrocytes. Recently, it has been suggested that ryanodine receptors (RyRs) and the α_2-NKA cooperate with NCXs to generate calcium transients, and a local RyRs-NCXs–α_2-NKA interaction in oligodendrocyte processes might influence myelin synthesis (Bassetti et al, 2020). Interestingly, our studies showed that the 4 days, but not the 2-days BED treatment protocol significantly and transiently downregulated the α_2-NKA protein levels at 1 day of washout. The reason for this transient alteration remains to be clarified but may be linked to the rapid $[Na^+]_i$ and $[Ca^{2+}]_i$ changes after prolonged NCX3 blocking and drug-free washout. For instance, early data showed that the activation of the Ca^{2+}/calmodulin-dependent kinase kinase β following $[Ca^{2+}]_i$ increase has been linked to AMP-activated kinase activation and NKA endocytosis (Gusarova et al, 2011). Our findings may also suggest that the low α_2-NKA expression, and possibly activity, would prime NCX for reverse mode exchange, consequently boosting oligodendrocyte development. In support of this hypothesis, and beside the specific role for the α_2 isoform as a regulator, via NCX exchanger, of calcium and contractility in the heart (Swift el al, 2008), Hamman et al. (2018) showed that knocking-down or blocking α_2-NKA activity with ouabain in oligodendrocytes increased NCX activity and anticipated the onset of MBP synthesis.

In agreement, we found that BED treatment for 4-days + 2 days of washout not only induced a significant higher calcium response in OPC soma and processes after acute D-Aspartate exposure, but also upregulated NCX3 expression along processes and accelerated oligodendrocyte maturation and myelin sheet formation. We found that Ca^{2+} concentrations

were always higher in processes than in the soma, either in absence of D-Asp. This finding is in line with previous studies showing that local Ca^{2+} events within processes of differentiating oligodendrocytes modulate MBP synthesis in vitro and in vivo (Krasnow et al, 2018, Baraban et al, 2018, Bassetti et al, 2020). We previously showed that D-Asp-induced calcium responses in oligodendrocytes promotes an orchestrated activation of glutamate transporters, glutamate AMPA and NMDA receptors, and NCX3 exchangers, and drives cell differentiation (Gautier et al, 2015, de Rosa et al, 2019). Hence, the upregulated expression and activity of NCX3 exchanger might contribute to the different kinetics of D-Asp response under control conditions and after 2 days of BED washout. In addition, in line with the characteristic stage-specific Ca^{2+} activity of oligodendrocyte lineage, BED-treated oligodendrocytes showed a more "flat" Ca^{2+} signaling, if compared to control cultures, that displayed characteristics OPCs oscillatory pattern with peak and plateau transients (Niu et al, 2016, Li et al, 2020).

Collectively, our findings demonstrated that the modulation of NCX3 exchanger may significantly influence intracellular $[Ca^{2+}]_i$ and $[Na^{+}]_i$ concentrations and related cellular processes, including myelin formation in oligodendroglia. Additionally, as a rebound activation of NCX3 exchanger may occur after the suspension of a drug that inhibits its function, particular attention should be paid to the use of NCX inhibitors in different pathophysiological conditions in which they have been proposed. Nevertheless, further studies will be necessary to understand the pharmacological effects of NCX3 inhibition in brain cells and whether the rebound activation of NCX3 following its pharmacological inhibition may represent a novel strategy to modulate NCX3 exchanger in demyelinating diseaseas.

Combined FAAH inhibitory activity and melatonin receptor agonism promoted neuroprotection against the neuroinflammatory damage.

In the second part of our study we showed that the newly synthetized compound UCM-1341, a bivalent ligand endowed with FAAH inhibitory activity and melatonin receptor agonism, exerts a potent neuroprotective effect against neuroinflammation-induced degeneration in hippocampal explants, if compared to the reference compounds URB-597 and melatonin, and benefits microglia M2 polarization during the neuroinflammatory insult.

Previous studies showed that LPS+IFN-γ induced inflammatory damage, by mimicking the microglia interaction with infiltrating peripheral immune T cells, triggers the release of massive proinflammatory and cytotoxic factors, and promotes an inflammatory neurodegeneration (Papageorgiou et al, 2010). In the present study we showed for the first time that this model of

cell degeneration, which preferentially occurred in the CA1 pyramidal region after 72 hours of LPS+INF-γ exposure, can be monitored by PI uptake in hippocampal slices. This model of damage may recapitulate the main hallmarks of CNS inflammatory demyelination (Boscia et al, 2020). By means of Western Blotting and confocal colocalization analyses, we showed that microglia and astrocyte activated early after the inflammatory insult in hippocampal slices, and is accompanied by a marked axonal demyelination and loss. It is widely documented that dysregulation in ECs levels and melatonin release take place in many chronic inflammatory disease conditions including neuroinflammatory, neurodegenerative and autoimmune diseases and may contribute to chronic associated brain cell dysfunction and disease progression (Leuti et al, 2020, Hardeland, et al, 2012). Hence, agents that increase the endogenous ECs levels and stimulate melatonin receptors may have therapeutic benefit to slow down disease progression (Chiuchiù et al, 2018, Abdulbaset et al, 2020).

Our expression studies showed that FAAH protein levels early increased in CA1 hippocampal neurons and astrocytes after the neuroinflammatory insult. At later time points, the increased FAAH immunosignal persisted in astrocytes, but not in neurons, and emerged in microglia, particularly in that one surrounding damaged cells. Consistently with these results, an increase in FAAH protein or mRNA levels were found in glial cells surrounding Aβ plaques in tissue samples from subjects with AD and Down syndrome, as well as in astrocytes at asymptomatic and acute EAE stage, respectively (Benito et al, 2007, Nu´nez et al, 2008, Moreno-García et al, 2020). Conversely, melatonin deficiency and a decline of MT1 and MT2 expression levels have been described in various neurodegenerative and neuroinflammatory diseases, including PD, AD, and ALS brains (Adi et al, 2010, Brunner et al, 2006, Savaskan et al, 2005, Zhang et al, 2013). Although a detailed characterization is still required to define the differential localization of melatoninergic receptors in brain cells under neuroinflammatory conditions, by using an antibody recognizing both plasma membrane melatonin receptor subtypes we found that MT1 levels persistently increased after LPS+IFN-γ exposure while MT2 proteins decreased after a transient upregulation. Interestingly, MT1 density was found to increase in hippocampal pyramidal neurons of AD brain, while a reduced expression was reported for MT2 receptors (Savaskan et al, 2002). Whether the imbalance between MT1 and MT2 levels observed in this latter study and in our model may reflect a compensatory effect, and to what extent it might be associated with signalling differences in neurons and glia under neuroinflammatory conditions remains to be investigated.

Our neuroprotection studies showed that while the damage occurring in the CA1 and the less vulnerable CA3 region in slices exposed to NMDA concentrations was not greatly affected by UCM-1341, the bivalent ligand exerted a marked dose-dependent neuroprotection against LPS+IFN-γ-induced neuroinflammatory damage and attenuated axonal demyelination. The neuroprotective effects of both ECs and melatonin in experimental models of CNS neuroinflammation have been documented by a number of studies. FAAH inhibition has therapeutic potential against different neuroinflammatory states including MS, traumatic brain injury, AD, PD, HD and stroke. Numerous *in vitro* and *in vivo* studies have established metabolic role underlying the neuroprotective role of ECs and, hence, for selective FAAH inhibitors. In several conditions, as an intrinsic neuroprotective response, the neuronal injury activates the ECs. Indirect potentiation of this salutary response through the pharmacological inhibition of the endocannabinoid-deactivating enzyme FAAH, offer site- and event-specific therapeutic relief in those tissues where endocannabinoids are being produced as part of a physiological protective mechanism (Janero et al, 2009a). Currently, FAAH inhibitors are in clinical evaluation for the treatment of cannabis use disorder, Tourette syndrome, and chronic pain (Egmond et al, 2020). Further support for beneficial effects of FAAH inhibition in MS has been demonstrated in the EAE model. FAAH deletion or pharmacological inhibition in mice produces a more substantial EAE remission, reduced synaptic dysfunction and spasticity (Webb et al, 2008, Rossi et al, 2011, Pryce et al, 2013). The beneficial effects of melatonin in MS have been reported by several studies showing that melatonin is effective in EAE mice and modulates adaptive immunity centrally and peripherally (Chen et al, 2016, Kashani et al, 2014). Melatonin has been identified as a powerful direct free radical scavenger (Reiter et al, 2007) and indirect antioxidant (Reiter et al, 2003, Reiter et al, 2004). It is also effective in reducing infiltration of Th1/Th17 lymphocytes, increasing Treg frequency during EAE, and improving disease clinical scores (Alvarez-Sanchez et al, 2015, Chen et al, 2016). Melatonin also inhibits demyelination and increases remyelination, and its local regulation by serotonin availability in white matter glia could play a role in the etiology, course and treatment of MS (Anderson et al, 2015).

Based on these observations, we hypothesized that melatonin could play an adjunct therapeutic role in treating CNS neuroinflammatory disease. We showed that cotreatment of slices with the reference compounds melatonin or URB-597 exerted a greater neuroprotection against LPS+IFN-γ exposure, if compared to single compounds. The combined effect was comparable

to that observed with UCM-1341, thus indicating that the reference compounds exerted a synergistic neuroprotective actions against LPS+IFN-γ-induced inflammatory damage.

It is largely documented that both ECs and melatonin may act as immunomodulators controlling innate immune activation and cytokine release during neuroinflammation (Cabral et al, 2015, Talarico et al, 2019). Our biochemical and confocal analyses showed that UCM1-341 has also protective effects on astrocyte and microglia cells and clearly polarized microglia/macrophages to a foamy phenotype. Microglia activation is recognized as a pivotal hallmark of neuroinflammation, and despite the well-documented detrimental effects exerted by activated microglial cells (Hong et al, 2016, Burma et al, 2017), it is now clear that they can also provide beneficial roles (Colton, 2009, Kigerl et al, 2009). It has been proven that the imbalance of pro- and anti-inflammatory microglia/macrophages plays an essential role in neurological disorders and neuroinflammatory diseases such as MS or AD (Boillee et al, 2006, Wang et al, 2015). Actually, as highly plastic cells, microglia could form continuum states with distinct phenotypes and functions in the brain (Hughes et al, 2012, Wang et al, 2013, Nakagawa and Chiba, 2015, Xiong et al, 2016, Lan et al, 2017). In particular, the anti-inflammatory M2 phenotype can orchestrate a neuroprotective or neurosupportive response by promoting tissue recovery, and improving brain reparation regeneration (Atri et al, 2018). Consistent with these observation, our Western blot and confocal analysis revealed that the *mannose receptor CD206*, an M2 macrophage marker, was intensely reduced in LPS+IFN–γ exposed slices, but significantly upregulated by UCM-1341 under the neuroinflammatory insult, indicating that UCM-1341-induced microglia M2 polarization may contribute to its beneficial effects. Recent studies demonstrated that both ECs and melatonin modulate microglia activation and regulate the activation of the immune system, reducing acute and chronic inflammation. In line with our findings, recent evidence demonstrated that the FAAH inhibitor URB-597 exerts a potent anti-inflammatory action by inhibiting BV-2 cell microglial polarization, promoting cytoskeleton reorganization via cell migration and phagocytosis processes, as well as by modulating the expression of pro- and anti-inflammatory markers (Grieco et al, 2021). Similarly, melatonin interacts in multiple ways with microglia, both directly and, indirectly thought astrocytes and neurons. Melatonin was shown to strongly influence their polarization in favor of the anti-inflammatory type M2 at the expense of the proinflammatory type M1 (Xia et al, 2019). Evidence suggest that the prevention of microglial inflammasome activation exerted by melatonin may be explained by the downregulation of toll-like receptor 4 (TLR4), the phosphorylation of Akt, mTOR (Cui et al, 2021, Zhou et al, 2008) and the stress kinases JNK

and p38, the prevention of NADPH oxidase activation/assembly (McCarty et al, 2021) and of caspase-3 cleavage (Yao et al, 2015). A common mechanism that is observed in many studies, that reflects the anti-inflammatory and antioxidant actions of melatonin in microglia, is the drug-induced suppression of NF-κB activation, which is often accompanied by Nrf2 upregulation (Park et al 2017, Merlo et al 2020, Caruso et al, 2021).

Collectively, our findings demonstrated that enhancing the of ECs and melatoninergic tone exert neuroprotective effects against and the neuroinflammatory damage in hippocampal organotypic slices. The modulation effects of UCM-1341 on microglia activities might contribute to the synergistic beneficial effects against the inflammatory injury. Nevertheless, further studies will be required to understand whether enhancing the ECs and melatoninergic tone with UCM-1341 may represent a novel neuroprotective strategy to treat neuroinflammatory conditions.

IV. References

Abdulbaset Abo Taleb H, Alghamdi BS, Neuroprotective Effects of Melatonin during Demyelination and Remyelination Stages in a Mouse Model of Multiple Sclerosis *Journal of Molecular Neuroscience* 70 (2020) 386–402

Alghamdi BS, AboTaleb HA, Melatonin improves memory defects in a mouse model of multiple sclerosis by up-regulating cAMP-response element-binding protein and synapse-associated proteins in the prefrontal cortex J Integr Neurosci 19 (2020) 229-237

Alghamdi BS, AboTaleb HA, Melatonin improves memory defects in a mouse model of multiple sclerosis by up-regulating cAMP-response element-binding protein and synapse-associated proteins in the prefrontal cortex J Integr Neurosci 19 (2020) 229-237

Álvarez-Sánchez N, Cruz-Chamorro I, López-González A, Utrilla JC, Fernández-Santos JM, Martínez-López A, Lardone PJ, Guerrero JM, Carrillo-Vico A, Melatonin controls experimental autoimmune encephalomyelitis by altering the T effector/regulatory balance Brain Behav Immun 50 (2015) 101-114

Álvaro MG, Bernal-Chico A, Colomer T, Rodríguez-Antigüedad A, Matute C, Mato Susana, Gene Expression Analysis of Astrocyte and Microglia Endocannabinoid Signaling during Autoimmune Demyelination Biomolecules 10 (2020) 9-1228

Andersona G, Rodriguez M, Multiple sclerosis: The role of melatonin and N-acetylserotonin Multiple sclerosis: Relat Disord 4 (2015) 112-23

Annunziato L, Boscia F, Pignataro G, Ionic transporter activity in astrocytes, mi-croglia, and oligodendrocytes during brain ischemia, J. Cereb. Blood Flow Metab. 33 (2013) 969–982

Annunziato L, Pignataro G, Di Renzo GF, Pharmacology of brain Na+/Ca2+ exchanger: from molecular biology to therapeutic perspectives. Pharmacol Rev. 56 (2004) 633-54

Araújo IM, Carreira BP, Pereira T, Santos PF, Soulet D, In´acio A, Bahr BA, Carvalho AP, Ambr´osio AF, Carvalho CM, Changes in calcium dynamics following the reversal of the sodium-calcium exchanger have a key role in AMPA receptor-mediated neurodegeneration via calpain activation in hippocampal neurons, Cell Death Differ. 14 (2007) 1635–1646

Armstrong RC, Dorn HH, Kufta CV, Friedman E, Dubois-Dalcq ME, Preoligodendrocytes from adult human CNS. J Neurosci 12 (1992) 1538–1547

Atherton J, Kurbatskaya K, Bondulich M, Croft CL, Garwood CJ, Chhabra R, Wray S, Jeromin A, Hanger DP, Noble W, Calpain cleavage and inactivation of the sodium calcium exchanger-3 occur downstream of Aβ in Alzheimer's disease, Aging Cell 13 (2014) 49–59

Atri C, Guerfali FZ, Laouini D, Role of Human Macrophage Polarization in Inflammation during Infectious Diseases Int J Mol Sci 19 (2018) 1801

Bano D, Young KW, Guerin CJ, Lefeuvre R, Rothwell NJ, Naldini L, Rizzuto R, Carafoli E, Nicotera P, Cleavage of the plasma membrane Na+/Ca2+ exchanger in excitotoxicity, Cell. 120 (2005) 275–285

Baraban M, Koudelka S, Lyons DA, Ca2+ activity signatures of myelin sheath formation and growth in vivo, Nat. Neurosci. 21 (2018) 19–23

Baraban M, Koudelka S, Lyons DA, Ca2+ activity signatures of myelin sheath formation and growth in vivo, Nat. Neurosci. 21 (2018) 19–23

Barateiro A, Fernandes A, Temporal oligodendrocyte lineage progression: in vitro models of proliferation, differentiation and myelination Biochim Biophys 1843 (2014) 1917-29

Barres BA, Raff MC, Axonal control of oligodendrocyte development. J Cell Biol 147 (1999) 1123-1128.

Bars DL, Thivolle P, Vitte PA, Bojkowski C, Chazot G, Arendt J, Frackowiak RS, Claustrat B, PET and plasma pharmacokinetic studies after bolus intravenous administration of melatonin in humans Int J Rad Appl Instrum B 199 (18) 1357-1362

Baumann N, Pham-Dinh D Biology of oligodendrocyte and myelin in the mammalian central nervous system. Physiol Rev 81 (2001) 871-927

Benamer N, Vidal M, Balia M, Angulo MC, Myelination of parvalbumin interneurons shapes the function of cortical sensory inhibitory circuits Nat Commun 11 (2020) 5151

Bergles DE, Richardson WD, Oligodendrocyte development and plasticity, Cold Spring Harb Perspect Biol 8 (2015) 020453

Black JA, Newcombe J, Trapp BD, Waxman SG, Sodium channel expression within chronic multiple sclerosis plaques, J. Neuropathol. Exp. Neurol. 66 (2007) 828–837

Boda E, Viganò F, Rosa P, Fumagalli M, Labat-Gest V, Tempia F, Abbracchio MP, Dimou L, Buffo A The GPR17 receptor in NG2 expressing cells: focus on in vivo cell maturation and participation in acute trauma and chronic damage. *Glia* 59 (2011)1958-1973

Boillée S, Yamanaka K, Lobsiger CS, Copeland NG, Jenkins NA, Kassiotis G, Kollias G, Cleveland DW Onset and progression in inherited ALS determined by motor neurons and microglia Science 312 (2006) 1389-1392.

Boscia F, Annunziato L, Taglialatela M. Retigabine and flupirtine exert neuroprotective actions in hippocampal slice cultures and adult rat brain. Neuropharmacology. 55 (2006) 428-439

Boscia F, Begum G, Pignataro G, Sirabella R, Cuomo O, Casamassa A, Sun D, Annunziato L, Glial Na(+) -dependent ion transporters in pathophysiological conditions, Glia 64 (2016) 1677–1697

Boscia F, Casamassa A, Secondo A, Esposito A, Pannaccione A, Sirabella R, Pignataro G, Cuomo O, Vinciguerra A, De Rosa V, Annunziato L, NCX1 exchanger cooperates with Calretinin to confer preconditioning-induced tolerance against cerebral ischemia in the striatum, Mol. Neurobiol. 53 (2016) 1365–1376

Boscia F, D'Avanzo C, Pannaccione A, Secondo A, Casamassa A, Formisano L, Guida N, Scorziello A, Di Renzo G, Annunziato L, New roles of NCX in glial cells: activation of microglia in ischemia and differentiation of oligodendrocytes, Adv. Exp. Med. Biol. 16 (2013) 961-307

Boscia F, D'Avanzo C, Pannaccione A, Secondo A, Casamassa A, Formisano L, Guida N, Sokolow S, Herchuelz A, Annunziato L, Silencing or knocking out the Na^+/Ca^{2+} exchanger-3 (NCX3) impairs oligodendrocyte differentiation, Cell Death Diff. 19 (2012) 562–572

Boscia F, de Rosa V, Cammarota M, Secondo A, Pannaccione A, Annunziato L, The Na^+/Ca^{2+} exchangers in demyelinating diseases. Cell Calcium 85 (2020) 102130

Boscia F, Esposito CL, Di Crisci A, de Franciscis V, Annunziato L, Cerchia L, GDNF selectively induces microglial activation and neuronal survival in CA1/CA3 hippocampal regions exposed to NMDA insult through Ret/ERK signalling, PLoS One 4 (2009) e6486

Boscia F, Esposito L, Casamassa A, de Franciscis V, Annunziato L, Cerchia L, The isolectin IB4 binds RET receptor tyrosine kinase in microglia, J. Neurochem. 126 (2013) 428–436

Boscia F, Ferraguti F, Moroni F, Annunziato L, Pellegrini-Giampietro DE, mGlu1alpha receptors are co-expressed with CB1 receptors in a subset of interneurons in the CA1 region of organotypic hippocampal slice cultures and adult rat brain, Neuropharmacology 55 (2008) 428–439

Boscia F, Pannaccione A, Ciccone R, Casamassa A, Franco C, Piccialli I, de Rosa V, Vinciguerra A, Di Renzo G, Annunziato L, The expression and activity of KV3.4 channel subunits are precociously upregulated in astrocytes exposed to Aβ oligomers and in astrocytes of Alzheimer's disease Tg2576 mice, Neurobiol. Aging 54 (2017) 187–198

Boscia F, Passaro C, Gigantino V, Perdona S, Franco R, Portella G, Chiffi S, Chieff P, High levels of GPR30 protein in human testicular carcinoma in situ and seminomas correlate with low levels of estrogen receptor-beta and indicate a switch in estrogen responsiveness, J. Cell. Physiol. 230 (2015) 1290–1297

Boscia F, Scorziello A, Sirabella R, Sokolow S, Herchuelz A, Di Renzo G, Annunziato L, A new concept: Aβ1-42 generates a hyperfunctional proteolytic NCX3 fragment that delays caspase-12 activation and neuronal death, J. Neurosci. 32 (2012) 10609–10617

Brustovetsky T, Bolshakov A, Brustovetsky N, Calpain activation and Na+/Ca2+ exchanger degradation occur downstream of calcium deregulation in hippocampal neurons exposed to excitotoxic glutamate J Neurosci Res 88 (2010) 1317–1328

Burma NE , Leduc-Pessah H, Fan CY, Trang T, Animal models of chronic pain: Advances and challenges for clinical translation (2016) J Neurosci Res 95 (2017) 1242-1256

Cammarota M, de Rosa V, Pannaccione A, Secondo A, Tedeschi V, Piccialli I, Fiorino F, Severino B, Annunziato L, Boscia F. Rebound effects of NCX3 pharmacological inhibition: a novel strategy to accelerate myelin formation in oligodendrocytes Biomedicine and Pharmacotherapy, 143 (2021) 112111

Caruso GI, Spampinato SF, Costantino G, Merlo S, Sortino MA, SIRT1-dependent upregulation of BDNF in human microglia challenged with Aβ: An early but transient response rescued by melatonin. Biomedicines 9 (2021) 466

Casamassa A, La Rocca C, Sokolow S, Herchuelz A, Matarese G, Annunziato L, Boscia F, Ncx3 gene ablation impairs oligodendrocyte precursor response and increases susceptibility to experimental autoimmune encephalomyelitis, Glia 64 (2016) 1124–1137

Cecon E, Oishi A, Jockers Ralf , Melatonin receptors: molecular pharmacology and signalling in the context of system bias Br J Pharmacol 175 (2018) 3263-3280

Centonze D, Finazzi-Agrò A, Bernardi G, Maccarrone M, The endocannabinoid system in targeting inflammatory neurodegenerative diseases Trends Pharmacol Sci 28 (2007) 180-187

Charcot JM, Histologie de la scle´rose en plaques Gaz Des hospitaux 41 (1868) 554-558

Chen D, Zhang T, Lee TH, Cellular Mechanisms of Melatonin: Insight from Neurodegenerative Diseases Biomolecules 10 (2020) 1158

Chen S, Shi L, Liang F, Xu L, Desislava D, Wu Q, Zhang J, Exogenous Melatonin for Delirium Prevention: a Meta-analysis of Randomized Controlled Trials Mol Neurobiol 53 (2016) 4046-4053

Chiurchiù V, van der Stelt M, Centonze D, Maccarrone M, The endocannabinoid system and its therapeutic exploitation in multiple sclerosis: Clues for other neuroinflammatory diseases Progress in Neurobiology 160 (2018) 82–100

Clapper JR et al. Anandamide suppresses pain initiation through a peripheral endocannabinoid mechanism. Nat Neurosci 13 (2010) 1265–1270

Claustrat B, Leston J, Melatonin: Physiological effects in humans Neurochirurgie 61 (2015) 77-84

Cohen CCH, Popovic MA, Klooster J, Weil MT, Möbius W, Nave KA, Kole HPM, Saltatory Conduction along Myelinated Axons Involves a Periaxonal Nanocircuit Cell 180 (2020) 311-322

Colton CA, Heterogeneity of microglial activation in the innate immune response in the brain J Neuroimmune Pharmacol 4 (2009) 399-418

Compston A, Coles A Multiple sclerosis. *Lancet* 359 (2002) 1221–1231

Compston A, Coles A The Lancet 372 (2008) 1502 – 1517

Correale J, Marrodan M, Ysrraelit MC, Mechanisms of Neurodegeneration and Axonal Dysfunction in Progressive Multiple Sclerosis Biomedicines 7 (2019) 1-14

Craner MJ, Hains BC, Lo AC, Black JA, Waxman SG, Co-localization of sodium channel Nav1.6 and the sodium-calcium exchanger at sites of axonal injury in the spinal cord in EAE, Brain 127 (2004) 294–303

Cui Y, Yang M, Wang Y, Ren J, Lin P, Cui C, Song J, He Q, Hu H, Wang K, Melatonin prevents diabetes-associated cognitive dysfunction from microglia-mediated neuroinflammation by activating autophagy via TLR4/Akt/mTOR pathway FASEB J. 35 (2021) e21485

Dawson MR, Polito LA, Levine JM, and Reynolds R, NG2-expressing glial progenitor cells: an abundan and widespread population of cycling cells in the adult rat CNS.Mol Cell Neurosci 24 (2003) 476-488

de Rosa V, Secondo A, Pannaccione A, Ciccone R, Formisano L, Guida N, Crispino R, Fico A, Polishchuk R, D'Aniello A, Annunziato L, Boscia F, DAspartate treatment attenuates myelin damage and stimulates myelin repair, EMBO Mol. Med. 11 (2019) e9278

Di Marzo V, Fontana A, Cadas H, Schinelli S, Cimino G, Schwartz JC, Piomelli D, Formation and inactivation of endogenous cannabinoid anandamide in central neurons Nature 372 (1994) 686–691

Di Marzo V, Piscitelli F, The Endocannabinoid System and its Modulation by Phytocannabinoids Neurotherapeutics 12 (2015) 692-698

Diarra C, Heldon S, Church J, In situ calibration and [H+] sensitivity of the fluorescent Na+ indicator SBFI, Am. J. Physiol. Cell Physiol. 280 (2001) 1623–1633

Du Y, Dreyfus CF, Oligodendrocytes as providers of growth factors. J Neurosci Res 68 (2002) 647–654

Dutta M, Hanna E, Das P, Steinhubl SR, Incidence and prevention of ischemic stroke following myocardial infarction: review of current literature. Cerebrovasc Dis 22 (2006) 331–339

Dutta R, Trapp BD Mechanisms of Neuronal Dysfunction and Degeneration in Multiple Sclerosis. Progress in neurobiology 93 (2011) 1-12

Dziedzic T, Metz I, Dallenga T, König FB, Müller S, Stadelmann C, Brück W, Wallerian degeneration: a major component of early axonal pathology in multiple sclerosis, Brain Pathol. 20 (2010) 976–985

Egemen S, Mohammed AA, Ravid R, Angeloni D, Fraschini F, Meier F, Eckert A, Müller-Spahn F, Jockers R, Reduced hippocampal MT_2 melatonin receptor expression in Alzheimer's disease J. Pineal Res. 38 (2004) 10–16

Egemen S, Olivieri G, Meier F, Brydon L, Jockers R, Ravid R, Wirz-Justice A, Müller-Spahn F, Increased melatonin 1a-receptor immunoreactivity in the hippocampus of Alzheimer's disease patients J Pineal Res 32 (2002) 59-62

Egmond N, Straub VM, van der Stelt M, Targeting Endocannabinoid Signaling: FAAH and MAG Lipase Inhibitors Annu Rev Pharmacol Toxicol 61 (2021) 441-463

Elbaz B, Popko B, Molecular Control of Oligodendrocyte Development Trends Neurosci 42 (2019) 263-277

Emery B, Regulation of oligodendrocyte differentiation and myelination, Science 330 (2010a) 779-782

Esposito F, Boscia F, Gigantino V, Tornincasa M, Fusco A, Franco R, Chieffi P, The high-mobility group A1-estrogen receptor β nuclear interaction is impaired in human esticular seminomas, J. Cell. Physiol. 227 (2012) 3749–3755

Eylar EH, Brostoff S, Hashim G, Caccam J, Burnett P Basic A1 protein of the myelin membrane, The complete amino acid sequence" J Biol Chem 246 (1971) 5770–5784

Fannon J, Tarmier W, Fulton D, Neuronal activity and AMPA-type glutamate receptor activation regulates the morphological development of oligodendrocyte precursor cells, Glia 63 (2015) 1021–1035

Ferguson B, Matyszak MK, Esiri MM, Perry VH, Axonal damage in acute multiple sclerosis lesions Brain 120 (1997) 393-399

Fernandez-Castaneda A, Gaultier, Adult oligodendrocyte progenitor cells - Multifaceted regulators of the CNS in health and disease Brain Behav Immun 57 (2016) 1-7

Fernández-Ruiz J , Gonzáles S, Cannabinoid control of motor function at the basal ganglia Handb Exp Pharmacol 2005 (168) 479-507

Fernández-Ruiz J, Romero J, Velasco G, Rosa M Tolón, José A Ramos, Manuel Guzmán Cannabinoid CB2 receptor: a new target for controlling neural cell survival? Trends Pharmacol Sci 28 (2007) 39-45

Filippi M, Bar-Or A, Piehl F, Preziosa P, Solari A, Vukusic S, Rocca MA, Mul-tiple sclerosis, Nat. Rev. Dis. Primers 4 (2018) 43

Foerster S, Hill MFE, Franklin RJM. Diversity in the oligodendrocyte lineage: Plasticity or heterogeneity? Glia 67 (2019) 1797-1805

Franklin RJM, ffrench-Constant C Remyelination in the CNS: from biology to therapy. Nature Reviews Neuroscience 9 (2008) 839-855

Freeman SA, Desmazières A, Fricker D, Lubetzki C, Sol-Foulon N Mechanisms of sodium channel clustering and its influence on axonal impulse conduction. *Cellular and Molecular Life Sciences* 73 (2016) 723-735

Friese MA, Schattling B, Fugger L, Mechanisms of neurodegeneration and axonal dysfunction in multiple sclerosis, Nat. Rev. Neurol. 10 (2014) 225–238

Friess M, Hammann J, Unichenko P, Luhmann HJ, White R, Kirischuk S, Intracellular ion signaling influences myelin basic protein synthesis in oligodendrocyte precursor cells, Cell Calcium 60 (2016) 322–330

Frischer JM, Weigand SD, Guo Y, Kale N, Parisi JE, Pirko I, Mandrekar J, Bramow S, Metz I, Brück W, Lassmann H, Lucchinetti C, Clinical and pathological insights into the dynamic nature of the white matter multiple sclerosis plaque Ann Neurol 78 (2015) 710-21

Gard AL, Pfeiffer SE, Oligodendrocyte progenitors isolated directly from developing telencephalon at a specific phenotypic stage: myelinogenic potential in a defined environment, Development 106 (1989) 119–132

Gautier HO, Evans KA, Volbracht K, James R, Sitnikov S, Lundgaard I, James F, Lao-Peregrin C, Reynolds R, Franklin RJ, K´arad´ottir RT, Neuronal activity regulates remyelination via glutamate signalling to oligodendrocyte progenitors, Nat. Commun 6 (2015) 8516–8518

Gerkau NJ, Lerchundi R, Nelson JSE, Lantermann M, Meyer J, Hirrlinger J, Rose CR, Relation between activity-induced intracellular sodium transients and ATP dynamics in mouse hippocampal neurons J. Physiol. 597 (2019) 5687–5705

Ghareghani M, Sadeghi H , Zibara K, Danaei N, Azari H, Ghanbari A, Melatonin Increases Oligodendrocyte Differentiation in Cultured Neural Stem Cells Cell Mol Neurobiol 37 (2017) 1319-1324

Ghareghani M, Scavo L , Jand Y, Farhadi N, Sadeghi H, Ghanbari A, Mondello Stefania, Arnoult D, Gharaghani S, Zibara K, Melatonin Therapy Modulates Cerebral Metabolism and Enhances Remyelination by Increasing PDK4 in a Mouse Model of Multiple Sclerosis Front Pharmacol 10 (2019) 147

Goldenberg MM, Multiple sclerosis review PT, 37 (2012) 175-84

Goldschmidt T, Antel J, König FB, Brück W, Kuhlmann T Remyelination capacity of the MS brain decreases with disease chronicity Neurology 72 (2009) 1914-1921

Gomez-Villafuertes R, Mellström B, Naranjo JR, Searching for a role of NCX/NCKX exchangers in neurodegeneration Mol Neurobiol 35 (2007) 195-202.

Gopalakrishnan G, Awasthi A, Belkaid W, Jr De Faria O, Liazoghli D, Colman DR, Dhaunchak AS, Lipidome and proteome map of myelin membranes, AS. J. Neurosci. Res. 91 (2013) 321–334.

Gourraud PA, Harbo HF, Hauser SL, Baranzini SE The genetics of multiple sclerosis: an up-to-date review Immunol 248 (2012) 87-103

Goverman JM, Immune Tolerance in Multiple Sclerosis, Immunological reviews 241 (2011) 228-240.

Greer JM, McCombe PA, Role of gender in multiple sclerosis: clinical effects and potential molecular mechanisms J Neuroimmunol 234 (2011) 7-18.

Gregus AM, Buczynski W M, Druggable Targets in Endocannabinoid Signaling Adv Exp Med Biol 1274 (2020) 177-201.

Griebel G, Stemmelin J, Lopez-Granca M, Fauchey V, Slowinski F, Pichat P, Dargazanli G, Abouabdellah A, Cohen C, Bergis OE, The selective reversible FAAH inhibitor, SSR411298, restores the development of maladaptive behaviours to acute and chronic stress in rodents 8 (2018) 2416

Grieco M, De Caris MG, Maggi E, Armeli F, Coccurello R, Bisogno T, D'Erme M, Maccarrone M, Mancini P, Businaro R, Fatty Acid Amide Hydrolase (FAAH) Inhibition Modulates Amyloid-Beta-Induced Microglia Polarization Int J Mol Sci 22 (2021) 7711

Grynkiewicz G, Poenie M, Tsien RY, A new generation of Ca^{2+} indicators with greatly improved fluorescence properties, J. Biol. Chem. 260 (1985) 3440–3450

Gulyas AI, Cravatt BF, Bracey MH, Dinh TP, Piomelli D, Boscia F, Freund TF, Segregation of two endocannabinoid-hydrolyzing enzymes into pre- and postsynaptic compartments in the rat hippocampus, cerebellum and am Eur J Neurosci 20 (2004) 441-58

Gusarova GA, Trejo HE, Dada LA, Briva A, Welch LC, Hamanaka RB, Mutlu GM, Chandel NS, Prakriya M, Sznajder JI, Hypoxia leads to Na, K-ATPase downregulation via Ca(2+) release-activated Ca(2+) channels and AMPK activation, Mol. Cell Biol. 31 (2011) 3546–3556

Hametner S, Wimmer I, Haider L, Pfeifenbring S, Brück W, Lassmann H. Ann Neurol, 74 (2013) 848–861

Hammann J, Bassetti D, White R, Luhmann HJ, Kirischuk S, α2 isoform of Na+,K+-ATPase via Na+,Ca2+ exchanger modulates myelin basic protein synthesis in oligodendrocyte lineage cells in vitro, Cell Calcium 73 (2018) 1–10

Hammann J, Bassetti D, White R, Luhmann HJ, Kirischuk S, α2 isoform of Na+, K+-ATPase via Na+,Ca2+ exchanger modulates myelin basic protein synthesis in oligodendrocyte lineage cells in vitro, Cell Calcium 73 (2018) 1–10

Hong S, Beja-Glasser VF, Nfonoyim BM, Frouin A, Li S, Ramakrishnan S, Merry KM, Shi Q, Rosenthal A, Barres BA, Lemere CA, Selkoe DJ, Stevens B, Complement and microglia mediate early synapse loss in Alzheimer mouse models Science 352 (2016) 712-716

Hu HJ, Wang SS, Wang YX, Liu Y, Feng XM, Shen Y, Zhu L, Chen HZ, Song M, Blockade of the forward Na^+ /Ca^{2+} exchanger suppresses the growth of glioblastoma cells through Ca^{2+} mediated cell death Br. J. Pharm. 176 (2019) 2691–2707

Hughes EG, Bergles DE, Hidden Progenitors Replace Microglia in the Adult Brain 82 (2014) 253-255

Hwang J, Adamson C, Butler D, Janero DR, Makriyannis A, Bahr BA, Enhancement of endocannabinoid signaling by fatty acid amide hydrolase inhibition: A neuroprotective therapeutic modality Br J Pharmacol. 153 (2008) 277–285.

Hwang J, Adamson C, Butler D, Janero DR, Makriyannis A, Bahr BA, Enhancement of endocannabinoid signaling by fatty acid amide hydrolase inhibition: A neuroprotective therapeutic modality Life Sci. 86 (2010) 615–622

Inglese M, Oesingmann N, Zaaraoui W, Ranjeva JP, Fleysher L, Sodium imaging as a marker of tissue injury in patients with multiple sclerosis Multiple Sclerosis and Related Disorders 2 (2013) 263-269

Iwamoto T, Kita S, YM-244769, a novel Na+/Ca2+ exchange inhibitor that preferentially inhibits NCX3, efficiently protects against hypoxia/reoxygenation-induced SH-SY5Y neuronal cell damage, Mol. Pharm. 70 (2006) 2075–2083

Jessen K, Glial cells, The International Journal of Biochemistry & Cell Biology 10 (2004), 1861–1867

Kanchandani R, Howe J G, Lhermitte's sign in multiple sclerosis: a clinical survey and review of the literature J Neurol Neurosurg Psychiatry 45 (1982) 308-312

Káradóttir R, Attwell D Neurotransmitter receptors in the life and death of oligodendrocytes. Neuroscience 145 (2007) 1426-1438

Kashani IR, Rajabi Z, Akbari M, Hassanzadeh G, Mohseni A, Eramsadati MK, Rafiee K, Beyer C, Kipp M, Zendedel A, Protective effects of melatonin against mitochondrial injury in a mouse model of multiple sclerosis Exp Brain Res 232 (2014) 2835-2846

Kiedrowski L, Brooker G, Costa E, Wroblewski J T, Glutamate impairs neuronal calcium extrusion while reducing sodium gradient Neuron (1994) 295-300

Kigerl KA, Gensel JC, Ankeny DP, Alexander JK, Donnelly DJ, Popovich PG, Identification of two distinct macrophage subsets with divergent effects causing either neurotoxicity or regeneration in the injured mouse spinal cord J Neurosci 29 (2009) 13435-13444

Kim JW, Jo J, Kim JY, Choe M, Leem J, Park JH, Melatonin Attenuates Cisplatin-Induced Acute Kidney Injury through Dual Suppression of Apoptosis and Necroptosis Biology 8 (2019) 3-64

Kornek B, and Lassmann H, Axonal pathology in multiple sclerosis. A historical note, Brain Pathol, 9 (1999) 651-656

Kornek B, Storch MK, Bauer J, Djamshidian A, Weissert R, Wallstroem E, Stefferl A, Zimprich F, Olsson T, Linington C, Schmidbauer M, Lassmann H, Distribution of a calcium channel subunit in dystrophic axons in multiple sclerosis and experimental autoimmune encephalomyelitis, Brain 124 (2001) 1114–1124

Krasnow AM, Ford MC, Valdivia LE, Wilson SW, Attwell D, Regulation of developing myelin sheath elongation by oligodendrocyte calcium transients in vivo, Nat. Neurosci. 21 (2018) 24–28

Kuhlmann T, Ludwin S, Prat A, Antel J, Brück & Hans W, Lassmann An updated histological classification system for multiple sclerosis lesions Acta Neuropathologica 133 (2016) 13-24

Kurnellas MP, Donahue KC, Elkabes S, Mechanisms of neuronal damage in multiple sclerosis and its animal models: role of calcium pumps and exchangers, Biochem. Soc. Trans. 35 (2007) 923–926.

Lan X, Han X, Li Q, Yang QW, Wang J, Modulators of microglial activation and polarization after intracerebral haemorrhage Nat Rev Neurol 13 (2017) 420-433

Lassmann H, Pathogenic Mechanisms Associated With Different Clinical Courses of Multiple Sclerosis Front Immunol 9 (2018) 3116

Lassmann H, Brück W, Lucchinetti C Heterogeneity of multiple sclerosis pathogenesis: implications for diagnosis and therapy Trends Mol Med 7 (2001) 115-121

Lee SL, YuQ ASL, Lyttonll J, Tissue-specific Expression of Na+-Ca2+ exchanger Isoforms, J. biowcical chemistry 269 (1994) 14849-14852

Leung D, Saghatelian A, Gabriel M, Cravatt Simon and Benjamin F, Inactivation of *N*-Acyl Phosphatidylethanolamine Phospholipase D Reveals Multiple Mechanisms for the Biosynthesis of Endocannabinoids Biochemistry 45 (2006) 4720–4726

Li C, Tropak MB, Gerlai R, Clapoff S, Abramow-Newerly W, Trapp B, Peterson A, Roder J Myelination in the absence of myelin-associated glycoprotein. Nature 30, 369 (1994)747-750

Li S, Stys PK, Mechanisms of ionotropic glutamate receptor-mediated excitotoxi-city in isolated spinal cord white matter, J. Neurosci. 84 (2000) 1190–1198

Li T, Wang L, Ma T, Wang S, Niu J, Li H, Xiao L, Dynamic calcium release from endoplasmic reticulum mediated by Ryanodine Receptor 3 is crucial for oligodendroglial. Differentiation, Front. Mol. Neurosci. 11 (2018) 162

Li Z, Matsuoka S, Hryshko LV, Nicoll DA, Bersohn MM, and Burke EP, Cloning of the NCX2 isoform of the plasma membrane Na+ -Ca2+ exchanger. JBiol Chem. 269 (1994) 17434-17439

Linnington C, Webb M, Woodhams PL, A novel myelin-associated glycoprotein defined by a mouse monoclonal antibody. J Neuroimmunol 6 (1984) 387-396

Liu J, Wang L, Harvey-White J, Huang BX, Kim HY, Luquet S, Palmiter DR, Krystal G, Rai R, Mahadevan A, Razdan RK, Kunos G, Multiple Pathways Involved in the Biosynthesis of Anandamide Neuropharmacology 54 (2008) 1–7

López HH, Webb SA, Nash S, Cannabinoid receptor antagonism increases female sexual motivation Pharmacol Biochem Behav 92 (2009) 17-24

Lublin FD, Reingold SC, Cohen JA, Cutter GR, Sørensen PS, Thompson AJ, Wolinsky JS, Balcer LJ, Banwell B, Barkhof F, Bebo B Jr, Calabresi PA, Clanet M, Comi G, Fox RJ, Freedman MS, Goodman AD, Inglese M, Kappos L, Kieseier BC, Lincoln JA, Lubetzki C, Miller AE, Montalban X, O'Connor PW, Petkau J, Pozzilli C, Rudick RA, Sormani MP, Stüve O, Waubant E, Polman CH Defining the clinical course of multiple sclerosis: The 2013 revisions. Neurology 83 (2014) 278-286

Lucchinetti C, Bruck W, Parisi J, Scheithauer B, Rodriguez M, Lassmann H, Heterogeneity of multiple sclerosis lesions: implications for the pathogenesis of demyelination Ann Neurol 47 (2000) 707–717

Filippi M, Preziosa P, Meani A, Ciccarelli O, Mesaro S, Rovira A, Frederiksen J, Enzinger C, Barkhof F, Gasperini C, Brownlee W, Drulovic J, Montalban X, Cramer SP, Pichler A, Hagens M, Ruggieri S, Martinelli V, Miszkiel K, MTintorè, Comi G, Dekker I, Uitdehaag B, Dujmovic-Basuroski I, Rocca MA. Prediction of a multiple sclerosis diagnosis in patients with clinically isolated syndrome using the 2016 MAGNIMS and 2010 McDonald criteria: a retrospective study. Lancet Neurol 17 (2018) 133–42

Marisca R, Hoche T, Agirre E, Hoodless LJ, Barkey W, Auer F, Castelo-Branco G, Czopka T, Functionally distinct subgroups of oligodendrocyte precursor cells integrate neural activity and execute myelin formation Nat Neurosci 23 (2020) 363-374

Marques S, Zeisel A, Codeluppi S, van Bruggen D, Falcão AM, Xiao L, Li H, Häring M, Hochgerner H, Romanov RA, Gyllborg D, Manchado AM, Manno LG, Lönnerberg P, Floriddia EM, Rezayee F, Ernfors P, Arenas E, Hjerling-Leffler J, Harkany T, Richardson WD, Linnarsson S, Castelo-Branco G, Oligodendrocyte heterogeneity in the mouse juvenile and adult central nervous system Science 352 (2016) 1326-1329

Martinez-Lozada Z, Waggener CT, Kim K, Zou S, Knapp PE, Hayashi Y, Ortega A, Fuss B, Activation of sodium-dependent glutamate transporters regulates the morphological aspects of oligodendrocyte maturation via signaling through calcium/calmodulin-dependent kinase IIβ's actin-binding/-stabilizing domain, Glia 62 (2014) 1543-1558

Mathes AM, Kubulus D, Weiler J, Bentley A, Waibel L, Wolf B, Bauer I, Rensing H, Melatonin receptors mediate improvements of liver function but not of hepatic perfusion and integrity after hemorrhagic shock in rats Crit Care Med 36 (2008) 24-9

McCarty MF, DiNicolantonio JJ, Lerner A, A Fundamental Role for Oxidants and Intracellular Calcium Signals in Alzheimer's Pathogenesis-And How a Comprehensive Antioxidant Strategy May Aid Prevention of This Disorder Int J Mol Sci 22 (2021) 2140

Menichella DM, Majdan M, Awatramani R, Goodenough DA, Sirkowski E, Scherer SS, Paul DL, Genetic and physiological evidence that oligodendrocyte gap junctions contribute to spatial buffering of potassium released during neuronal activity. J Neurosci Off J Soc Neurosci 26 (2006) 10984–10991

Merlo S, Luaces JP, Spampinato SF, Toro-Urrego N, Caruso GI, D'Amico F, Capani F, Sortino MA, SIRT1 mediates melatonin's effects on microglial activation in hypoxia: In vitro and in vivo evidence. Biomolecules 10 (2020) 364

Michel LY, Hoenderop JG, Bindels RJ, Towards understanding the role of the Na+-Ca^{2+} exchanger isoform 3, Rev. Physiol. Biochem. Pharmacol. 168 (2015) 31–57

Molinaro P, Cuomo O, Pignataro G, Boscia F, Sirabella R, Pannaccione A, Secondo A, Scorziello A, Adornetto A, Gala R, Viggiano D, Sokolow S, Herchuelz A, Schurmans S, Di Renzo G, Annunziato L, Targeted disruption of Na +/Ca2+ exchanger 3 (NCX3) gene leads to a worsening of ischemic brain damage, J. Neuro-sci. 28 (2008) 1179–1184

Molinaro P, Viggiano D, Nisticò R, Sirabella R, Secondo A, Boscia F, Pannaccione A, Scorziello A, Mehdawy B, Sokolow S, Herchuelz A, Di Renzo GF, Annunziato L, Na+-Ca2+ exchanger (NCX3) knock-out mice display an impairment in hippocampal long-term potentiation and spatial learning and memory, J. Neurosci. 31 (2011) 7312–7321

Montag D, Giese KP, Bartsch U, Martini R, Lang Y, Blüthmann H, Karthigasan J, Kirschner DA, Wintergerst ES, Nave KA, Mice deficient for the myelin-associated glycoprotein show subtle abnormalities in myelin. Neuron 13 (1994) 229-246

Moreno-Sanz G, Duranti A, Melzig L, Fiorelli C, Ruda GF, Colombano G, Mestichelli P, Sanchini S, Tontini A, Mor M, Bandiera T, Scarpelli R, Tarzia G, Piomelli D, Synthesis and structure-activity relationship studies of O-biphenyl-3-yl carbamates as peripherally restricted fatty acid amide hydrolase inhibitors. J Med Chem 56 (2013) 5917–5930

Nakagawa Y, Chiba K, Diversity and plasticity of microglial cells in psychiatric and neurological disorders Pharmacol Ther 154 (2015) 21-35

Nave KA, Trapp BD, Axon-glial signaling and the glial support of axon function, Annu. Rev. Neurosci. 31 (2008) 535–561

Newcombe J, Uddin A, Dove R, Patel B, Turski L, Nishizawa Y, Smith T, Glutamate receptor expression in multiple sclerosis lesions, Brain Pathol. 18 (2008) 52–61

Nikhil A, Mash DC, Ali Y, Singer C, Shehadeh L, Papapetropoulos S, Melatonin MT1 and MT2 receptor expression in Parkinson's disease Med Sci Monit 16 (2010) BR61-7

Nikić I, Merkler D, Sorbara C, Brinkoetter M, Kreutzfeldt M, Bareyre FM, Brück W, Bishop D, Misgeld T, Kerschensteiner M, A reversible form of axon damage in experimental autoimmune encephalomyelitis and multiple sclerosis, Nat. Med. 17 (2011) 495–499

Nishiyama A, Lin XH, Giese N, Heldin CH, Stallcup WB, Interaction between NG2 proteoglycan and PDGF alpha-receptor on O2A progenitor cells is required for optimal response to PDGF. J Neurosci Res 43 (1996) 315-330

Niu J, Li T, Yi C, Huang N, Koulakoff A, Weng C, Li C, Zhao CJ, Giaume C, Xiao L, Connexin-based channels contribute to metabolic pathways in the oligodendroglial lineage, J. Cell Sci. 129 (2016) 1902–1914

Nunez E, Benito C, Tolon RM, Hillard CJ, Griffin WS, Romero J, Glial expression of cannabinoid CB(2) receptors and fatty acidamide hydrolase are beta amyloid-linked events in Down's syn-drome Neuroscience 151 (2008) 104–110

Okamoto Y, Morishita J, Tsuboi K, Tonai T, Ueda N, Molecular characterization of a phospholipase D generating anandamide and its congeners J Biol Chem 279 (2004) 5298-305

Osório MJ, Goldman SA, Neurogenetics of Pelizaeus-Merzbacher disease Handb Clin Neurol 148 (2018) 701-722

Pan S, Chan JR, Regulation and dysregulation of axon infrastructure by myelinating glia, J. Cell Biol. 216 (2017) 3903–3916

Pannaccione A, Boscia F, Scorziello A, Adornetto A, Castaldo P, Sirabella R, Taglialatela M, Di Renzo G, Annunziato L, Up-regulation and increased activity of KV3.4 channels and their accessory subunit MinK-related peptide 2 induced by amyloid peptide are involved in apoptotic neuronal death, Mol. Pharm. 72 (2007) 665–673

Papa M, Canitano A, Boscia F, Castaldo P, Selitti S, Porzing H, Taglialatela M, Annunziato L, Differential expression of the Na^{+}/ Ca^{2+} exchangerer tran-scripts and proteins in rat brain regions. J Comp Neurol. 461 (2003) 31-48

Papageorgiou IE, Lewen A, Galow LV, Cesetti T, Scheffel J, Regen T, Hanisch UK, Kann O.
TLR4-activated microglia require IFN-γ to induce severe neuronal dysfunction and death in situ Proc Natl Acad Sci U S A 113 (2016) 212-7

Park E, Chun HS, Melatonin attenuates manganese and lipopolysaccharide-induced inflammatory activation of BV2 microglia Neurochem. Res. 42 (2017) 656–666

Patrikios P, Stadelmann C, Kutzelnigg A, Rauschka H, Schmidbauer M, Laursen H, Sorensen P S, Brück W, Lucchinetti C, Lassmann H, Remyelination is extensive in a subset of multiple sclerosis patients Brain 129 (2006) 3165-72.

Patterson E, Lazzara R, Szabo B, Liu H, Tang D, Li Y, Scherlag BJ, Po SS, Sodium-Calcium Exchange Initiated by the Ca^{2+} Transient Journal of the American College of Cardiology 47, (2006)

Petrocellis LD, Di Marzo V, Role of endocannabinoids and endovanilloids in Ca^{2+} signalling Cell Calcium 45 (2009) 611-24.

Pfeiffer SE, Warrington AE, Bansal R, The oligodendrocyte and its many cellular processes

Piomelli D, Tarzia G, Duranti A, Tontini A, Mor M, Compton TR, Dasse O, Monaghan EP, Parrott JA, Putman D, Pharmacological profile of the selective FAAH inhibitor KDS-4103 (URB597) CNS Drug Rev Spring 12 (2006) 21-38.

Plemel JR, Liu WQ, Yong VW, Remyelination therapies: a new direction and challenge in multiple sclerosis, Nature Reviews Drug Discovery 16 (2017) 617–634

Pringle NP, Mudhar HS, Collarini EJ, Richardson WD PDGF receptors in the rat CNS: during late neurogenesis, PDGF alpha-receptor expression appears to be restricted to glial cells of the oligodendrocyte lineage. Development 115 (1992) 535-551.

Pryce G, Cabranes A, Fernandez-Ruiz J, Bisogno T, Di Marzo V, Long JZ, Control of experimental spasticity by targeting the degradation of endocannabinoids using selective fatty acid amide hydrolase inhibitors Mult Scler 19 (2013) 1896-1904

Quednau BD, Nicoll DA, Philipson KD, Tissue specificity and alternative splicing of the Na+/Ca2+ exchanger isoforms NCX1, NCX2, and NCX3 in rat Journal of Physiology-Cell Physiology 272 (1997) 1250-1261

Readhead C, Takasashi N, Shine H D, Saavedra R, Sidman R, Hood L, Role of myelin basic protein in the formation of central nervous system myelin Ann N Y Acad Sci 5 (1990) 605:280

Reiter RJ Melatonin: clinical relevance Best Pract Res Clin Endocrinol Metab 17 (2003) 273-85

Reiter RJ , Tan D, Pappolla MA, Melatonin relieves the neural oxidative burden that contributes to dementias Ann N Y Acad Sci 1035 (2004) 179-96

Reiter RJ, Acuna-Castroviejo D, Tan D, Melatonin therapy in fibromyalgia Curr Pain Headache Rep 11 (2007) 339-342

Ren W, Liu G, Chen S, Yin J, Wang J, Tan B, Wu G, Bazer F W, Peng Y, Li Tiejun, Reiter R J, Yin Y, Melatonin signaling in T cells: Functions and applications J Pineal Res 62 (2017) 3

Reynolds R, Wilkin GP, Development of macroglial cells in rat cerebellum. II. An in situ immunohistochemical study of oligodendroglial lineage from precursor to mature myelinating cell. Development 102 (1988) 409–425

Rivara S, Pala D, Bedini A, Spadoni, Therapeutic uses of melatonin and melatonin derivatives: a patent review 25 (2014) 425-441

Rossi S, Furlan R, De Chiara V, Muzio L, Musella A, Motta C, Cannabinoid CB1 receptors regulate neuronal TNF-alpha efects in experimental autoimmune encephalomyelitis Brain Behav Immun. 25 (2011) 1242-1248

Saher G, Brügger B, Lappe-Siefke C, Möbius W, Tozaw Ra, Wehr MC, Wieland F, Ishibashi S, Nave KA High cholesterol level is essential for myelin membrane growth Nature Neuroscience 8 (2005) 468-475

Sasso O, Bertorelli R, Bandiera T, Scarpelli R, Colombano G, Armirotti Andrea, Moreno-Sanz G, Reggiani A, Piomelli D, Peripheral FAAH inhibition causes profound antinociception and protects against indomethacin-induced gastric lesions. Pharmacol Res 65 (2012) 553–563

Sasso O, Wagner K, Morisseau C, Inceoglu Bora, D Hammock B, Piomelli D, Peripheral FAAH and soluble epoxide hydrolase inhibitors are synergistically antinociceptive. Pharmacol Res 97 (2015) 7–15

Scolding NJ, Frith S, Linington C, Morgan BP, Campbell AK, Compston DA, Myelin-oligodendrocyte glycoprotein (MOG) is a surface marker of oligodendrocyte maturation, *J.* Neuroimmunol 22 (1989) 169–176

Scorziello A, Savoia C, Sisalli MJ, Adornetto A, Secondo A, Boscia F, Esposito A, Polishchuk EV, Polishchuk RS, Molinaro P, Carlucci A, Lignitto L, Di Renzo G, Feliciello A, Annunziato L, NCX3 regulates mitochondrial Ca^{2+} handling through the AKAP121-anchored signaling complex and prevents hypoxiainduced neuronal death, J. Cell Sci. 126 (2013) 5566–5577

Scotter EL, Abood ME, Glass M, The endocannabinoid system as a target for the treatment of neurodegenerative disease Br J Pharmacol 160 (2010) 480-98

Secondo A, Pignataro G, Ambrosino P, Pannaccione A, Molinaro P, Boscia F, Cantile M, Cuomo O, Esposito A, Sisalli MJ, Scorziello A, Guida N, Anzilotti S, Fiorino F, Severino B, Santagada V, Caliendo G, Di Renzo G, Annunziato L, Pharmacological characterization of the newly synthesized 5-amino-N-butyl-2-(4-ethoxyphenoxy)-benzamide hydrochloride (BED) as a potent NCX3 inhibitor that worsens anoxic injury in cortical neurons, organotypic hippocampal cultures, and is-chemic brain, ACS Chem. Neurosci. 6 (2015) 1361–1370

Secondo A, Staiano IR, Scorziello A, Sirabella R, Boscia F, Adornetto A, Canzoniero LM, Di Renzo G, Annunziato L, Ann NY, The Na+/Ca2+ exchanger isoform 3 (NCX3) but not isoform 2 (NCX2) and 1 (NCX1) singly transfected in BHK cells plays a protective role in a model of in vitro hypoxia, Acad Sci. 5 (2007) 481–485

Slivicki RA, Xu Z, Mali SS, Hohmann GA, Brain permeant and impermeant inhibitors of fatty-acid amide hydrolase suppress the development and maintenance of paclitaxel induced neuropathic pain without producing tolerance or physical dependence in vivo and synergize with paclitaxel to reduce tumor. Pharmacol Res 142 (2019) 267–282

Smith KJ, Blakemore WF, McDonald WI Central remyelination restores secure conduction. Nature 280 (1979) 395–396

Sokolow S, Manto M, Gailly P, Molgó J, Vandebrouck C, Vanderwinden JM, Her-chuelz A, Schurmans S, Impaired neuromuscular transmission and skeletal muscle fiber necrosis in mice lacking Na +/Ca2+ exchanger 3, J. Clin. Invest. 113 (2004) 265–273.

Sommer I, Schachner M Monoclonal antibodies (O1 to O4) to oligodendrocyte cell surfaces: an immunocytological study in the central nervous system. Dev Biol 30, 83(1981) 311-327

Sorbara CD, Wagner NE, Ladwig A, Nikić I, Merkler D, Kleele T, Marinković P, Naumann R, Godinho L, Bareyre FM, Bishop D, Misgeld T, Kerschensteiner M, Pervasive axonal transport deficits in multiple sclerosis models, Neuron 84 (2014) 1183–1190

Sprinkle TJ, 2', 3'-cyclic nucleotide 3'-phosphodiesterase, an oligodendrocyte-Schwann cell and myelin-associated enzyme of the nervous system Crit Rev Neurobiol 4 (1989) 235-3012

Stys PK, General mechanisms of axonal damage and its prevention, J. Neurol. Sci. 233 (2005) 3–13

Stys PK, Lopachin RM, Mechanisms of calcium and sodium fluxes in anoxic myelinated central nervous system axons, Neuroscience 82 (1998) 21–32

Stys PK, Waxman SG, Ransom BR, Ionic mechanisms of anoxic injury in mammalian CNS white matter: role of Na+ channels and Na (+)-Ca2+ exchanger, J. Neurosci. 12 (1992) 430–439.

Swift F, Tovsrud N, Sjaastad I, Sejersted OM, Niggli E, Egger M, Functional coupling of alpha(2)-isoform Na(+)/K(+)-ATPase and Ca(2+) extrusion through the Na(+)/Ca(2+)-exchanger in cardiomyocytes, Cell Calcium 48 (2010) 54–60

Syed YY, McKeage K, Scott JL, Delta-9-tetrahydrocannabinol/cannabidiol (Sativex®): a review of its use in patients with moderate to severe spasticity due to multiple sclerosis Drugs 74 (2014) 563-78

Talarico G, Trebbastoni A, Bruno G, de Lena C, Modulation of the Cannabinoid System: A New Perspective for the Treatment of the Alzheimer's Disease Neuropharmacology, Curr Neuropharmacol 17 (2019) 176-183

Tanaka M, Yagyu K, Sackett S, Zhang Y, Anti-Inflammatory Effects by Pharmacological Inhibition or Knockdown of Fatty Acid Amide Hydrolase in BV2 Microglial Cells Cells 8 (2019) 491

Tanasescu R, Constantinescu CS, Cannabinoids and the immune system: an overview Immunobiology 215 (2010) 588-597

Tekkok SB, Goldberg MP, Ampa/kainate receptor activation mediates hypoxic ol-igodendrocyte death and axonal injury in cerebral white matter, J. Neurosci. 21 (2001) 423–424

Thompson AJ, Banwell BL, Barkhof F, Carroll WM, Coetzee T, Comi G, Correale J, Fazekas F, Filippi M, Freedman MS, Fujihara K, Galetta SL, Hartung HP, Kappos L, Lublin FD, Marrie RA, Miller AE, Miller DH, Montalban X, Mowry EM, Sorensen PS, Tintoré M, Traboulsee AL, Trojano M, Uitdehaag BMJ, Vukusic S, Waubant E, Weinshenker B G, Reingold SC, Cohen JA Diagnosis of multiple sclerosis: 2017 revisions of the McDonald criteria Lancet Neurol 17 (2018) 162–173

Thompson AJ, Baranzini SE, Geurts J, Hemmer B, Ciccarelli O, Multiple sclerosis Lancet 39 (2018) 11622-1636

Tong XP, Li XY, Zhou B, Shen W, Zhang ZJ, Xu TL, Duan S, Ca^{2+} signalling evoked by activation of Na^{+} channels and Na^{+}/Ca^{2+} exchangers are required for GABA-induced NG2 cell migration, J. Cell Biol. 186 (2009) 113–128

Trapp BD, Nave KA, Multiple sclerosis: an immune or neurodegenerative disor-der? Annu, Rev. Neurosci. 31 (2008) 247–269

Trapp BD, Peterson J, Ransohoff RM, Rudick R, Mörk S, Bö L, Axonal transection in the lesions of multiple sclerosis, N. Engl. J. Med. 338 (1998) 278–285

Trapp BD, Peterson J, Ransohoff RM, Rudick R, Mörk S, Bö L, Axonal transection in the lesions of multiple sclerosis, N. Engl. J. Med. 338 (1998) 278–285

Trapp BD, Stys PK, Virtual hypoxia and chronic necrosis of demyelinated axons in multiple sclerosis, Lancet Neurol. 8 (2009) 280–291

van Egmond N, Straub VM, van der Stelt M, Targeting Endocannabinoid Signaling: FAAH and MAG Lipase Inhibitors Annu Rev Pharmacol Toxicol 61 (2021) 441-463

van Esbroeck ACM, Janssen APA, Cognetta AB, Ogasawara D, Shpak G, van der Kroeg Mark, Kantae V, Baggelaar MP, de Vrij FMS, Deng H, Allarà M, Fezza F, Lin Z, van der Wel T, Soethoudt M, Mock ED, den Dulk H, Baak IL, Florea IB, Hendriks G, De Petrocellis L, Herman Overkleeft S, Hankemeier T, De Zeeuw CI, Di Marzo V, Maccarrone Mauro, Cravatt BF, Kushner SA, van der Stelt M, Activity-based protein profiling reveals off-target proteins of the FAAH inhibitor BIA 10-2474 Science 356 (2017) 1084-1087

Verkhratsky A, Toescu EC, Endoplasmic reticulum Ca(2+) homeostasis and neuronal death, J. Cell. Mol. Med. 7 (2003) 351–361

Vincze A, Mazlo M, Seress L, Komoly S, Abraham H A correlative light and electron microscopic study of postnatal myelination in the murine corpus callosum. *Int J Dev Neurosci 26* (2008) 575-584

Waggener CT, Dupree JL, Elgersma Y, Fuss B, CaMKIIβ regulates oligodendrocyte maturation and CNS myelination, J. Neurosci. 33 (2013) 10453–10458

Wallace JB, Dan RA, Ferran P, Miszkiel KA, Eshaghi A, Gandini CAM, Kingshott Wheeler B, Ciccarelli O, Early imaging predictors of long-term outcomes in relapse-onset multiple sclerosis Brain 142 (2019) 2276–2287

Wang Q, Liu Y, Zhou J, Neuroinflammation in Parkinson's disease and its potential as therapeutic target Translational Neurodegeneration 4 (2015)

Waxman SG, Acquired channelopathies in nerve injury and MS, Neurology 56 (2001) 1621–1627

Waxman SG, Axonal conduction and injury in multiple sclerosis: the role of sodium channels, Nat. Rev. Neurosci. 7 (2006) 932–941

Wen J, Ariyannur PS, Ribeiro R, Tanaka M, Moffett JR, Kirmani BF , Namboodiri AM, Zhang Y, Efficacy of N-Acetylserotonin and Melatonin in the EAE Model of Multiple Sclerosis J Neuroimmune Pharmacol 11 (2016) 763-773

Wen J, Ariyannur PS, Ribeiro R, Tanaka M, Moffett JR, Kirmani BF, Namboodiri AMA, Zhang Y, Efficacy of N-Acetylserotonin and Melatonin in the EAE Model of Multiple Sclerosis J Neuroimmune Pharmacol 11 (2016) 763-773.Ghareghani M, Sadeghi H, Zibara K, Danaei N, Azari H, Ghanbari A, Melatonin Increases Oligodendrocyte Differentiation in Cultured Neural Stem Cells Cell Mol Neurobiol 37 (2017) 1319-1324

Wilkins A, Majed H, Layfield R, Compston A, Chandran S Oligodendrocytes promote neuronal survival and axonal length by distinct intracellular mechanisms: a novel role for oligodendrocyte-derived glial cell line-derived neurotrophic factor. J Neurosci Off J Soc Neurosci 23 (2003) 4967–4974

Witte ME, Schumacher AM, Mahler CF, Bewersdorf JP, Lehmitz J, Scheiter A, Sanchez P, Williams PR, Griesbeck O, Naumann R, Misgeld T, Kerschensteiner M, Calcium influx through plasma-membrane nanoruptures drives axon degeneration in a model of multiple sclerosis, Neuron 101 (2019) 615–624

Wu YH, Ursinus J, Zhou JN, Scheer Frank AJL, Ai-Min B, Jockers R, van Heerikhuize J, Swaab DF, Alterations of melatonin receptors MT1 and MT2 in the hypothalamic suprachiasmatic nucleus during depression J Affect Disord 148 (2013) 357-367

Xia Y, Zhang G, Han C, Ma K, Guo X, Wan F, Kou L, Yin S, Liu L, Huang J, Xiong N, Wang T, Microglia as modulators of exosomal alpha-synuclein transmission Cell Death Dis 10 (2019) 174

Xiong XY, Liu L, WuYang Q, Functions and mechanisms of microglia/macrophages in neuroinflammation and neurogenesis after stroke in Neurobiology 142 (2016) 23-44

Yang B, Zhang LY, Chen Y, Bai YP, Jia J, Feng JG, Liu KX, Zhou J, Melatonin alleviates intestinal injury, neuroinflammation and cognitive dysfunction caused by intestinal ischemia/reperfusion. Int. Immunopharmacol. 85 (2020) 106596

Yang J, Weimer RM, Kallop D, Olsen O, Wu Z, Renier N, Uryu K, Tessier-Lavigne M, Regulation of axon degeneration after injury and in development by the endogenous calpain inhibitor calpastatin, Neuron 80 (2013) 1175–1189

Yao L, Lu P, Ling EA, Melatonin suppresses toll like receptor 4-dependent caspase-3 signaling activation coupled with reduced production of proinflammatory mediators in hypoxic microglia. PLoS ONE 11 (2016) e0166010

Young EA, Fowler CD, Kidd GJ, Chang A, Rudick RA, Fisher E, Trapp BD, Imaging correlates of decreased axonal Na+/K+ ATPase in chronic multiple sclerosis lesions, Ann. Neurol. 63 (2008) 428–435

Yu L, Colvin RA, Regional differences in expression of transcripts for Na+/Ca2+ exchanger isoforms in rat brain Brain Res Mol Brain Res 50 (1997) 285-292

Zhang Q, Zhou Z, Lu G, Song B, Guo J, Melatonin improves bladder symptoms and may ameliorate bladder damage via increasing HO-1 in rats Inflammation 36 (2013) 651-657

Zhang SC, Defining glial cells during CNS development. Nat Rev Neurosci 2 (2001) 840–843

Zhou J, Zhang S, Zhao X, Wei T, Melatonin impairs NADPH oxidase assembly and decreases superoxide anion production in microglia exposed to amyloid-β1-42 J. Pineal Res. 45 (2008) 157–165

Zou S, Kumar U, Cannabinoid Receptors and the Endocannabinoid System: Signaling and Function in the Central Nervous System Int J Mol Sci 19 (2018) 833